DSPACE

https://dspace.org/

Assessment of South African coals in a bubbling fluidised bed combustion testing facility

Papo, Gladwin Thabo

2015-05-07
http://hdl.handle.net/10539/17663

Downloaded from a DSpace repository. https://dspace.org/

ASSESSMENT OF SOUTH AFRICAN COALS IN A BUBBLING FLUIDISED BED COMBUSTION TESTING FACILITY

Gladwin Thabo Papo

A dissertation submitted to the Faculty of Engineering and Built Environment, University of the Witwatersrand, in fulfilment of the requirement for the degree of Master of Science in Engineering.

October, 2014

DECLARATION

I declare that this dissertation is my own unaided work. It is being submitted for the degree of Master of Science in Engineering to the University of the Witwatersrand, Johannesburg. It has not been submitted before for any degree or examination to any other University.

……..

(Gladwin Thabo Papo)

…… day of ……. ……..

ACKNOWLEDGMENTS

I would like to thank the Almighty God for giving me the strength and ability to have furthered my education to this point. Special quote "*Keep faith and never lose hope in the God of mount Zion*"

I would like to express my gratitude to my colleagues, family and friends who have been a part of this journey;

- To the combustion facility manager, Mr Nyangwa, and the PSFBTF test team, thanks for the endless support and encouragement.
- Professor Rosemary Falcon, your words of encouragement and supervision has been a pillar of strength in concluding this study.
- To my parents, Mr and Mrs Papo, you are perfect models for my aspirations.

ABSTRACT

South Africa is one of the world's largest coal producers and exporters. However the quality of coal being mined is declining and hence beneficiating is required to meet export quality. Through beneficiation, waste coal (discard coal and duff coal) is produced and its accumulation is increasing yearly. The storage of waste coal can lead to environmental issues and is an eyesore to local and international sightseers in the highvelds. Therefore utilisation of waste coal, or land reformation of their sites is a necessity. In order to utilise waste coals, international coal consumers have applied fluidised bed combustion (FBC) technology. Fluidised bed combustion is a fuel-flexible technology, capable of burning waste coal with reduced nitrogen oxides and sulphur dioxide emissions.

The objective of this research was to evaluate the combustibility of high-ash coals in a bubbling fluidised bed combustor. This study proposed that high ash coal will combust in the BFBC with reduced emissions as well as without ash agglomeration. The research carried out entailed coal and limestone analysis (chemical, elemental and mineral analysis), coal combustion tests in a pilot scale BFBC facility (at different combustion temperatures and different limestone feedrates), fly ash analysis (elemental and mineral quantifications) and data consolidation.

On average, fly ashes from the three coals tested had a carbon fraction lower than 0.1%. Coal C had the lowest carbon-in-ash residue at all testing conditions. The addition of limestone without adjustment of the air/fuel ratio impacted negatively on the combustion efficiency at the highest Ca/S ratio. Coal A had the highest sulphur self-capture and retention, and the highest amount of decomposed calcite and dolomite. Overall limestone addition reduces the amount of SO_2 emitted. The BFBC test displayed low NO_x emissions which were lower than the minimum emission standard for new plants. NO_x emission increased with increasing bed temperature and N_2O emission decreased with increasing bed temperature. No ash agglomerations or slagging was detected during tests and the post-test reactor observation. Coal B has the lowest slagging propensity.

Overall, this study has shown that low quality coals can be combusted in the BFBC. The results showed that the considered coals can be combusted effectively with reduced emissions, without ash agglomeration, and with lower carbon-in-ash.

CONTENTS

DECLARATION I

ACKNOWLEDGMENTS II

ABSTRACT III

LIST OF FIGURES VII

LIST OF TABLES X

ABBREVIATIONS XII

CHAPTER 1 : INTRODUCTION 1

1.1 Background and Motivation 1

1.2 Objective of the Dissertation 2

1.3 Research Questions 3

1.4 Overview of the Dissertation 3

CHAPTER 2 : LITERATURE REVIEW 4

2.1 Introduction 4

2.2 Fluidisation Fundamentals 4

2.2.1 Minimum Fluidising Velocity 6

2.2.2 Bubble Formation 9

2.2.3 Particle Size 10

2.3 Fluidised Bed Combustion: An Overview 11

2.3.1 The Technology 11

2.3.2 Developments in FBC 13

2.3.3 Advantages and Disadvantages 15

2.4 Coal Combustion in Fluidised Bed 15

2.4.1 Coal Drying and Devolatilisation 16

2.4.2 Combustion of volatile matter 17

2.4.3 Char Combustion 18

2.5 Emissions from Fluidised Beds 18

2.5.1 NO_x and N_2O Emission 19

2.5.2 SO_2 Emission 21
2.6 Mineralogy and Chemistry of Fluidised Bed Ashes 24
2.6.1 Analyses of Coal and Fly Ash 24
2.6.2 Mineralogy of Fly Ash 25
2.7 South African Perspectives on BFBC 28
2.8 Summary 30
CHAPTER 3 : METHODOLOGIES 32
3.1 Introduction 32
3.2 Selected Coals for Testing 32
3.3 The BFBC Testing Facility 32
3.3.1 Overview of the testing facility 32
3.3.2 Testing Methodology 38
3.3.3 Gas Analysers 40
3.4 Laboratory Analysis 40
3.5 Computational Methods 41
3.5.1 Gas Species 42
3.5.2 Slagging Propensity 43
CHAPTER 4 : RESULTS AND DISCUSSIONS 45
4.1 Introduction 45
4.2 Analysis of Coal and Sorbent 45
4.3 Pilot Scale Test Results 49
4.3.1 Reactor Temperature Profiles 49
4.3.2 Carbon Efficiency 50
4.3.3 Sulphur Retention 52
4.3.4 Nitrogen Oxides Formation 53
4.3.5 Fly Ash Analysis 55
4.4 Discussion of the Results 59

4.4.1 Differences in Carbon-in-Ash 59

4.4.2 Local Impact of BFBC SO_2 Emission 61

4.4.3 Local Impact of NO_x Emissions 65

4.4.4 Ash Depositions in BFBC 68

CHAPTER 5 : CONCLUSIONS AND RECOMMENDATIONS 71

4.5 Conclusion 71

4.6 Recommendations 72

REFERENCES 73

APPENDIX A: COAL AND SORBENT ANALYSIS DATA 77

APPENDIX B: COAL A TEST RESULTS 84

APPENDIX C: COAL B TEST RESULTS 87

APPENDIX D: COAL C TEST RESULTS 90

APPENDIX E: FLY ASH ANALYSIS DATA 93

APPENDIX F: EXAMPLES OF EMISSION CONVERSION AND SULPHUR RETENTION 99

LIST OF FIGURES

FIGURE 1-1: DOMESTIC RATION OF COAL USAGE (EBERHARD, 2011) 1

FIGURE 2-1: FLUIDISATION REGIMES (PERRY *ET AL*, 1997) 5

FIGURE 2-2: SCHEMATIC OF A FLUIDISED BED (ESCUDERO, 2010) 6

FIGURE 2-3: PRESSURE DROP VERSUS FLUIDISING VELOCITY, (A) IDEAL (B) REAL (FUEYO AND DOPAZO, 1995) 7

FIGURE 2-4: GELDART PARTICLE CLASSIFICATION CHART (FUEYO AND DOPAZO, 1995) 10

FIGURE 2-5: PRINCIPLE OUTLINE OF FBC BOILERS (A) BFBC (B) CFBC (JOHNSSON, 2007) 12

FIGURE 2-6: COAL COMBUSTION IN FLUIDISED BED (ZHANGFA WU, 2003) 16

FIGURE 2-7: THE FORMATION PATTERN OF NO IN FBC (KONTTINEN *ET AL*, 2013) 20

FIGURE 2-8: SULPHATION PATTERNS (ANTHONY AND GRANATSTEIN, 2001) 23

FIGURE 3-1: ILLUSTRATION OF THE BFBC REACTOR 33

FIGURE 3-2: SCHEMATIC OF THE BUBBLING FLUIDISED BED COMBUSTION TESTING FACILITY 35

FIGURE 3-3: CONTROL PANEL PICTURE OF THE BFBC SYSTEM 36

FIGURE 3-4: CONTROL PANEL PICTURE OF THE REACTOR, GAS-SOLID SEPARATOR AND THE ASH REMOVAL SYSTEM. 37

FIGURE 4-1: COAL ASH ELEMENTAL ANALYSIS 46

FIGURE 4-2: COAL MINERALOGY ASSESSMENT 47

FIGURE 4-3: SORBENT ASH ELEMENTAL ANALYSIS 48

FIGURE 4-4: SORBENT MINERAL PROPORTION ANALYSIS 48

FIGURE 4-5: REACTOR TEMPERATURE PROFILES AVERAGED FOR THE THREE COALS 50

FIGURE 4-6: COMBUSTION EFFICIENCY GRAPH 51

FIGURE 4-7: SULPHUR RETENTION TRENDS 52

FIGURE 4-8: COAL A - NO_X AND N_2O GASEOUS EMISSIONS 53

FIGURE 4-9: COAL B - NO_X AND N_2O GASEOUS EMISSION 54

FIGURE 4-10: COAL C - NO_X AND N_2O GASEOUS EMISSION 54

FIGURE 4-11: MASS FRACTIONS ANHYDRITE, CALCITE, DOLOMITE, CAMG-SULPHATE AND CHAR 57

FIGURE 4-12: PROPORTION OF THE REACTED AND UNREACTED CAO AND CAMGO 58

FIGURE 4-13: CARBON-IN-ASH AT THE DIFFERENT TEMPERATURES AND CALCIUM SULPHUR RATIOS 59

FIGURE 4-14: TYPICAL POWER STATION CARBON-IN-ASH COMPARED TO THAT IN BFBC 60

FIGURE 4-15: BFBC SO_2 EMISSION COMPLIANCY TO NEM: AQA 2004 62

FIGURE 4-16: EQUIVALENCE BFBC SO_2 TO ESKOM AND VARIOUS REGULATORS 64

FIGURE 4-17: BFBC NO_X EMISSION COMPLIANCY TO NEM: AQA 2004 65

FIGURE 4-18: EQUIVALENCE OF BFBC NO_X EMISSIONS TO ESKOM AND VARIOUS REGULATORS 66

FIGURE 4-19: FLY ASH MINERALOGY FROM COAL A 69

FIGURE 4-20: FLY ASH MINERALOGY FROM COAL B 69

FIGURE 4-21: FLY ASH MINERALOGY FROM COAL C 70

FIGURE A-1: MINERALOGY ASSESSMENT GRAPH FOR COAL A 78

FIGURE A-2: MINERALOGY ASSESSMENT GRAPH FOR COAL B 80

FIGURE A-3: MINERALOGY ASSESSMENT GRAPH FOR COAL C 82

FIGURE B-1: CARBON CONVERSION FOR COAL A 85

FIGURE B-2: NO_X EMISSIONS FOR COAL A 85

FIGURE B-3: N_2O EMISSIONS FOR COAL A 86

FIGURE B-4: SO_2 EMISSIONS FOR COAL A 86

FIGURE C-1: CARBON CONVERSION FOR COAL B 88

FIGURE C-2: NOX EMISSIONS FOR COAL B 88

FIGURE C-3: N_2O EMISSIONS FOR COAL B 89

FIGURE C-4: SO_2 EMISSIONS FOR COAL B 89

FIGURE D-1: CARBON CONVERSION FOR COAL C 91

FIGURE D-2: NOX EMISSIONS FOR COAL C 91

FIGURE D-3: N_2O EMISSIONS FOR COAL C 92

FIGURE D-4: SO_2 EMISSIONS FOR COAL C 92

FIGURE E-1: ASH ELEMENTAL OF FLY ASH FROM COAL A, 850 °C TESTS 93

FIGURE E-2: ASH ELEMENTAL OF FLY ASH FROM COAL B, 850 °C TESTS 95

FIGURE E-3: ASH ELEMENTAL OF FLY ASH FROM COAL C, 850 °C TESTS 97

LIST OF TABLES

TABLE 2-1: ERGUN'S EQUATION SELECTED DERIVATIONS (SUKSANKRAISON ET AL, 2001) 8

TABLE 2-2: TECHNOLOGY STATUS OF FBC TECHNOLOGY (IEA-CLEAN COAL CENTRE, JUNE 2006) 13

TABLE 2-3: SUMMARY OF THE DIFFERENCE BETWEEN CONVENTIONAL COMBUSTION ASHES AND FBC ASHES (SULOVSKY, 2002) 26

TABLE 2-4: DECOMPOSITION AND MELTING TEMPERATURES OF SELECTED MINERALS FOUND IN COAL AND FLY-ASH (MATJIE, 2008) 27

TABLE 2-5: SOME APPLICATIONS OF FBC IN SOUTHERN AFRICA (NORTH, 2012) 30

TABLE 3-1: THE TEST MATRIX FOR COAL A, B AND C WITH AND WITHOUT LIMESTONE 39

TABLE 3-2: CHEMICAL ANALYSIS REQUIRE FOR COAL 40

TABLE 4-1: COAL PROXIMATE AND ULTIMATE ANALYSIS ON AIR-DRIED BASES 45

TABLE 4-2: TEMPERATURE READING ACROSS THE BED AND THE FREE-BOARD 49

TABLE 4-3: COAL A - ASH ELEMENTAL RESULTS FOR THE TESTS AT 850 ˚C 55

TABLE 4-4: COAL B - ASH ELEMENTAL RESULTS FOR THE TESTS AT 850 ˚C 56

TABLE 4-5: COAL C - ASH ELEMENTAL RESULTS FOR THE TESTS AT 850 ˚C 56

TABLE 4-6: MINIMUM EMISSION STANDARDS FOR SOLID FUEL COMBUSTION INSTALLATIONS 62

TABLE 4-7: SLAGGING PROPENSITY OF THE COALS 68

TABLE A-1: CHEMICAL ANALYSIS DATA FOR COAL A 77

TABLE A-3: CHEMICAL ANALYSIS DATA FOR COAL B 79

TABLE A-5: CHEMICAL ANALYSIS DATA FOR COAL C 81

TABLE A-7: CHEMICAL ANALYSIS OF LIMESTONE 83

TABLE B-1: EXPERIMENTAL TEST DATA FOR COAL A 84

TABLE C-1: TESTING RESULTS FOR COAL B WITH AND WITHOUT LIMESTONE 87

TABLE D-1: TABLE RESULTS FOR COAL C WITH AND WITHOUT LIMESTONE 90

TABLE E-1: MINERALOGY ASSESSMENT OF FLY ASH FROM COAL A, 850 ℃ TESTS 94

TABLE E-2: MINERALOGY ASSESSMENT OF FLY ASH FROM COAL B, 850 ℃ TESTS 96

TABLE E-3: MINERALOGY ASSESSMENT OF FLY ASH FROM COAL C, 850 ℃ TESTS 98

ABBREVIATIONS

ACRONYMS

Ai	Alkaline Index
B/A	Base/Acid Ratio
BFBC	Bubbling fluidised bed combustion
BHEL	Bharat Heavy Electrical Ltd
CAPEX	Capital Expenditure
CCSEM	Coal Characterisation Scanning Electron Microscope
CFBC	Circulating fluidised bed combustion
CSIR	Council of Scientific and Industrial Research
CV	Caloric Value
DEA	Department of Energy
Eskom	Electricity supply commission
etc.	From Latin, abbreviation of '*et cetera'*, meaning 'and other things' or 'and so on'
FBC	Fluidised bed combustion
FGD	Flue gas desulphurisation
Fi	Fouling Index
IEA	International Energy Agency
ISO	International Organisation of Standardization
OEM	Original Equipment Manufacture
OPEX	Operational Expenditure
NEM : AQA	National Emission Management: Air Quality Act
QEMSCAN	Quantitative Evaluation of Mineralogy by Scanning Electron Microscopy
SABS	South African Bureau of Standards
SANAS	South African National Association of Standards
SASOL	South African Synthetic Oil Limited
SCR	Selectively catalytic reduction
SEM	Scanning Electron Microscope
Si	Slagging Index
SNCR	Selective non-catalytic reduction
SR	Silica Ratio
STP	Standard Temperature and Pressure (1 atm, O °C)
XRF	X-ray fluorescence

CHEMICAL FORMULAS

Symbols	**Descriptions**
Al	Aluminium
C	Carbon
Ca	Calcium
$CaCO_3$	Calcite
CaO	Calcium Oxide
$CaO.MgCO_3$	Calcium-magnesium Oxide
$CaSO_4$	Calcium Sulphate
CH_4	Methane

CO	Carbon Monoxide
CO_2	Carbon Dioxide
Fe	Iron
H_2	Hydrogen
H_2O	Water
HCN	Hydrogen cyanide
K	Potassium
O_2	Oxygen
Mg	Magnesium
Mn	Manganese
N_2	Nitrogen
N_2O	Nitrous Oxide
Na	Sodium
NH_3	Ammonia
NO_x	Nitrogen oxides
P	Phosphorus
S	Sulphur
Si	Silica
SO_2	Sulphur dioxide

SYMBOLS

Symbol	**Description**	**Unit**
Ar	Argon's number	
d_p	Diameter of the particles,	m
ε	Bed's void fraction	
g	Gravitation acceleration	$m.s^{-2}$
L	Bed Height	m
MW_e	Megawatt electricity sent out	MW
MW_{th}	Megawatt thermal	MW
ρ_g	Gas density	$kg.m^{-3}$
ρ_s	Particle density	$kg.m^{-3}$
ΔP	Differential Pressure	atm
Re_{mf}	Reynold Number	
ϕ	Particles' sphericity	
μ	Fluid dynamic viscosity	$kg.m^{-2}$
U_{mf}	Minimum fluidisation velocity	$m.s^{-1}$

CHAPTER 1 : INTRODUCTION

1.1 Background and Motivation

South Africa is one of the top producers and exporters of coal. It has the world's largest coal export terminal and its geographical position (between the Atlantic and the Pacific oceans) allows the South African coal producers to export competitively to either Europe or the East (Eberhard, 2011). World Coal Association stated in its Coal Fact 2012 publication that 42% of the electricity generated in the world is from coal and that South Africa generated 93% of electricity locally from coal.

South Africa's coal reserves are estimated between 15 and 55 billion tonnes (Eberhard, 2011) with the majority of the mines situated in the Central Basin (the Emalahleni, Highvelds and Ermelo coal fields). However the quality of the export coal produced in South Africa is declining, and coal with lower heating value and higher ash content is being mined and beneficiated to meet export specifications. Steam coal for domestic use is taken from the middling and large amounts of discard coal are produced at a rate of about 60 million tonnes per year (Eberhard, 2011). Eskom uses 70% of the domestic steam coal for electricity generation, 20% by SASOL in its coal-to-liquid processes and the rest by other industries as shown in Figure 1.1.

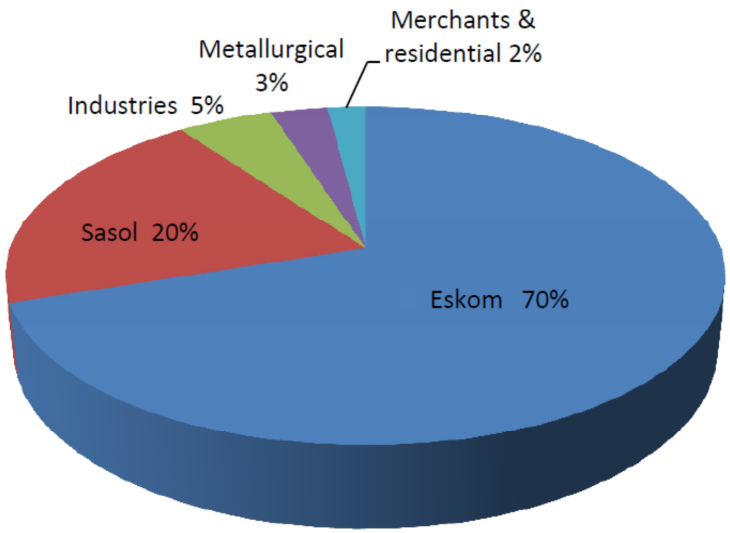


Figure 1-1: Domestic ration of coal usage (Eberhard, 2011)

The stockpiles of discard coal are an eyesore and an environmental concern; however these stockpiles can also be a source of energy. Discard coals have a high amount of ash, low volatile matter, high sulphur and lower heating value (<14 MJ/kg). Petrie (1985) stated that fluidised bed combustion is an attractive technology for burning coal not suited for the conventional coal-fired power plants. Lloyd (2000) also stated that the reason for not burning discard coal is that boilers have not been developed to use materials as abrasive as discard coal. This author further mentions that the 'better' quality discard coal is situated in Mpumalanga, a water scarce region, where water would be required if this coal was to be used to generate power.

Therefore a clean coal technology has to be adapted to burn the discard coals efficiently and in an environmentally friendly procedure. In light of the above and with the advantages that fluidised bed combustion (FBC) holds in the future, a comprehensive research program was devised with the aim of combining local combustion experience with international experience in fluidised beds.

FBC is generally regarded as a robust technology with unique characteristics, rendering its suitable to a host of different applications. In 1990, the turnkey for the construction and commissioning of a pilot scale bubbling fluidised bed combustion (BFBC) for Eskom was completed. The aim was to evaluate the suitability of FBC for South African application with regards to electricity generation. This specific study aims to assess how different coals behave inside a pilot scale BFBC reactor with reference to the extent of reaction of the constituents in the coals and sorbents, and compares the differences based on the combustion efficiency, gaseous emissions and the composition of fly ash.

1.2 Objective of the Dissertation

The objectives of this study are:

- To establish the combustibility of high-ash coals (power station and discard coals) with and without sorbent in the pilot BFBC, and
- To determine the effect of temperature, fluidising velocity and excess air on the performance of the pilot BFBC.

1.3 Research Questions

To accomplish these objectives, the following main 'research' question is presented;

- Can South African coal be effectively combusted using a bubbling fluidised bed combustion technology?

To obtain the answers to this question, three sub-questions are introduced and answers to these will consequently lead to the main solution. These sub-questions are;

- How does the carbon-in-ash differ for the coals at the different temperature?
- How are the gaseous emissions impacted by utilising the BFBC technology?
- How do the coal constituents affect ash deposition and agglomeration in BFBC?

1.4 Overview of the Dissertation

The dissertation is divided into five chapters;

Chapter one introduces the objectives of this study and also states the questions that need to be answered.

Chapter two is a literature review of FBC technology and highlights other uses of the BFBC technology locally and international. The chapter also includes a background on fluidisation, coal combustion chemistry and sulphur capture chemistry.

Chapter three describes the methodologies adopted in this study to obtain both the technical and analysis data. It describes the test equipment used and the procedure followed to eliminate any discrepancies between the tests.

Chapter four outlines the experimental test work data and results; it also focuses on the analysis of the fly-ash obtained from the pilot BFBC. In this chapter the discussions are aimed at providing solutions to the questions in chapter 1.

Chapter five outlines the conclusions derived from this study and the recommendations for further work based on the study.

CHAPTER 2 : LITERATURE REVIEW

2.1 Introduction

Perry and Green (2007) state that gas-solid fluidised bed systems are generally for contacting purposes, but in some instances the presence of the gas or solid is solely used to provide a fluidised bed to accomplish the desired result. Solids are of great importance in the chemical process industry, mineral processing, pharmaceutical production, energy-related processes, etc. (Avidan et al, 1997). These solid particles are either used as catalysts in some processes, or undergo chemical conversion as in ore processing or physical transformation like drying as noted by Petrie (1985).

Chapter one introduced the motivation behind this work as the need to assess the combustibility of high-ash, low CV coals in Eskom's pilot scale bubbling fluidised bed combustion facility for future utilisation in power generation. Chapter two's objectives are to conduct a literature review on the following elements,

- The fundamentals of fluidisation,
- Coal combustion in FBC technology,
- The effects of the operating parameters,
- Mineralogy of ash from FBC systems,
- International perspectives on BFBC and
- South African view on fluidisation.

2.2 Fluidisation Fundamentals

When a liquid or a gas at low velocity passes through a bed of solid particles, the particles do not move. If the fluid velocity is steadily increased, the pressure drop and the drag force on individual particles increase, and eventually the particles start to move and become suspended in the fluid. This phenomenon where a solid bed acquires fluid-like properties is called fluidisation. The fluidisation medium can either be liquid, gas or liquid-gas arising to fluidised systems of liquid-solid, gas-solid and liquid-gas-solid. The fluidised system of

interest in this study is the gas-solid system. Figure 2-1 depicts the progression stages of a gas-solid fluidised system.

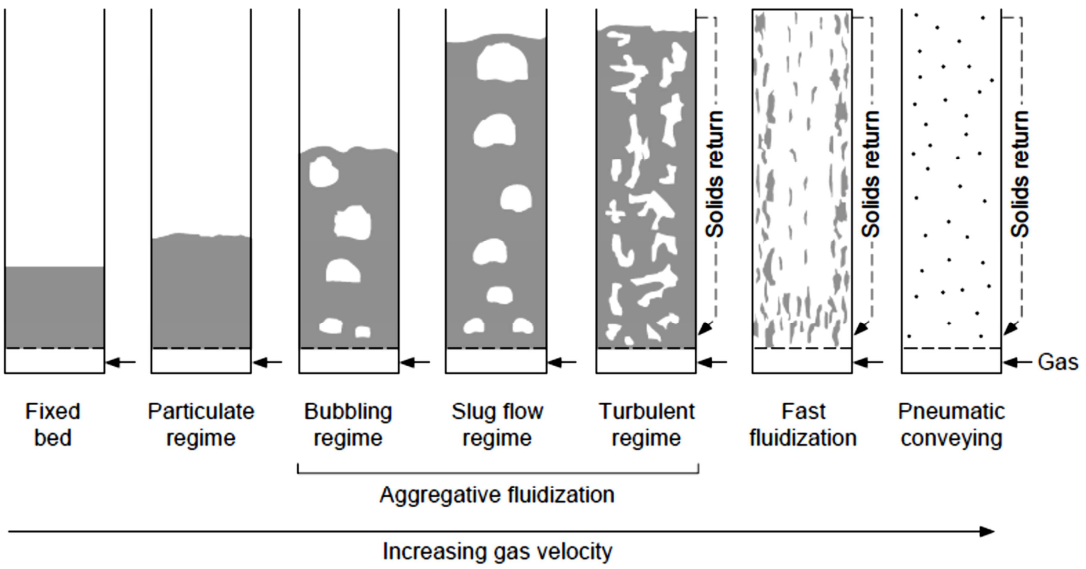


Figure 2-1: Fluidisation regimes (Perry *et al*, 1997)

A typical gas-solid fluidised bed system comprises of an air plenum, a distributor, a bed region and a free-board region. In a gas-solid system, air enters the reactor via the air plenum and distributed across the bed by the distributor. Solids are placed on top of the distributor plate through which air passes and at the correct velocity, fluidisation is achieved. Solids entrained by the air from the bed region passes into the free-board region before exiting the FBC reactor. A typical schematic of an FBC reactor is shown in Figure 2-2.

Publications on the fundamentals of fluidisation are available from numerous authors and institutes. These publications provide information on solid classification, bubble formation, minimum fluidisation velocity, gas flow pattern, etc. The objective of this section is to summarise some of these fundamentals that are applicable to BFBC assessment.

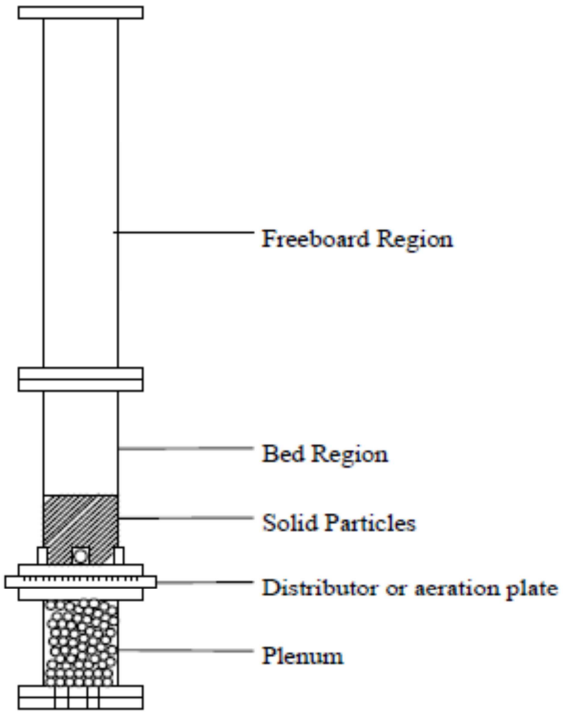


Figure 2-2: Schematic of a Fluidised Bed (Escudero, 2010)

2.2.1 Minimum Fluidising Velocity

In a gas-solid system, minimum fluidising velocity is the velocity of gas where the drag force exerted on the solids equals the weight of the solid particles per unit area. Fueyo and Dopazo (1995) state, the minimum fluidising velocity is probably the single most important parameter in determining the performance of a FBC. Figure 2-1 shows the impact of gas velocity and differential pressure on a bed packed with solid particles. At low velocity, the particles do not move (fixed bed). If the velocity is gradually increased, the pressure drop (ΔP) across the packed bed will also increase until fluidisation in initiated at the minimum fluidisation velocity (Figure 2-3). Beyond the minimum fluidisation velocity, in an ideal environment the differential pressure across the bed should remain constant. However in real environments the behaviour of the differential pressure is different as depicted in Figure 2-3.

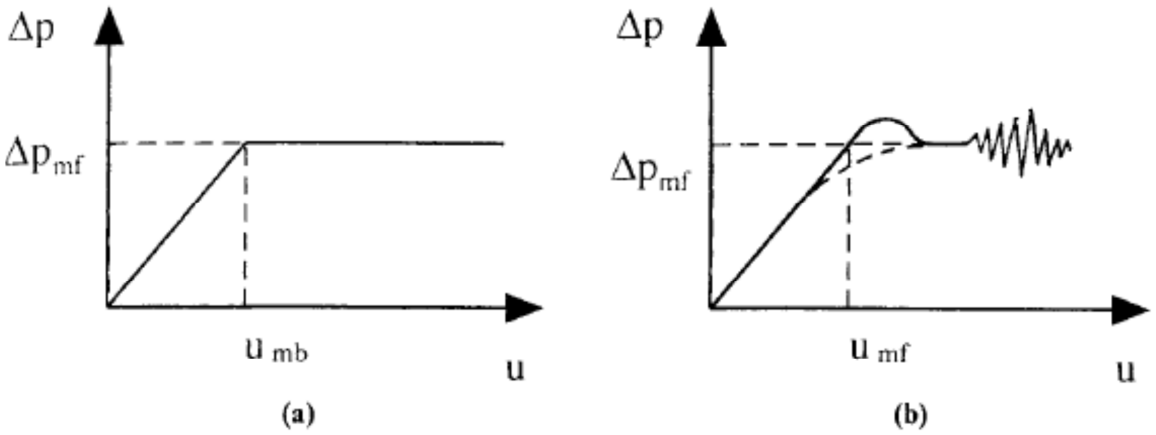


Figure 2-3: Pressure drop versus fluidising velocity, (a) ideal (b) real (Fueyo and Dopazo, 1995)

Minimum fluidisation velocity can be predicted by using a correlation between differential pressure and gas velocity according to Ergun's correlation,

$$\Delta P = L\left(\frac{150(1-\varepsilon_{mf})\mu U_{mf}}{\phi_s^2 \varepsilon_{mf}^3 d_p^2} + \frac{1.75(1-\varepsilon_{mf})\, U_{mf}^2 \rho_g}{\phi_s\, \varepsilon_{mf}^3 d_p}\right) \qquad \text{Equation 2-1}$$

where L is the bed height, μ is the fluid dynamic viscosity, ϕ is the particles' sphericity, d_p is the diameter of the particles, ρ_g is the gas density and ε is the bed's void fraction. Differential pressure at a fluidisation point is determined by the following equation,

$$\Delta P = L(\rho_s - \rho_g)g(1-\varepsilon_{mf}) \qquad \text{Equation 2-2}$$

where g is the gravitation acceleration and ρ_s is the particle density. For a system with Reynolds number less than 20, i.e. laminar flow, Ergun's equation can be simplified to determine the minimum fluidisation velocity;

$$U_{mf} = \frac{d_p^2(\rho_s-\rho_g)g}{150\mu}\left(\frac{\varepsilon^3\phi_s^2}{1-\varepsilon}\right) \qquad \text{Equation 2-3}$$

However using Ergun's equation requires knowledge of parameters that are difficult to acquire for real systems (parameters like the voidage at fluidisation and the sphericity). Suksankraisorn et al (2001) observed the prediction of the minimum fluidisation velocity by Wu and Baeyens (1991) from various correlations.

Table 2-1: Ergun's Equation Selected Derivations (Suksankraison et al, 2001)

Author	Equation
Wen and Yu	$U_{mf} = \frac{\mu_g}{\rho_g d_p}(\sqrt{1135{,}7 + 0.048Ar} - 33.7)$
Baeyens and Geldart	$Ar = 1823Re_{mf}^{1.07} + 21.27Re_{mf}^{2}$
Leva *et al*	$U_{mf} = \frac{7.39 d_p^{1.82}(\rho_p - \rho_g)^{0.94}}{\rho_g^{0.06}}$
Goroshoko *et al*	$U_{mf} = \frac{\mu_g}{\rho_g d_p}\left(\frac{Ar}{1400 + 5.2\sqrt{Ar}}\right)$
Leva	$U_{mf} = \frac{7.169 \times 10^{-4} d_p^{1.82}(\rho_p - \rho_g)^{0.94} g}{\rho_g^{0.006}\mu_g^{0.88}}$
Bena	$U_{mf} = \frac{\mu_g}{\rho_g d_p}\left(\frac{1.38 \times 10^{-3} Ar}{(Ar + 19)^{0.11}}\right)$
Rowe and Henwood	$U_{mf} = \frac{8.1 \times 10^{-3} d_p^2(\rho_p - \rho_g) g}{\mu_g}$
Miller and Logwinuk	$U_{mf} = \frac{0.00125 d_p^2(\rho_p - \rho_g)^{0.9}\rho_g^{0.1} g}{\mu_g}$
Frants	$U_{mf} = \frac{1.065 \times 10^{-3} d_p^2(\rho_p - \rho_g) g}{\mu_g}$
Davies and Richardson	$U_{mf} = \frac{7.8 \times 10^{-4} d_p^2(\rho_p - \rho_g) g}{\mu_g}$
Pillai and Raja Rao	$U_{mf} = \frac{7.01 \times 10^{-4} d_p^2(\rho_p - \rho_g) g}{\mu_g}$
Broadhurst and Becker	$U_{mf} = \frac{\mu_g}{\rho_g d_p}\left(\frac{Ar}{2.42 \times 10^5 Ar^{0.85}\left(\frac{\rho_p}{\rho_g}\right)^{0.13} + 37.7}\right)^{0.5}$
Saxena and Vogel	$U_{mf} = \frac{\mu_g}{\rho_g d_p}\left(\sqrt{25.28^2 + 0.0571Ar} - 25.28\right)$
Babu *et al*	$U_{mf} = \frac{\mu_g}{\rho_g d_p}\left(\sqrt{25.25^2 + 0.0651Ar} - 25.25\right)$
Richardson and Da St. Jeromino	$U_{mf} = \frac{\mu_g}{\rho_g d_p}\left(\sqrt{25.7^2 + 0.0365Ar} - 25.7\right)$
Doichev and Akhmakov	$U_{mf} = \frac{\mu_g}{\rho_g d_p}(1.08 \times 10^{-3} Ar^{0.947})$
Thonglimp	$U_{mf} = \frac{\mu_g}{\rho_g d_p}\left(\sqrt{31.6^2 + 0.042Ar} - 31.6\right)$
Bourgeois and Grenier	$U_{mf} = \frac{\mu_g}{\rho_g d_p}\left(\sqrt{25.46^2 + 0.03824Ar} - 25.46\right)$

Suksankraisorn et al (2001) measured the minimum fluidised velocity at temperatures above ambient and compared their results to the correlations in Table 2-1: Ergun's Equation Selected Derivations (Suksankraison et al, 2001) Although most of the correlations were consistent with their laboratory determined minimum fluidisation velocity at the different temperatures, none were capable of accurately predicting the minimum fluidisation velocity. Suksankraisorn et al (2001) recommended that correlation for the prediction of minimum fluidising velocity should be a rough guideline only.

Escudero (2010) found that the minimum fluidising velocity is proportional to the solid particles density. This author states that for solid particles of higher density, a higher superficial gas velocity is required to establish fluidisation. Hence, minimum fluidising velocity is a function of the gas and solid particle properties.

2.2.2 Bubble Formation

Bubbles generally form at the holes of the distributor and propagate through the bed. A bubble within a cloud of bubbles rises faster than one in isolation, except for those in beds of larger mean particle diameter of 1 mm, where the rise rate tends to be slower (Howard and Elliot, 1983). Howard further mentions that as a bubble rises through the bed it grows by collection of gases from the surrounding phase and through coalescence. Olsson (2008) states that bubbles and gas channelling affects the efficiency of FBC negatively, and that bubble size, rise velocity, shape, distribution, frequency and flow pattern are of interest in the determining the interaction of bubbles with bed materials.

Bubbles play an important role in some aspects of the fluidised bed performance; some of these aspects are (Fueyo and Dopazo, 1995):

- *Mixing* – the upward motion of bubbles in a fluidised system greatly enhances mixing, and hence promotes the uniformity of bed properties (e.g. heat and mass transfer),
- *Bed expansion* – The bed height is a function of the bubble-phase volume within the bed,
- *Through flow* – Fast-moving bubbles carry with them a cloud of gas and particles that circulate through the bubble but are not exchanged with its surroundings. This through-flow hampers mixing, and may cause the elutriation of unburned particles, and

- *Elutriation* – The phenomenon of elutriation is compounded by the bursting of bubbles at the bed surface, which throws particles into the freeboard zone.

The behaviour of bubbles within the fluidisation system can be described by Geldart's particle classification chart which is shown in Figure 2-4.

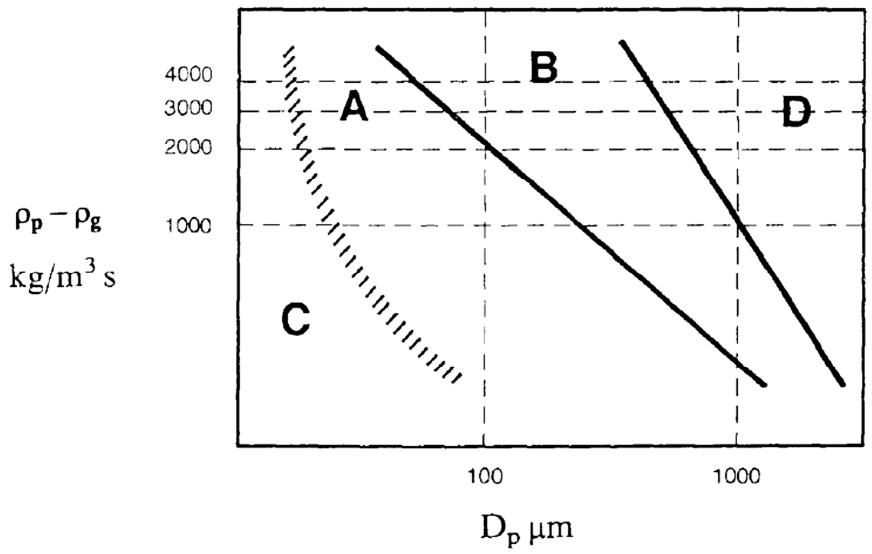


Figure 2-4: Geldart Particle Classification Chart (Fueyo and Dopazo, 1995)

Holdich (2002) explains these regions in terms of bubble formation and fluidisation impact as follows;

- Group A: Aeratable, may not bubble, if it does then bed expands before bubbling, may have fast moving bubbles less than 100mm
- Group B & D: Large bubbles may form slugs. Group D gives slow bubbles
- Group C: Cohesive, high inter-particle forces leads to difficult fluidisation, may form channels or slugs instead

Bubbles in fluidised beds belonging to groups A and B in the Geldart particle classification chart are typically spherical cap-shaped (Olsson, 2008). The size of a bubble in a fluidised bed changes continuously due to coalescence and splitting.

2.2.3 Particle Size

Fluidisation of a system depends on the type and size of particles being used. The size and type of particles used impacts on the minimum fluidisation velocity and the formation of

bubbles within the fluidisation system. Geldart's particle classification is based on their mean diameters (Group A, B, C and D) and the difference in density between the fluidising medium and the particles ($\rho_p - \rho_g$) as shown in Figure 2-4 above.

Most solid fuels used in commercial fluidised bed combustion of solid fuels belong to group B which contains most of the material of medium-range size and density (Johnsson, 2007). Fluidised beds employing group B particles have coinciding minimum bubbling and minimum fluidising velocities (Olsson, 2008). Wu (2003) states that the solid particle sizes in the bed (0.5 mm to 1.5 mm in BFBC and 150 μm in CFBC) is determined by the feed particle size (2 – 6 mm for BFBC).

2.3 Fluidised Bed Combustion: An Overview

Fluidised bed combustion had been thoroughly research and extensively reported in a number of publications. This section provides an overview of this established technology with a focus on BFBC.

2.3.1 The Technology

The fluidised bed combustion technology applies the principle of fluidisation which implies that the particles are suspended in air and, at this stage, the mixture of air and solids behave like a fluid (Zhangfa Wu, 2003). For coal combustion, fine coal particles in the reactor are suspended in air where they are free to move and react to produce heat, gases and solid residue. Two types of fluidised bed combustion technologies boilers dominate the FBC market; bubbling fluidised bed combustion (BFBC) and circulating fluidised bed combustion (CFBC). These are illustrated in Figure 2-5.

Johnsson (2007) lists the characteristics of the reactor of fluidized bed units applied in combustion are as follows;

- A height to diameter (aspect) ratio of the riser of the order of or less than 10,
- A ratio of the static bed height to riser diameter of less than 1,
- Fluidised solids belonging to group B in the Geldart classification, and
- For CFBC units a solids net flux typically ranging from 0.5 to 20 $kg/m^2 \cdot s$.

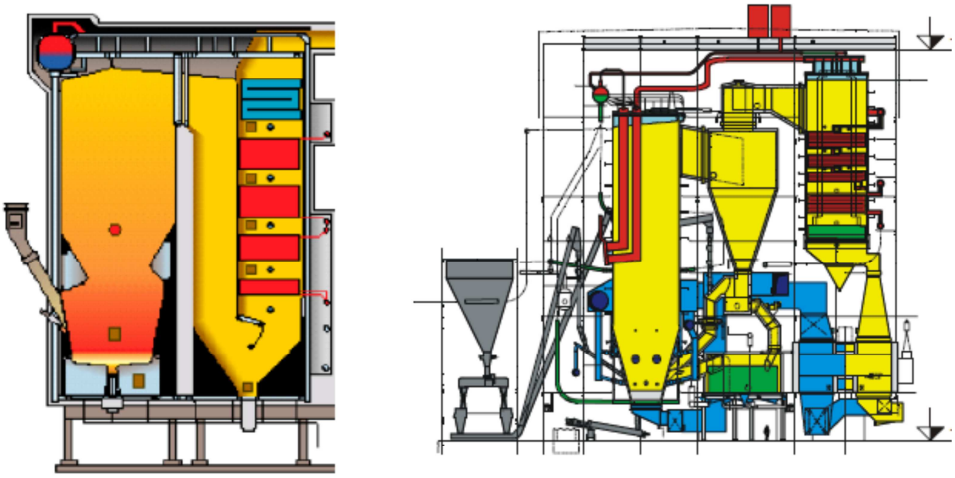


Figure 2-5: Principle outline of FBC boilers (a) BFBC (b) CFBC (Johnsson, 2007)

Mladenovic *et al* (2012) mentions that the differences in combustion conditions between BFBC and CFBC boilers are a consequence of different CFBC hydrodynamics; namely smaller inert material particle size, higher fluidisation velocity, different particle concentration, different mixing, and fuel particle circulation up to the total burn-out. However two important parameters for the combustion process are the same; combustion temperature and excess air. Some other facts that influence combustion in the two systems are listed below (Mladenovic *et al*, 2012);

- In both types, bed temperature is practically the same (800-850 °C), but in CFBC it is constant along furnace height, while in BFBC a significant difference between bed and freeboard temperature can exist, which depends very much on coal rank (volatile matter content), char reactivity and particle size distribution. However, conditions in the bottom bed of CFBC are similar to those in BFBC,
- Mixing of fuel particles, gas mixing and inert particle mixing are more intensive in CFBC regimes, so the convection component of heat transfer is higher in CFBC conditions. The height of the CFBC boiler furnace is chosen to allow higher burn-out rates of small particles in one pass. Large particles are circulated until maximum burn-out is achieved. Due to these facts, for the same fuel applied, combustion efficiency is higher in CFBC than in BFBC,

- Limestone particle sizes are smaller and hence have larger specific surface area available for reaction. The degree of desulphurisation in CFBC is greater than in BFBC because of the longer residence time due to re-circulation, and
- Due to the staged combustion, NO_x emission in CFBC is lower than in BFBC.

2.3.2 Developments in FBC

IEA-Clean Coal Centre (June 2006) profiled the developments of FBC technology based on difference in operating pressure (atmospheric and pressurised) of the two systems. This is shown in Table 2-2.

Table 2-2: Technology status of FBC Technology (IEA-Clean Coal Centre, June 2006)

	BFBC	PBFBC	CFBC	PCFBC
Unit size	Up to 300 MWth	Up to 360 MWe	Up to 460 MWe	Pilot Scale
Steam conditions	Sub-critical	7 Sub-critical and 1 supercritical	Sub-critical and 1 supercritical	
Plant Efficiency	30% with industrial boilers	Up to 44% with sub-critical, 44% with supercritical	38-40% with sub-critical, 43% with supercritical	
Plant availability	>90	Not available	90-98	
NO_x Emissions, mg/m^3	<400	<400	<400	
Sulphur retention efficiency	Lower than CFBC/PBFBC	90% at Ca/S ratios of 1.8-2.0	90% at Ca/S ratio 2	
Particulate emissions, mg/m3	<50 with ESP/bag filter	3.5-76	<50% with ESP/bag filter	
Future development	Continuous development	Uncertain	Major development	Uncertain
Market potential	Favourable	Unfavourable	Strong	Unfavourable

BFBC has been used at relatively small unit sizes rating up to 300 MW_{th}. The steam conditions of BFBC are generally lower than CFBC and therefore plant efficiencies (energy transfer from coal to electricity) are normally around 30% with plant availabilities over 90%. NO_x emissions are lower than conventional PF combustion boilers due to the low combustion temperatures. If air staging (primary and secondary air) is applied, NO_x emissions can be lower than 40 mg/m^3. Table 2-2 also indicates that sulphur removal in BFBC is lower than the CFBC.

PBFBC is currently at the demonstration phase with eight plants world-wide. Table 2-2 indicate that there were seven subcritical plants of 70–250 MW_e and one supercritical plant of 360 MW_e installed by 2006. Plant efficiency of 44% with the supercritical PBFBC plant has been attained. NO_x emissions are similar to those of BFBC, but sulphur removal is higher.

Larger industries involved in chemicals and electricity production favour the CFBC. These units are mostly subcritical and their sizes rate up to 300 MW_e. Plant efficiency for CFBC range between 38-40%, and have plant availability at 90-98% as shown in Table 2-2. The supercritical CFBC Łagisca plant has plant efficiency of 43%. Its NO_x emission is similar to those of BFBC and PBFBC and sulphur removal is higher than both versions of the BFBC (IEA-Clean Coal Centre, June 2006).

IEA-Clean Coal Centre (November 2013) illustrates current developments in CFBC plants with the world's largest CFBC plant located in China at 600 MW_e commissioned in 2013 and the planned 550 MW_e CFBC plant in South Korea. Utt and Giglio (2011) state that the Łagisza plant has been used to show the validity of Foster Wheeler's design of 4X500 MW_e CFBC units in South Korea, which are set for commission in 2015.

BFBCs are excellent solid mixer, capable of ensuring homogeneous operating temperatures and a good contact between coal, sorbent and the gas phase, although part of the gas tends to short-circuit the bed (Kovacs, 2001). To lessen this, bed height is increased which also increases the differential pressure across the bed. However, the bed height in BFBC expands to only one or two meters above the distributor. Combustion temperature in both systems is controlled by in-furnace cooling surfaces located in the furnace walls. For BFBC the cooling possibilities are limited to cooling by the furnace wall or in-bed cooling surfaces (Johnsson, 2007).

2.3.3 Advantages and Disadvantages

There are some advantages and disadvantages associated with FBC technology when compared with the conventional pulverised coal boilers. The advantages of FBC are as follows (Zhangfu Wu, 2003 and Kovacs, 2001);

- Bed temperatures are typically between 800 °C and 900 °C, above which ash may melt and form slag,
- The low operating temperature reduces NO_x formation,
- In-situ sulphur capturing with either limestone or dolomite can reduce SO_2 emissions,
- The turbulence of the fluidised mixture increases the rate of heat transfer between the particles and the water tubes, and
- A variety of fuels or fuel blends can be burned in the FBC boiler, including low-quality fuels with a high level of ash or moisture content.

The disadvantages and limitations of FBC include (Zhangfa Wu, 2003 and Kovacs, 2001);

- A relatively high pressure-drop is required to fluidise a bed of granular particles,
- Relatively large amounts of ash is generated (esp. with sorbent addition),
- The flue gas carries a high dust load,
- Higher carbon-in-ash levels,
- Increased N_2O formation due to the lower combustion temperatures, and
- Limited operating experience with fluidised bed combustors.

2.4 Coal Combustion in Fluidised Bed

Coal is a fossil fuel formed by the decomposition of plant matter under high pressure and at high temperatures over millions of years. Coal is composed of organic matter (macerals), mineral matter, moisture and some impurities. It is classified according to age or maturity (formation years) with the youngest coal called lignite, then sub-bituminous, bituminous and the oldest, anthracite. When coal is heated, its organic matter undergoes pyrolysis and evolves as volatiles. The residue solid, char, is made up of carbon and mineral matter. Coal combustion in principle is the combustion of carbon as well as the volatile matter (Shen, 2009).

For fluidised bed combustion systems, coal combustion involves the following steps (Zhangfa Wu, 2003);

- Drying (with or without shrinkage of the particles),
- Devolatilisation (with or without swelling and fragmentation),
- Combustion of volatile matter, and
- Combustion of the residual char particles.

These combustion steps are illustrated in Figure 2-6 below.

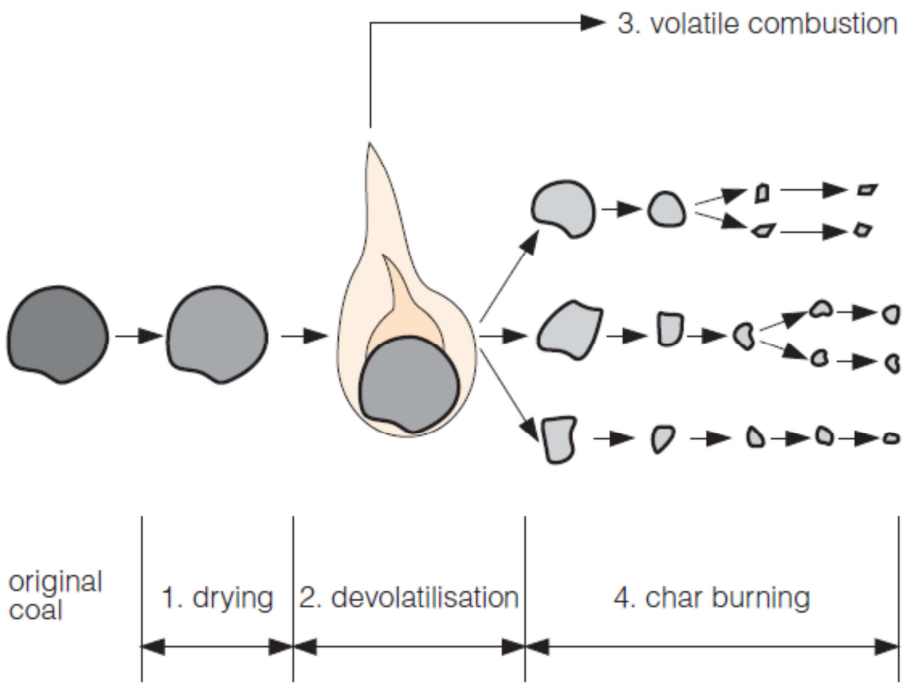


Figure 2-6: Coal Combustion in Fluidised Bed (Zhangfa Wu, 2003)

The result of these processes in an air-fired system is a gaseous exhaust (mainly CO, CO_2, SO_2, NO_x, N_2, O_2, and H_2O) and solid residues (mineral matter) composed mainly of clay, pyrite and calcite. The objective of this section is to create an understanding of coal combustion in a BFBC system.

2.4.1 Coal Drying and Devolatilisation

Upon entering a hot FBC furnace, the moisture in coal is evaporated as the initial step. Moisture in coal is present as both surface and inherent moisture, the former is evaporated first and the latter follows suit. The moisture content of coal can be as high as 70 % (as with

lignite), however the coal of interest in this work is bituminous coal and its moisture content is normally lower than 20 %.

During coal devolatilisation, the organic matter of coal is pyrolised and a variety of products such as tar, hydrocarbon gases, hydrogen, carbon monoxide, carbon dioxide and methane (Zhangfa Wu, 2003) is produced. The volatile matter content in coal varies from a few percentages up to 70 – 80 % (Shen, 2009). After coal drying and devolatilisation, a carbonaceous solid residue referred to as char remains.

2.4.2 Combustion of volatile matter

Shen (2009) states that gases released during coal devolatilisation are combusted in the presence of oxygen in a rapid process. The combustion reactions of some of the volatiles are listed by Zhangfa Wu (2003) as follows;

Combustion of carbon monoxide;

$$CO + {}^{1}/_{2}\, O_2 \rightarrow CO_2 \qquad \text{Equation 2-4}$$

Combustion of hydrogen

$$2H_2 + O_2 \rightarrow 2H_2O \qquad \text{Equation 2-5}$$

Combustion of methane

$$CH_4 + {}^{3}/_{2}\, O_2 \rightarrow CO + 2H_2O \qquad \text{Equation 2-6}$$

Combustion of NH_3

$$NH_3 + {}^{5}/_{4}\, O_2 \rightarrow NO + {}^{3}/_{2}\, H_2O \qquad \text{Equation 2-7}$$

$$NH_3 + {}^{3}/_{4}\, O_2 \rightarrow {}^{1}/_{2}\, N_2 + {}^{3}/_{2}\, H_2O \qquad \text{Equation 2-8}$$

The combustion of these gases provides the energy required to initialise the combustion of char.

2.4.3 Char Combustion

Shen (2009) stated that the residual char particles are often spherical, very porous and have many cracks due to coal devolatilisation. The burning of these residual char particles is the final stage in coal combustion.

Char contains carbon, mineral matter, nitrogen and sulphur and is oxidised at temperatures higher than the measured bed temperatures to forms gaseous products (CO, CO_2, N_2O, NO_x, and SO_2) and ash.

The principle char reactions for carbon are;

$$C + {}^{1}/_{2}\, O_2 \rightarrow CO \qquad \text{Equation 2-9}$$

$$C + O_2 \rightarrow CO_2 \qquad \text{Equation 2-10}$$

$$CO + {}^{1}/_{2}\, O_2 \rightarrow CO_2 \qquad \text{Equation 2-11}$$

$$C + CO_2 \rightarrow 2CO \qquad \text{Equation 2-12}$$

The principle reactions for nitrogen are;

$$N + {}^{1}/_{2}\, O_2 \rightarrow NO \qquad \text{Equation 2-13}$$

$$NO + {}^{1}/_{2}\, O_2 \rightarrow N0_2 \qquad \text{Equation 2-14}$$

$$N + NO \rightarrow N_2O \qquad \text{Equation 2-15}$$

The principle reaction for sulphur is;

$$S + O_2 \rightarrow SO_2 \qquad \text{Equation 2-16}$$

These reactions are slower than the combustion of volatile matter and their rate of reaction is affected by the coal types, unit operating pressure and temperature, oxygen level in the unit and the properties of char. Zhangfa Wu (2003) states that in fluidised bed combustion char particles continuously reduce in size due to char particle burnout, particle fragmentation and particle attrition. These leads to the formation of char fines and consequently char entrainment into the freeboard region. This entrainment also contributes to combustion inefficiency.

Nitrogen in the furnace comes from air and coal. The formation of thermal NO_x, from nitrogen in the air, is reduced to a minimum by the relatively low operating temperature associated with fluidised beds. Therefore NO_x and N_2O are primarily formed from the reaction of oxygen with the coal-bound nitrogen. The nitrogen in coal is present in both the volatile matter and char.

Sulphur in coal is oxidised to from sulphur dioxide. The emission of SO_2 is reduced when it reacts with calcium oxides (CaO) and/or with the calcium-magnesium oxide ($CaO.MgCO_3$) to form calcium-sulphates and/or calcium-magnesium compounds. In the absence of calcium based sorbent, the reactive char-bound calcium will react with some of the formed SO_2. The extent of sulphur-self retention depends on the amount of char-bound calcium and its reactivity.

2.5 Emissions from Fluidised Beds

Gaseous products from coal combustion have an impact on the environment. Large amounts of CO_2 are emitted, which has global warming impact. Substantial amounts of SO_2 are emitted, a precursor of fine particulate and acid rain. Significant amounts of NO_x (NO & NO_2) are emitted, which influences tropospheric ozone, methane formation, particulate and mercury formation (Shindell and Faluvegi, 2010).

The objective of this section is to review the formation of NO_x and SO_x, and the relevant reduction options.

2.5.1 NO_x and N_2O Emission

During devolatisation, nitrogen in the volatiles is released as ammonia (NH_3), hydrogen cyanide (HCN) and tar-nitrogen. These compounds will react in the presence of air to form mostly NO and small amounts of N_2O. However some of the volatile-nitrogen reduces to N_2. During char combustion, char-nitrogen oxidises in the presence of oxygen to form NO and N_2O. The principle reaction equations for nitrogen are shown in section 2.4. These reactions are shown pictorially in Figure 2-7.

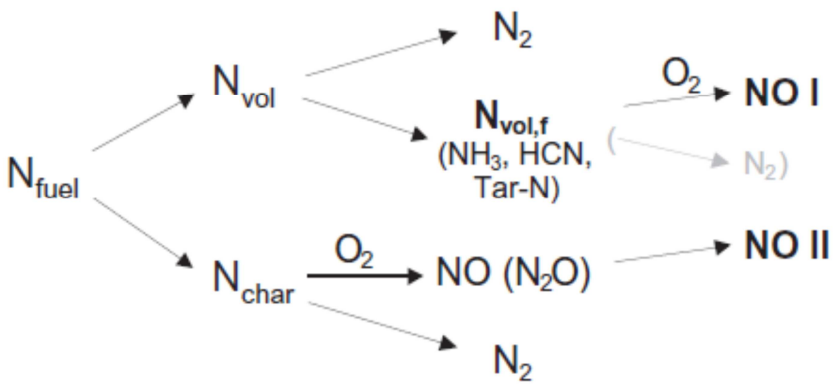


Figure 2-7: The formation pattern of NO in FBC (Konttinen *et al*, 2013)

The reaction involving the oxidation of NO to NO_2 is influenced by temperature and is limited by the low equilibrium concentration. Hence 90% of the NO_x in FBC exhaust gases is NO (Zhangfa Wu, 2003). The bed temperature, amongst other factors, has an impact of the amount of NO_x and N_2O in the exhaust gas. The low temperatures and other reducing conditions that are suitable for producing low NO_x have a contrary effect of increasing the production of N_2O emissions. N_2O is a global warming potential gas.

At temperatures of 800 °C – 900 °C, NO and N_2O reduce to form N_2, H_2O and CO in the presence of char, NH_3 and CO. The reduction reactions are shown by Zhangfa Wu (2003);

NO reduction by NH_3, CO and char;

$$NO + NH_3 + {}^1/_4\, O_2 \rightarrow N_2 + {}^3/_2\, H_2O \qquad \text{Equation 2-17}$$

$$NO + {}^2/_3\, NH_3 \rightarrow {}^5/_6\, N_2 + H_2O \qquad \text{Equation 2-18}$$

$$NO + Char \rightarrow {}^1/_2\, N_2 + CO \qquad \text{Equation 2-19}$$

$$NO + CO \rightarrow {}^1/_2\, N_2 + CO_2 \qquad \text{Equation 2-20}$$

N_2O reduction by temperature, char and CO;

$$N_2O \rightarrow N_2 + {}^1/_2\, O_2 \qquad \text{Equation 2-21}$$

$$N_2O + Char \rightarrow N_2 + CO \qquad \text{Equation 2-22}$$

$$N_2O + CO \rightarrow N_2 + CO_2$$ Equation 2-23

Konttinen *et al* (2013) conducted a study on the tendency of NO formation and concluded that the standard fuel analysis is not enough to provide the required inputs for NO emission predictions in large scale fluidized bed combustion. Their combustion test results show that the maximum cumulative conversion of fuel nitrogen to NO under lean, non-staged fluidized bed combustion is 20–50% (850 °C with O_2 in excess). Zhangfa Wu (2003) also states that the fuel N_2 that is converted to NO_x is between 5 % and 40 %, whereas less than 10% is converted to N_2O.

A study conducted by Valentim *et al* (2006) showed that SA coals produce higher NO and N_2O than their Columbian and USA counterparts. In their study, the authors showed that the emission of NO decreased for the vitrinite-rich coals (Columbian and USA) and increased for the inertinite-rich coals (SA) with increasing combustion temperature. N_2O emissions decreased with an increase in combustion temperature.

The reduction of NO and N_2O depends highly on the catalytic activity of coal ash and that of the sorbent (limestone or dolomite). This would affect the concentration of these species in the flue gas. The abatement of the emission of NO_x and N_2O can be achieved by employing staged combustion, or by installing well-established selectively catalytic reduction (SCR) or selective non-catalytic reduction (SNCR) technologies.

2.5.2 SO_2 Emission

During coal combustion, sulphur in coal is converted to SO_2 (Equation 2-16). The amount of SO_2 emitted is directly proportional to the amount of S in the coal. FBC technology has an advantage of capturing SO_2 in-situ by use of a calcium-based sorbent (limestone or dolomite). The sulphur capture reactions that occur in the FBC are (Anthony and Granatstein, 2001);

Calcination of limestone:

$$CaCO_3 = CaO + CO_2$$ Equation 2-24

Sulphation of lime:

$$CaO + SO_2 + {}^1/_2\, O_2 = CaSO_4$$ Equation 2-25

In pressurised system, limestone calcination does not occur. Sulphur capture is this type of system is governed by the following equation:

$$CaCO_3 + SO_2 + {}^1/_2\, O_2 = CaSO_4 + CO_2$$ Equation 2-26

Where a dolomite is used, calcination of the dolomite is as follows:

$$CaMg(CO_3)_2 = CaCO_3.MgO + CO_2$$ Equation 2-27

Sulphation of dolomite:

$$CaCO_3.MgO + SO_2 + {}^1/_2\, O_2 = CaSO_4.MgO + CO_2$$ Equation 2-28

In pressurised system, dolomite calcination does not occur. Sulphur capture is this type of system is governed by the following equation (Zhangfa Wu, 2003):

$$CaMg(CO_3)_2 + SO_2 + {}^1/_2\, O_2 = CaSO_4.MgO + 2CO_2$$ Equation 2-29

A degree of reduction is associated with the oxidation of some elements; the same is applicable to the reduction of some elements where a degree of oxidation will occur. Zhangfa Wu (2003) noted that C and CO have the potential to reduce $CaSO_4$ in the oxygen deficient bed zone at temperatures above 850 °C.

$$CaSO_4 + CO = CaO + SO_2 + CO_2$$ Equation 2-30

Calcination of limestone and dolomite is a process where the non-porous rock gets transformed into a porous calcite rock that would allow the diffusion of SO_2 into the CaO cleats and slits. Physical properties of the limestone or dolomite have an impact on the degree of sulphation that can occur. For limestone, the porosity can change from 0.3-12 % to over 50 % (Zhangfa Wu, 2003).

Sulphation will continue to happen in the calcined limestone or dolomite until the pores are blocked with $CaSO_4$, thus impeding the diffusion of SO_2. Therefore sorbent utilisation in FBC technologies is typically lower than 50%. Sorbent utilisation has no relationship to chemical composition, except for a week catalytic effect of iron oxide on reactivity (Zhangfa Wu, 2003).

Furthermore, the effectiveness of the reaction between SO_2 and CaO depends on the ability of SO_2 to diffuse into the particle through $CaSO_4$ on the surface and in the pores of the limestone/dolomite as displayed in Figure 2-8. Therefore the notion that the maximum sulphur capture efficiency is approximately at 850 °C might not generally be valid (Anthony and Granatstein, 2001).

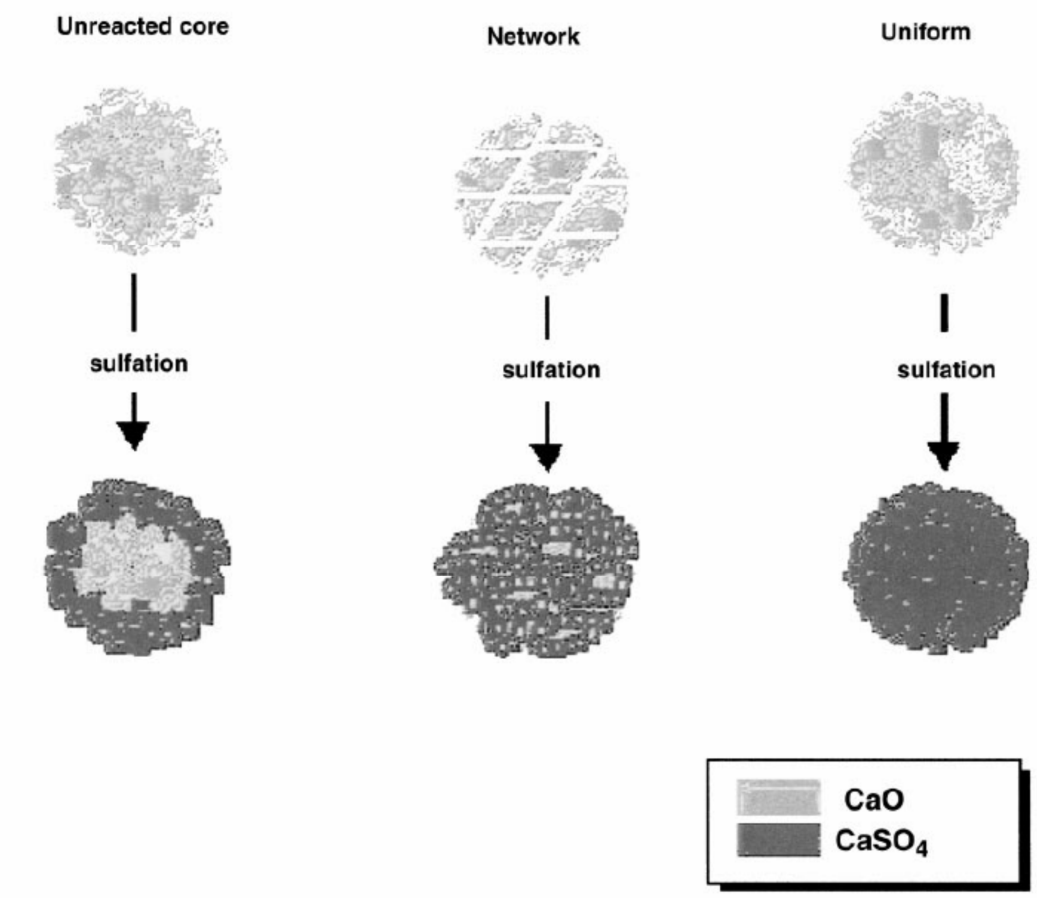


Figure 2-8: Sulphation patterns (Anthony and Granatstein, 2001)

2.6 Mineralogy and Chemistry of Fluidised Bed Ashes

During coal combustion, fly-ash is produced as a by-product of the process. The finely divided fly ash particles, solidify while suspended in the exhaust gases and are collected by the de-ashing systems employed in the plant. The physical, chemical and mineralogy characteristics of fly ash can vary greatly and will mainly depend on the combustion method and coal properties used at a particular power plant (Pando et al, 2006). Primary factors that influence the mineralogy of coal fly ash are;

- Chemical and mineral composition of coal,
- Coal combustion processes including coal pulverisation, combustion, flue gas clean up, and fly ash collection operations, and
- Additives used, including oil additives for flame stabilization and corrosion control additives.

Fly ash from FBC differ from that of conventional pulverised coal-fired combustion operations; the main differences result from different combustion temperatures and differing systems of desulphurisation (in-situ/post-combustion). Both these factors influence the chemical and phase compositions as well as the speciation of trace elements (Sulovsky, 2002). The addition of calcite sorbents to capture sulphur dioxide in-situ also influences the mineralogy and chemistry of FBC fly ash. This section discusses the mineralogy and chemistry of fly ash attained from fluidised bed combustion.

2.6.1 Analyses of Coal and Fly Ash

To understand the mineralogy and chemistry of fly ash, it is important to understand the mineralogy and chemistry of the parent coal. As noted above, the chemical composition of coal influences the mineralogy and chemistry of fly ash.

Alphen (2005) stated that proximate (ash, volatiles, inherent moisture, and fixed carbon) and ultimate (carbon, hydrogen, nitrogen, sulphur and oxygen) are routine analyses for coal, and that elemental analysis (Si, Al, Fe, Ca, Mg, Na, K, P, Mn and S) is used extensively to determine the slagging propensity of coal, mineral composition and fly ash composition.

Falcon and Snyman (1986) noted that the organic composition of coal which relates to maceral quantification (a petrographic analytical technique) is used to determine the rank and

reactivity of coal. Macerals may be grouped or counted individually, with vitrinite, liptinite, exinite and inertinite quantified according to their reflectance measurement. Maceral quantifications are carried out by use of a reflected light optical microscope at a total magnification between 250 and 500. Singh (2011) found that the Quantitative Evaluation of Materials by Scanning Electron Microscope (QEMSCAN) can also be used to quantify macerals. This method uses elemental proportions (sulphur, carbon and oxygen values) to achieve this.

2.6.2 Mineralogy of Fly Ash

Fly ash consists mainly of stone (aluminosilicate and quartz), pyrite cleats (iron oxide), calcite/dolomite cleats (calcium oxide and calcium magnesium oxide), and molten ash spheres. Other elements; such as magnesium, potassium, sodium, titanium and sulphur; are also present to a lesser degree.

The mineralogy of fly ashes from conventional coal-fired plants are relatively well known, although mostly on bulk level, while FBC products (bottom ash, fly ash) are known to a much lesser degree (Sulovsky, 2002). The difference between the mineralogy and chemistry of conventional pulverised coal-fired and FBC ashes for the two systems are shown in Table 2-3.

The mineral matter composition of coal controls the mode of occurrence of some of these potentially hazardous minerals whose concentration levels increase due to combustion of coal. The differences between fly ashes from the different combustion systems, is a result of the different burning temperature and the sulphur removal method used as shown by the distinct difference in Table 2-3. These minerals are responsible for the sintering and slagging of ash in boilers.

The lower operating temperature experienced in FBC application prevents the devolatilisation of certain minerals. This influences the mineralogy and composition of FBC fly ash, which is slightly similar to that of coal, and creates residues enriched in potentially hazardous elements. However, the addition of calcite sorbent neutralises the acidity of the residue by forming insoluble compounds with the hazardous elements (Sulovsky, 2002).

Table 2-3: Summary of the difference between conventional combustion ashes and FBC ashes (Sulovsky, 2002)

Factor or Process	Conventional combustion	Fluidised bed combustion
Usual combustion temperature	1400 – 1500 °C	820 – 850 °C
Coal grain heating rate	1 °C.s^{-1}	1000 °C.s^{-1}
Furnace retention time	Seconds	➢ 20 minutes
Input material	Coal	Coal + additive
Mineral melting/glass formation	Massive	Scarce
Volatilisation	Hg, Se, Pb, ZnO, $Ba(OH)_2$, As_2O_3 etc	None
Ash grain forms	Globular, rounded	Irregular, rather sharp-edged
Grain size	Smaller that original	Original
Thermal metamorphism	Strong	Weaker
Recrystallisation	Abundant	Scarce
Mineral neoformation	Massive, many species	Massive, limited to few species
Change of trace element bonding	Massive	Limited
Major phases	Glass, mullite, anortite, quartz, cristoballite, magnetire and other spinels, gehlenite	Haematite, quartz, metaillite, metakaolinite, anhydrite, perislase, lime, portlandite
Prevalent Fe oxide	Magnetite	Haematite
Amorphous phases	Glass	Metaillite, meakaolinite
Neoformation of mineral phase	Extensive, may phases	Extensive, few phases (anhydrite, mete-clays)
Changes in PHE speciation	Distinct	Limited
Concentration of volatile elements	Lower (major portion escapes with flue gas)	Higher (up to 95% of the amount present in coal
Surface enrichment	Pronounced, higher	Visible, lower

Matjie (2008) mentions that fly ash particles fuse and crystallise to form slag deposits, vaporises and condenses to form deposits and interacts with each other or internal boiler components to produce corrosion. However it is the high concentrations of alkali elements in mineral matter that are responsible for slagging and fouling at elevated temperatures higher than 1000 °C (Matjie, 2008 & Alphen, 2005). These and other minerals decompose and melt at different temperatures as shows in Table 2-4.

Table 2-4: Decomposition and Melting Temperatures of selected minerals found in coal and fly-ash (Matjie, 2008)

Minerals	Composition	Decomposition[(d)] and Melting points (°C)
Kaolinite	$Al_2Si_2O_5(OH)_4$	800-1000[d], 1810
Illite	$K_{1.5}Al_4(Si_{6.5}Al_{1.5})O_{20}(OH)_4$	400-1167[d], 1200-1350
Pyrite	FeS_2	800[d], 1171
Apatite	$Ca_5F(PO_4)_3$	>1230
Calcite	$CaCO_3$	925[d]
Dolomite	$CaMg(CO_3)_2$	775[d]
Siderite	$FeCO_3$	525[d]
Quartz	SiO_2	1710
Anhydrite	$CaSO_4$	1450
Lime	CaO	2570
Haematite	Fe_2O_3	1567
Magnetite	Fe_3O_4	1592
Mullite	$Al_6Si_2O_{13}$	1850

During coal combustion the minerals identified in Table 2-4 will either decompose or melt to form other materials, or they do not change form. A summary of the actions that occur during coal combustion are listed below (Matjie, 2008);

- Quartz do not change form nor react,
- Kaolinite and illite decompose to form mullite, silicon and aluminium compounds, and hydroxyl water,
- Calcite and Dolomite decompose to form lime and CO_2, lime consequently reacts with SO_2 and water depending on the temperature to form anhydrite and portlandite ($Ca(OH)_2$) respectively, and
- Pyrite decomposes into haematite, magnetite and sulphur compounds.

These minerals form the basis of fly/bottom ash, and depending on the melting points of the different minerals, they can cause ash deposition and slagging. The occurrence of these minerals in coal and fly/bottom ash can be quantified by applying various mineralogy assessment techniques.

Alphen (2005) compared different mineralogy assessment techniques and found that the Coal Characterisation Scanning Electron Microscope (CCSEM) was the method used by the

majority of coal scientists and engineers to quantify and identify minerals in coal and phases/minerals in fly ash and slag deposits.

Alphen (2005) also cited the round robin tests of Galbreath *et al* (1996) where North American coals were sent to different laboratories using different SEM instruments for mineral quantification. Their results resolved that the QEMSCAN gave the most precise analytic results.

French and Ward (2009) studied the applicability of QEMSCAN to examine mineral distribution and mineral association, and provided information to assess ash behaviour in FBC plants. The mineralogy of the bottom ash, economiser ash and fly ash were found to be similar. The ash was composed of calcite, lime, portlandite, aluminosilicate, calcium sulphate, quartz and other amorphous components. The study concluded that QEMSCAN provides unique information not readily obtainable by other techniques. More particular, data can be obtained on particle size and shape, phase identification and abundance, as well as the mode of occurrence and association of the identified phases (French and Ward, 2009).

The QEMSCAN is an integrated system designed by CSIRO, Australia, and was originally designed to service the base and precious metal mining industry and not the coal industry. Mineral identification is based on elemental proportions, elemental ratios and the type of elements present. Mineral identification rules are determined by acquiring standard X-ray spectra of the minerals in coal and the phases in fly ash. QEMSCAN can also determine the organic component of coal (Alphen, 2005).

The QEMSCAN can provide data on mineral or phase proportions, oxide elemental composition, associated characteristics of minerals in coal and phases in fly ash, size variation of the different minerals, and elemental deportment, and the proportion of included minerals compared to that of excluded minerals.

2.7 South African Perspectives on BFBC

The work on FBC in South Africa started in the 1970's with research focused on the combustibility of low grade coal (duff coal, discard coal and fine coal) in the BFBC boilers (Petrie, 1985). Research later focused on the use of limestone or dolomite to reduce the associated emissions of SO_2. The technology has been put to minimal use within South

Africa for electricity generation, it has been utilised by some industries to incinerate waste, biomass and co-fire coal for different applications, but it hasn't been installed for large-scale electricity generation in South Africa.

Aziz and Dittus (2011) evaluated suitable technology for Kuyasa Mining and also provided a CFBC conceptual design for the planned 4 x 150 MW_e boilers. They selected a CFBC as a suitable boiler for Kuyasa Mining and established a key advantage over the conventional pulverised coal-fired boilers as fuel-flexibility and the ability to combust discard coal. Seeing that South Africa is under immerse pressure to increase its generating capacity, plants like the CFBC planned for Kuyasa will be play a crucial role to ease the stress on the electricity grid.

Anglo American is also in the process of procuring a 3 x 150 MW_e CFBC plant that will be located in the south of Emalahleni in Mpumalanga, South Africa (Hall *et al*, 2011). This Khanyisa plant will utilise discard coal from the surrounding mine dumps. To reduce the cost related to limestone usage, the feed coal will be beneficiated to reduce sulphur and ash content. These CFBCs are set for commission in 2015 (Hall *et al*, 2011).

Moodley (2007) tested the performance of South African discard coals in the presence of a sorbent in a pilot scale BFBC. The aim was to assess the changes in gaseous emissions and the combustion efficiency of the coal, intended to provide information on possible coals and sorbents for any future built FBC based power station.

North (2010) evaluated a range of fuels in a pilot scale BFBC facility. These fuels were; high ash discard coals, high fines duff coals, high water content slurry coals and biomass sludge (for co-firing). It was concluded that discard coal can be burnt at good thermal and combustion efficiencies and that the FBC is capable of incinerating a wide range of opportunity fuels.

Botha *et al* (2011) reported that a FBC reactor in Kwa-Zulu Natal utilising sewage sludge has been operating since 2000 and is in compliance with the emission standards set by the DEA. The facility employs a drier to dry some of the sewage sludge and it supplies this to the FBC in pellet form as a supplementary fuel, to maintain the bed temperature at 850 °C. Lessons learned from the operation of the facility have concluded that waste energy recovery for electricity generation is a viable option for South Africa.

Table 2-5: Some Applications of FBC in Southern Africa (North, 2012)

Plant	Type	Feedstock
AECI Modderfontien	BFBC	C-Rich Fly Ash, coal
Mondi Merebank	BFBC	Waste, bark, sawdust, flyash, coal, SASOL gas
Slagment	BFBC	Duff coals, Organic Waste
Eastcourt KZN	BFBC	Coffee Ground
SASOL	BFBC	High S Pitch
Phalaborwa Mining Co.	BFBC	Coal
FBC HGGS	BFBC	Waste, bark, sawdust, flyash, coal, SASOL gas
SAPPI Tugela	BFBC	Wood waste, coal
Mondi Merebank	BFBC	Wood,waste, coal and gas
Soda Ash Botswana	BFBC	Coal

North (2012) noted a number of FBC application in Southern Africa, Table 2-5 groups the finding in his study. Babcock Engineering has been the leading supplier of BFBC boiler in Southern Africa.

Pilot scale fluidised bed research facilities exist at the CSIR, Eskom, Mintek (primarily for minerals treatment), SASOL (for Fischer-Tropsch reaction research), and various universities (North, 2012).

2.8 Summary

Literature reports that coal combustion in an FBC boiler occurs in four steps; drying, devolatilisation, volatile combustion, and char combustion. These operations are influenced by temperature, pressure, excess air and fuel concentration within the bed. In the current research, these parameters will be monitored and at times kept constant to eliminate discrepancies between coal combustion tests.

FBC has been shown to be capable of burning a variety of fuels (biomass, domestic waste, industrial waste, duff coals, discard coals, lignite and all other coals) with reduced NO_x and SO_2 emissions. In the current research BFBC tests with and without sorbent addition will be carried out to assess how these emissions behave.

Lower carbon efficiency, N_2O formation and large amounts of ash have been reported to be some of the negative factors associated with FBC operations. N_2O emission and carbon

efficiency attained during the current tests will be compared to values from conventional pulverised coal-fired plant to assess this disadvantage for South African coal.

It has been shown that vitrinite-rich coals emit less NO and N_2O than inertinite-rich coal. However the production of NO increases with increasing temperature and that of N_2O decreases with increasing temperature. The test work will assess the validity of this statement for South African coals.

Literature has also proved that when a calcite sorbent is added for sulphur capturing, its utilisation factor is lowered by $CaSO_4$ formed, blocking the pore and cleats on the calcite sorbent particles, thus impeding the diffusion SO_2. Sorbent utilisation is lower than 50 % and is assumed to be at a maximum at a temperature of 850 °C. This too will be tested in the current research.

The mineralogy of ash has been reported as being influenced by coal composition, combustion technology, and combustion additives. Therefore the mineralogy of the coals and sorbent, together with that of the fly ash of the current samples will be determined to assess these influences as well as look at the conversion of reaction of various elements in the coals and sorbent.

Literature has reported that the composition of ash from FBC is different from the ash found in conventional pulverised coal-fired boilers. This is due to the difference in operating temperature and the desulphurisation method. This too will be verified in the current research.

In summary, numerous BFBC plants have been installed in South Africa for different applications; i.e. hot gas generation, process steam, waste incineration, and so forth. But none of the installations are for large scale electricity generation. Kuyasa Mining has conducted a conceptualised design of a possible CFBC power plant using discard coal. This would the first large scale FBC plant generating electricity in South Africa. However, no detailed test work on actual coal combustion performance and emissions of South African coals burnt in large pilot scale plant have been reported as yet. For these reasons, the current research may be considered the first attempt at undertaking such detailed research into the performance of such high ash, low grade coals including discards for large scale BFBC power generation.

CHAPTER 3 : METHODOLOGIES

3.1 Introduction

To thoroughly assess South African type coal in a bubbling fluidised bed combustion testing facility, experimental tests and analytical assessment were conducted on selected coals, sorbent and combustion products. The techniques applied in this dissertation are detailed in this chapter. The facility utilised to conduct the combustion tests is also described in this chapter.

3.2 Selected Coals for Testing

Three coals from the Waterberg and Highveld regions were selected for this research.

- Coal A: A typical high-ash power station coal from the Highveld region
- Coal B and C: Discard coals from the Waterberg region, extracted from the same basin but different seams.

3.3 The BFBC Testing Facility

3.3.1 Overview of the testing facility

The BFBC testing facility is a Bharat Heavy Electrical Ltd (BHEL) bubbling fluidised bed design which can be operated as either a combustion reactor or a gasification reactor by removing the in-bed cooler used during combustion and replacing it with a refractory plug. This FBC/G design is a pressurised system, which can be operated at pressures ranging from 12 kPa up to 300 kPa. The reactor is a seven meter high-refractory lined pressure vessel, with a bed zone region that has a diameter of 230 mm and a freeboard region that expands to a diameter of 360 mm. Figure 3-1 shows an illustration of the BFBC reactor.

The illustration in Figure 3-1 shows the entry point of the fluidising air, the coal and the sorbent. It also shows the exit point of the gaseous products, the fly ash and the coarse ash. Also shown in the illustration is the bed-zone region which has six thermocouples that measure bed temperature and three pressure differential instruments used to calculate the bed depth during testing. The freeboard region has four thermocouples with the last located at the

exit point. These thermocouples are instrumental in controlling the reactor temperature as well as profiling the reactor temperature. A heat exchanger (in-bed coil) is also shown as an integral part of temperature control in the bed region.

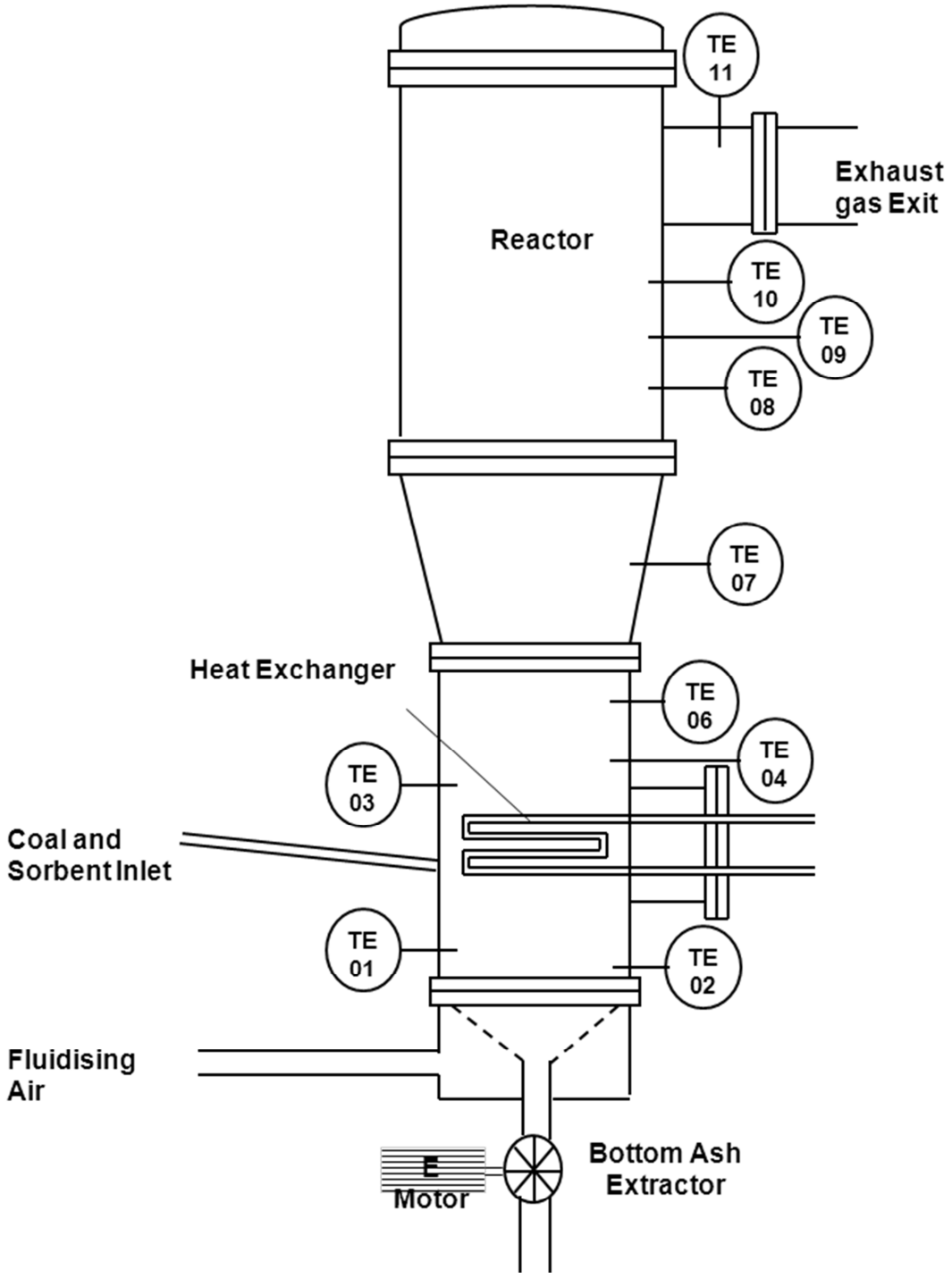


Figure 3-1: Illustration of the BFBC Reactor

The reactor is the heart of any process plant; however it is complimented by interlinking process units that aid in achieving the purpose of the plant. Figure 3-2 shows an illustration of the BFBC inclusive of the auxiliary units that make coal combustion tests in the facility materialise.

The reactor has downstream and upstream processes that complement the operation of the BFBC reactor. Upstream processes like the coal preparations unit, the coal and sorbent pressure lock feeding system, the air compressor and air conditioning system ensure that the operating conditions as per design or per test requirements are accomplished. The coal preparation unit is a stand-alone unit and has not been shown in Figure 3-2. Downstream processes like the solid-gas separator, gas clean-up unit and the stack ensure that the pilot plant is environmental friendly/competent. Other essential downstream processes like the gas-sampling and analysing system and the fly-ash sampling system ensure that adequate test data and test chemistry is accounted for during the data evaluation session post the tests.

The plant is also equipped with pressure, flow and temperature indicators and readers which are displayed in the on-line DSP system installed in the control room. Pictures taken from the DSP display unit depicting some of the upstream and downstream processes are shown below in Figure 3-3 and Figure 3-4

Figure 3-3 shows the coal, sorbent and air injection arrangement. Air from a compressor is stored in the air header (max 400 kPa) and passes through a 37 kW electric air heater where an exit temperature of 300 °C is kept during testing. For research purposes the system was designed with ad-hoc oxygen header and steam generator. The coal and sorbent feeding systems each have 50 kg silos equipped with double air-lock systems to create a pressure barrier between the pressurised BFBC and the atmosphere. The prepared solid feeds are manually fed into the silos and discharged from the second air-lock by a variable speed drive controlled volumetric feeder. These solids are pneumatically conveyed into the reactor with pressurised air at a set velocity to eliminate settling of the solid along the pipes. The solids can either be fed into the bed or just above the bed height.

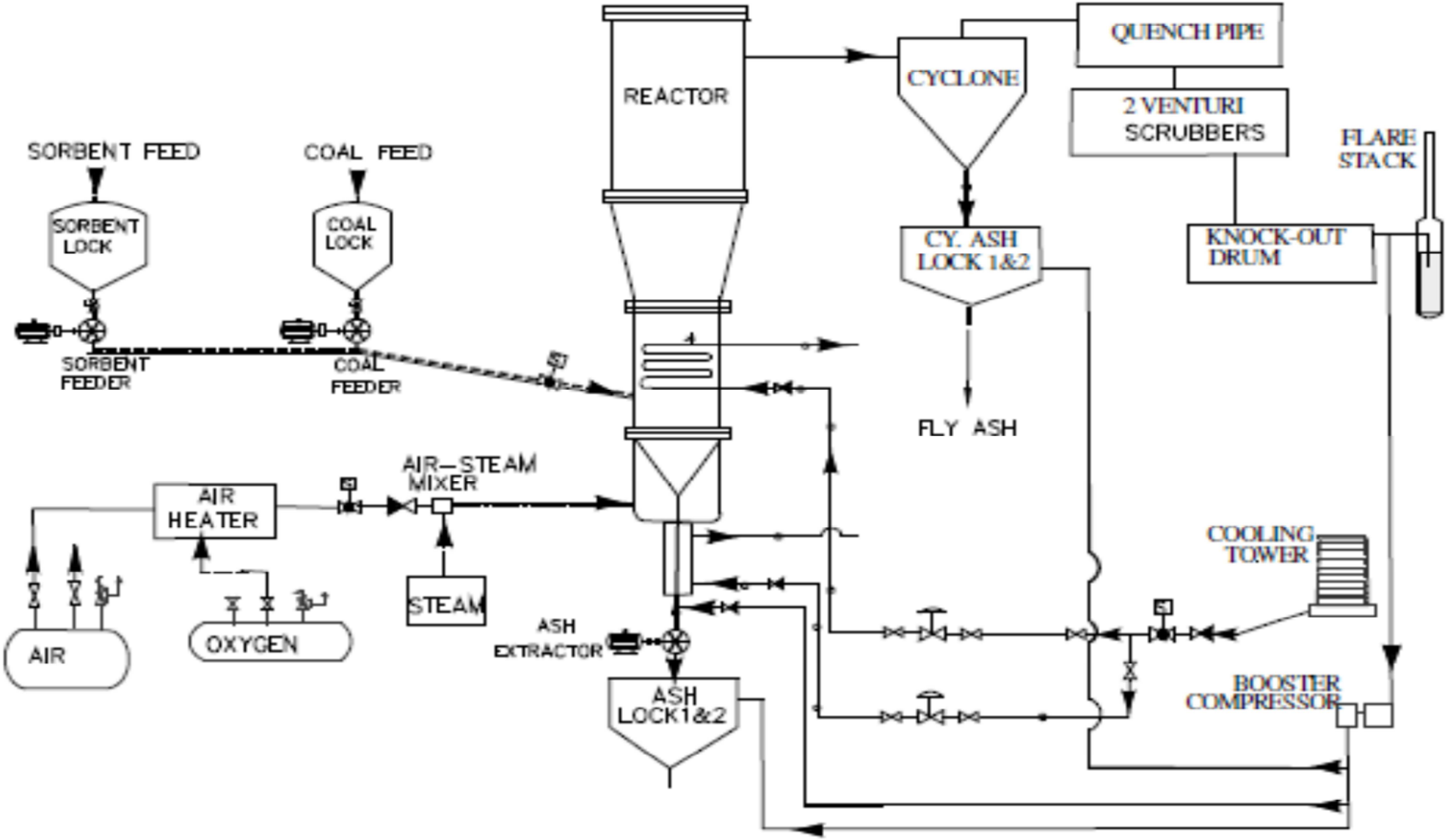


Figure 3-2: Schematic of the Bubbling Fluidised Bed Combustion Testing Facility

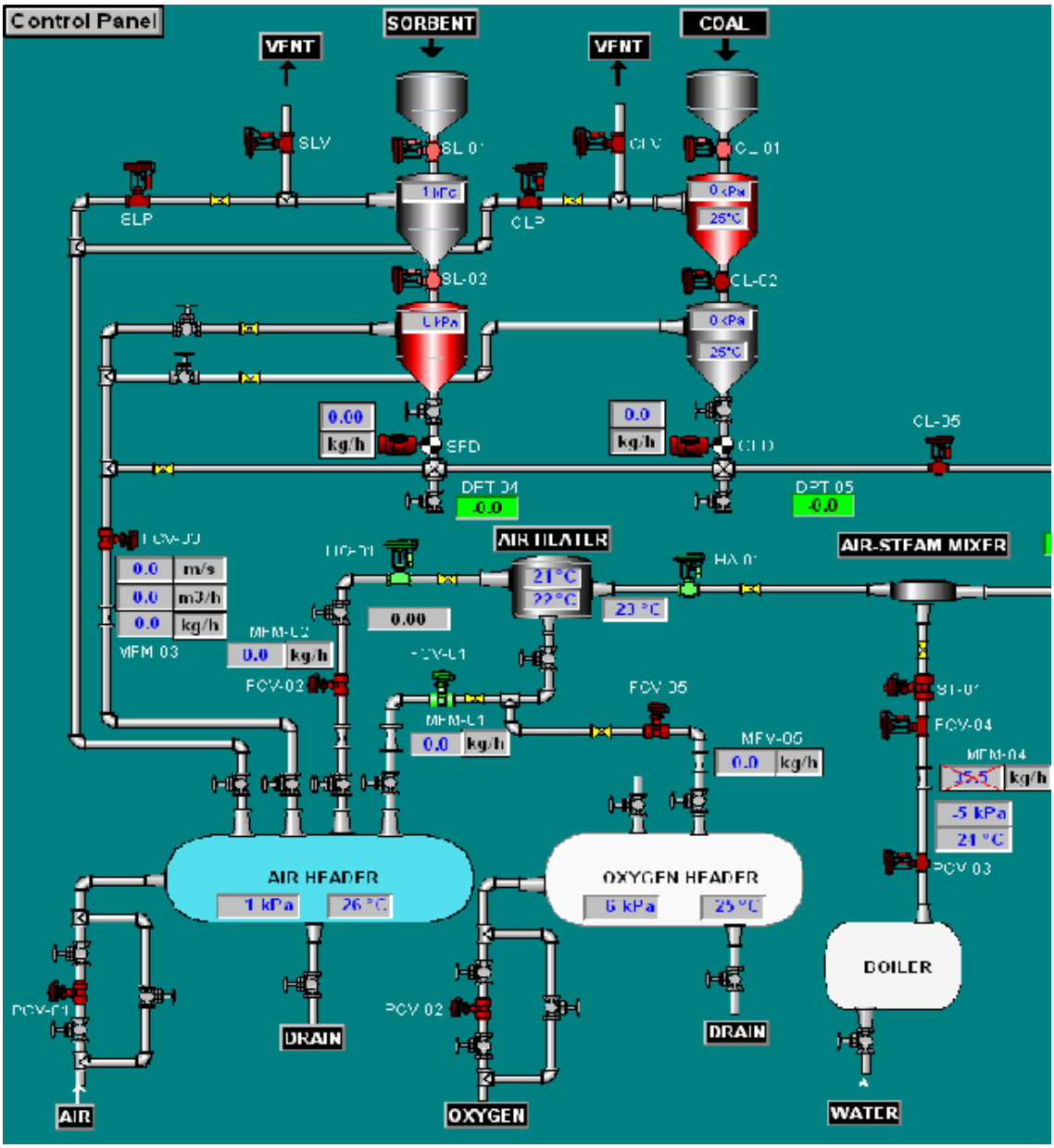


Figure 3-3: Control Panel Picture of the BFBC system

To maintain pressure in the reactor the coarse ash and fly-ash removal systems are also equipped with the double air-lock system as shown in Figure 3-4. Figure 3-4 also shows the solid-gas separator unit, the cyclone, where gas produced in the reactor leaves the cyclone at the top and the fly-ash at the bottom. A gas sampling system is installed on the gas duct after the cyclone to condition the sampled gas prior to being analysed by the online gas analysers.

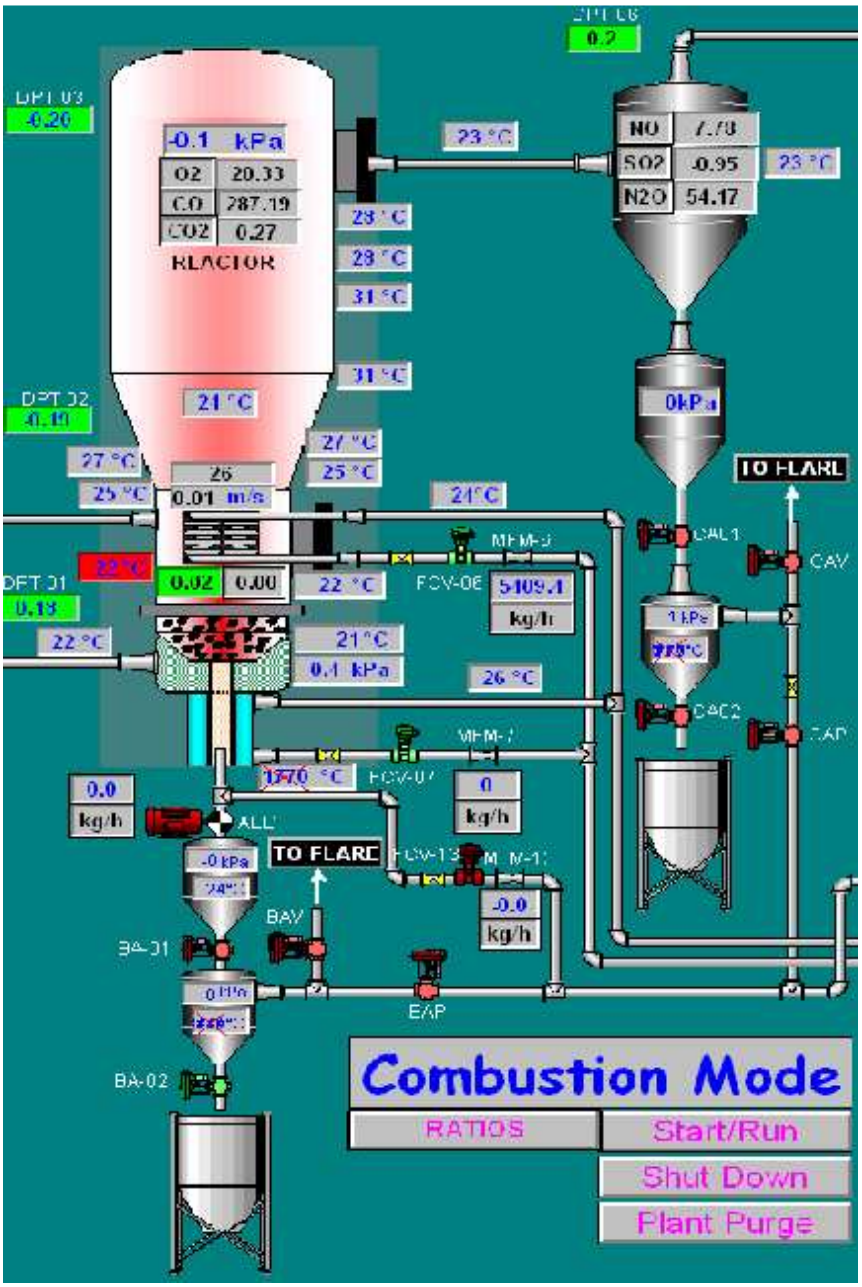


Figure 3-4: Control Panel Picture of the reactor, gas-solid separator and the ash removal system.

The reactor is shown in Figure 3-4 with the location of the temperature and differential pressure sensors and transmitters, the inlet points, the in-bed coil and the gas exit point. A gas-solid separator is used to remove particulates from the fly ash and is instrumental is obtaining fly ash samples during coal combustion test.

3.3.2 Testing Methodology

The operation of the pilot plant is systematically arranged to cover all aspect of the plant to ensure that the plant is not prone to problems whenever it is operated. The OEM provided operating manuals that describe the steps to be adhered to every time the plant is operated. These steps are; pre-start checks, reactor pre-heat, coal and sorbent testing, and plant shut-down. However this sub-section details the coal and sorbent testing procedure only, as adopted and modified for the purpose of this dissertation.

The preceding steps to the combustion tests are very important to the integrity of the tests; if there is air leakage the gases might not balance, and if the right temperatures are not reached combustion might be affected. Once these steps are complete, then the tests can commence. Firstly test coal is loaded into the silo and then it is injected into the reactor to begin testing. Test conditions are determined from the chemical analysis of the coal and sorbent, and the test matrix as tabulated in Table 3-1.

The matrix in Table 3-1 indicates that a baseline test for each coal is required to be able to compare results for each of the coals. The baseline test is also conducted without limestone to assess the capability of sulphur-self capturing. Further tests are conducted at different calcium to sulphur (Ca/S) molar ratio to evaluate the extent of sulphur in-situ capturing and also to assess the impact sorbent injection on the other operating parameters.

To maintain the same base and eliminate potential discrepancies, a generic testing procedure was adopted,

- Ensure the correct coal and sorbent are in the hoppers,
- Set the coal and sorbent feeder rates as per the test matrix
- Control the flow of water through the bed coil to ensure the right bed temperature as per the test matrix is achieved,
- Allow the system to stabilise before commencing with test,
- Clear the cyclone and the fly-ash lock system to eliminate contamination in the sample,
- Once the system is stable (gaseous species and temperature trends should constant), commence test and capture the following data (reactor pressure, differential pressure, temperature, flowrates and gas species) manually, and

- At the end of each test, clear the cyclone and obtain a sample of fly-ash for analysis.

This procedure is repeated for each test and a systematic approach is followed at all times. The duration of the each test is about 30 minutes, this exclude the time it takes the reactor to stabilise.

Table 3-1: The Test Matrix for Coal A, B and C with and without Limestone

	Units	Test 0.1	Test 0.2	Test 0.3	Test 0.4	Test 0.5	Test 0.6	Test 0.7	Test 0.8	Test 0.9
Coal										
Coal A										
Coal B										
Coal C										
Sorbent										
Limestone										
Molar Ratio										
Ca/S		0	0	0	1	1	1	2	2	2
Bed Temperature										
830	^{0}C			X			X	X		
850	^{0}C		X		X				X	
870	^{0}C	X				X				X
Coal Flow	kg/hr	8,00	8,00	8,00	8,00	8,00	8,00	8,00	8,00	8,00
Sorbent Flow	kg/hr	0,00	0,00	0,00	0,40	0,40	0,40	0,79	0,79	0,79

		Test 1.1	Test 1.2	Test 1.3	Test 1.4	Test 1.5	Test 1.6	Test 1.7	Test 1.8	Test 1.9
Coal										
Coal A										
Coal B										
Coal C										
Sorbent										
Limestone										
Molar Ratio										
Ca/S		0	0	0	1	1	1	2	2	2
Bed Temperature										
830	^{0}C	X					X	X		
850	^{0}C		X			X			X	
870	^{0}C			X	X					
Coal Flow	kg/hr	8,50	8,50	8,50	8,50	8,50	8,50	8,50	8,50	8,50
Sorbent Flow	kg/hr	0,00	0,00	0,00	0,70	0,70	0,70	1,50	1,50	1,50

		Test 2.1	Test 2.2	Test 2.3	Test 2.4	Test 2.5	Test 2.6	Test 2.7	Test 2.8	Test 2.9
Coal										
Coal A										
Coal B										
Coal C										
Sorbent										
Limestone										
Molar Ratio										
Ca/S		0	0	0	1	1	1	2	2	2
Bed Temperature										
830	^{0}C	X			X			X		
850	^{0}C		X			X			X	
870	^{0}C			X			X			X
Coal Flow	kg/hr	8,50	8,50	8,50	8,50	8,50	8,50	8,50	8,50	8,50
Sorbent Flow	kg/hr	0,00	0,00	0,00	0,59	0,59	0,59	1,18	1,18	1,18

3.3.3 Gas Analysers

The gas sampling system is equipped with a filter and line heaters to maintain gas temperature at 180 ℃, and a Peltier drier to remove the moisture and cool the gases to 40 ℃ as per the upstream requirements of the online analysers.

The online analysers are calibrated as per OEM requirements and verified for accuracy before the tests commence. Verification gases were used to verify the analysers. These on-line analysers measure O_2, CO, CO_2, N_2O, NO, NO_2 and SO_2 on a dry basis.

3.4 Laboratory Analysis

The raw coals utilised during the experimental work described above were subjected to chemical analysis. The samples were prepared according to SABS 0135 Part II – 1977. The analyses tabled in Table 3-2 were carried on the coal samples.

Table 3-2: Chemical Analysis require for coal

	Units	Standard
Proximate Analysis		
Inherent Moisture	%	SABS 925
Volatile Matter	%	ISO 562:1998
Ash Content	%	IS0 1171:1997
Fixed Carbon	%	By difference
Ultimate Analysis		
Carbon	%	ISO 12902
Nitrogen	%	ISO 12902
Hydrogen	%	ISO 12902
Total Sulphur	%	IS0 351
Oxygen	%	By difference
Gross Caloric Value	MJ/kg	SABS ISO 1928

Fixed carbon is calculated by subtracting the sum of the inherent moisture, ash and volatile matter from 100.

Fixed carbon (%) = 100 - (inherent moisture + ash + volatile matter). Equation 3-1

Oxygen was calculated as a difference from 100 by the sum of the inherent moisture, ash, carbon, hydrogen, nitrogen, total sulphur and carbonate.

Oxygen (%) = 100 - (inherent moisture + ash + carbon + hydrogen + nitrogen + total sulphur + carbonate) Equation 3-2

Sorbent, coals and fly-ash samples were subjected to non-destructive analysis using the X-ray Fluorescence (XRF) detection method and the QEMSCAN. For XRF analysis, a bead for every sample was prepared by mixing 1 gram of the sample with 9 grams of lithium flux. The XRF technique employed provides the following ash elemental analysis; silicon (as SiO_2), aluminium (as Al_2O_3), iron (as Fe_2O_3), titanium (as TiO_2), phosphorus (as P_2O_5), calcium (as CaO), magnesium (as MgO), sodium (as Na_2O), potassium (as K_2O), sulphur (as SO_3), and manganese (as MnO). These are oxides; therefore coal and sorbent samples were initially ashed prior to preparing the bead.

The coals, sorbent and the fly-ash were also subjected to mineralogical analysis to obtain the mineral content of the coals as well as that of the fly-ash. The QEMSCAN was utilised for this function. It is routinely used to determine the mineral and phase proportions in coal, fly ash and clinkers. Carnauba wax polished sections were prepared for QEMSCAN analysis. The following data were obtained from QEMSCAN analysis;

- Mass-% mineral or phase proportions in pulverised fuel or fly ash, respectively.
- Association characteristics of minerals in coal and phases in fly ash.
- Elemental behaviour
- Proportion of included minerals compared to proportion of extraneous minerals

3.5 Computational Methods

Results herein are computed on the basis of test data (temperature, mass flowrate, pressure, (gaseous emissions), coal and sorbent analysis (proximate, ultimate, ash elementals and mineralogy assessment), and fly ash analysis (ash elemental and mineralogy assessment).

3.5.1 Gas Species

The calculations related to the normalisation of gas species measurements to 6 % O_2 and converting to mg/Nm^3 at 6 % O_2, and the calculations related to determining the amount of sulphur retentions was discussed by Moodley (2007). An example of these calculations is shown in Appendix F.

In essence the gas readings are normalised to 6 % O_2,

$$X_{i,ppm\ at\ 6\%02} = \frac{X_{i,ppm\ at\ actual\ O2}}{1+\left(\frac{6-O_{2,actual}}{20,95-6}\right)} \quad \text{Equation 3-3}$$

Then converted to mg/Nm^3 at 6 % O_2,

$$X_{i,mg/Nm3\ 6\%} = X_{i,ppm\ at\ 6\%02} \times \rho_i \quad \text{Equation 3-4}$$

where ρ_i is the gas component's density at the specified temperature and pressure.

For sulphur capturing, the following process was followed. Theoretical SO_2 emission is determined from coal flowrate and sulphur content.

$$\dot{m}_{theoSO2} = \dot{m}_{coal} \times n_{S\ in\ coal} \times 2 \quad \text{Equation 3-5}$$

The gas analysers and the coal analysis results, and air mass fractions are used to determine the total gas mass by firstly converting the volume fractions into mass unit.

$$m_i = v_i \times M_{molar,i} \times 100 \quad \text{Equation 3-6}$$

Ultimately adding the mass units together to obtain the mass of gas in equation 3-7

$$m_{gas\ mass} = m_{CO} + m_{CO2} + m_{NO} + m_{NO2} + m_{N2O} + m_{SO2} + m_{N2} +$$

$$m_{O2} + m_{H2O} \quad \text{Equation 3-7}$$

Then the mass fraction of SO_2 in the gas is determined

$$X_{mass\%SO2} = m_{SO2} \div m_{gas\ mass} \times 100 \quad \text{Equation 3-8}$$

In the absence of flue gas mass flowrate readings, a mass balance across the reactor is used to determine the flowrate of flue gas.

$$\dot{m}_{flue\ gas} = \dot{m}_{total\ air} + \left({}^{X_{moisture}}/_{100} + {}^{X_{volatiles}}/_{100}\ {}^{X_{fixed\ carbon}}/_{100} \right) \times \dot{m}_{coal}$$ Equation 3-9

Therefore the mass flowrate of SO_2 emitted can be calculated from Equation 3-8 and 3-9.

$$\dot{m}_{SO2emitted} = \dot{m}_{flue\ gas} \times \left({}^{X_{mass\%SO2}}/_{100} \right)$$ Equation 3-10

Taking the results of equation 3-5 and 3-10, sulphur retention is calculated as such

$$S_{retention} = \left(1 - {}^{\dot{m}_{SO2emitted}}/_{\dot{m}_{theoSO2}} \right)$$ Equation 3-11

3.5.2 Slagging Propensity

Slagging propensity of a coal can be determined either the Ash Fusion Temperature or by calculation from the chemical composition of the ash. The method employed in this research was based on the chemical composition of ash (Alphen, 2005) (Coal Technology, 2013).

- Silica Ratio (SR)

$$SR = \frac{\%SiO_2}{\%SiO_2 + \%Fe_2O + \%CaO + \%MgO}$$ Equation 3-12

Low	> 72
Medium	72 - 65
High	< 65

- Alkaline Index (Ai)

$$Ai = \frac{\%Na_2O + 0{,}657 \times \%K_2O}{\%Ash_{coal}}$$ Equation 3-13

Low	< 0,3
Medium	0,3 - 0,45
High	0,45 - 0,6
Very high	> 0,6

- Slagging Index (Si)

$$Si = \left(\frac{\%Fe_2O_3 + \%Na_2O + \%K_2O + \%CaO + \%MgO}{\%SiO_2 + \%Al_2O_3 + \%TiO_2}\right) \times \%S_{Total} \qquad \text{Equation 3-14}$$

Low	< 0,6
Medium	0,6 - 2,0
High	2,0 - 2,6
Very high	> 2,6

- Fouling Index (Fi)

$$Fi = Si \times \left(\frac{\%Na_2O + \%K_2O}{\%S_{Total}}\right) \qquad \text{Equation 3-15}$$

Low	< 0,6
Strong	0,6 - 40
Very strong	> 40

- Base/Acid Ratio (B/A)

$$B/A = \frac{\%Fe_2O_3 + \%Na_2O + \%K_2O + \%CaO + \%MgO}{\%SiO_2 + \%Al_2O_3 + \%TiO_2} \qquad \text{Equation 3-16}$$

Dry Firing	0,1 - 0,5
Slag Tap Furnace	0,3 - 1,0

The smaller, the lower is the slagging propensity

CHAPTER 4 : RESULTS AND DISCUSSIONS

4.1 Introduction

The principle objective of this research is to assess the combustibility of South African coals as well as to determine the impact of reactor parameters on the products of combustion in a pilot scale bubbling fluidised bed combustion testing facility. This chapter discusses the data and results obtained from use of the methodologies discusses in Chapter 3.

4.2 Analysis of Coal and Sorbent

Coal basically consists of stone (mudstone, siltstone and sandstone), pyrite cleats, carbonate cleats (calcite/dolomite) and clay quartz in carbon rich particles. The analysis of raw coal and sorbent was performed as a pre-requisite for the experimental FBC test matrix. The proximate and ultimate analyses are shown in Table 4-1.

Table 4-1: Coal Proximate and Ultimate Analysis on air-dried bases

		Coal A	Coal B	Coal C
Inherent Moisture	%	2.10	2.70	2.80
Volatile Matter	%	19.80	19.70	18.10
Ash	%	36.30	52.50	45.20
Fixed Carbon	%	41.80	25.10	33.90
Total Carbon	%	48.65	32.78	37.52
Hydrogen	%	2.34	2.12	1.92
Nitrogen	%	1.11	0.58	0.76
Total sulphur	%	1.79	1.41	2.67
Carbonate (as CO_2)	%	1.81	1.45	2.35
Oxygen	%	5.90	6.46	6.78
Gross Caloric Value (HHV)	MJ/kg	18.63	13.60	14.54

Coal A possesses the lowest ash content (36.6% ad.) and coal B the highest (52.5% ad.). Whereas Coal A has the highest CV (18.63 MJ/kg ad.) and coal B the lowest CV (13.60 MJ/kg ad.). However, all three coals have similar volatile matter content.

The ash elemental composition of the three coals is shown in Figure 4-1.

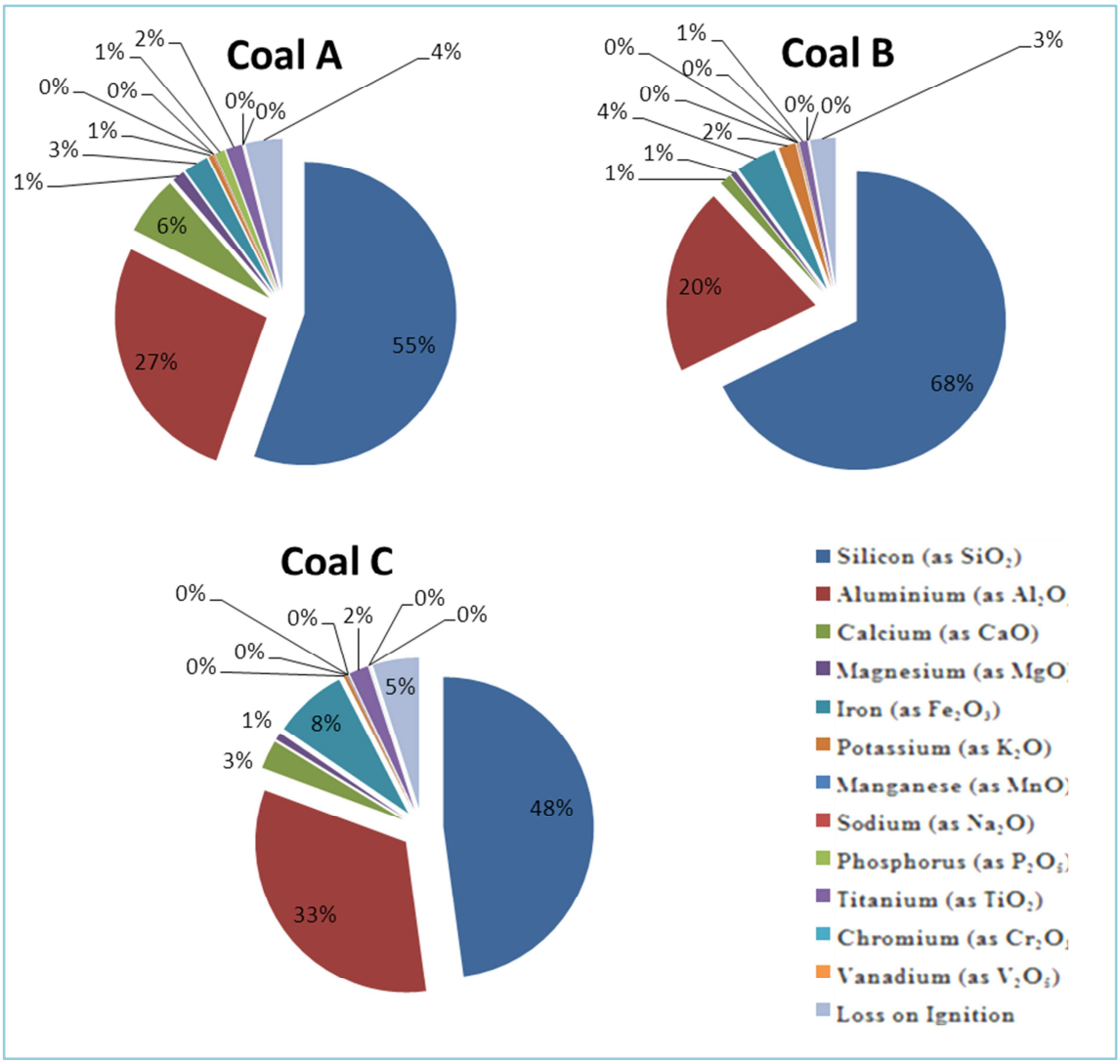


Figure 4-1: Coal Ash Elemental Analysis

Calcium and magnesium compounds in the ash are of particular importance to the sulphur self-capture mechanism experienced in FBC. It is noted that Coal A-ash has the highest calcium oxide (6.1%) and Coal B-ash the lowest (1.23%). The coals have similar magnesium oxide contents (approximately 1%). In the absence of coal-calcium and magnesium reactivity, it can be assumed that Coal A will have the highest sulphur-self capture rate and Coal B the least. However, QEMSCAN was used to determine amount of calcium and magnesium and also quantify the mineralogy of various elements.

The mineralogy of the coals is shown in Figure 4-2 below.

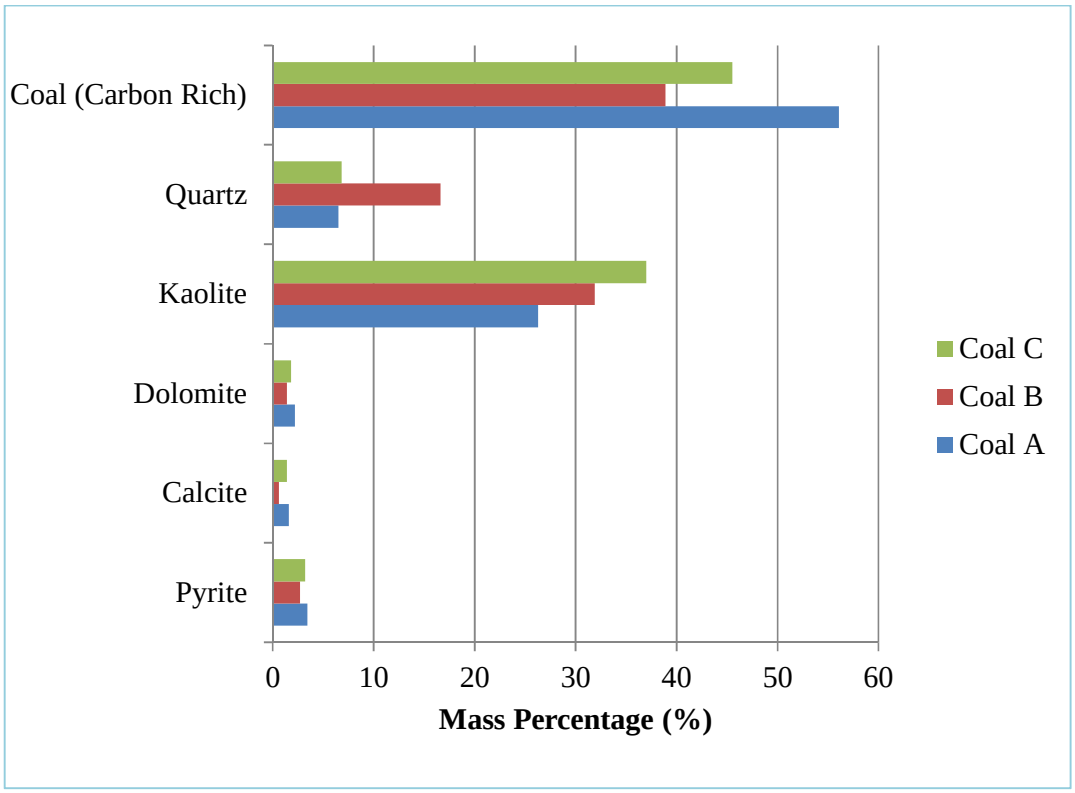


Figure 4-2: Coal Mineralogy Assessment

Coal mineralogy shows similar trends as observed from the chemical and ash elemental analyses. Coal A has the highest calcite and dolomite (1.6% and 2.2%), and Coal B the least (0.6% and 1.4%); a similar finding from the ash elemental analysis (calcium and magnesium content). Coal A has the lowest amount of kaolite and quartz (26.3% and 6.5%), and Coal B the highest (31.6% and 16.6%); a similar finding in proximate analysis (ash percent). Hence the QEMSCAN is used extensively to quantify the contents of coal.

A point of interest to FBC is the proportion of pyrite, calcite and dolomite in the coals. The QEMSCAN, in particular, is able to identify calcium in the different compounds such as calcite, dolomite and apatite. These compounds can be used to estimate the reactivity of CaO, as seen in ash elemental analysis, and therefore the rate of sulphur self-capture.

An advantage of FBC over the conventional pulverised coal-fired boilers; is the ability to capture sulphur in-situ through the addition of calcium- and/or calcium-magnesium-based sorbent. Figure 4-3 and Figure 4-4shows the ash elemental and mineralogy analyses of the sorbent used during the combustion tests.

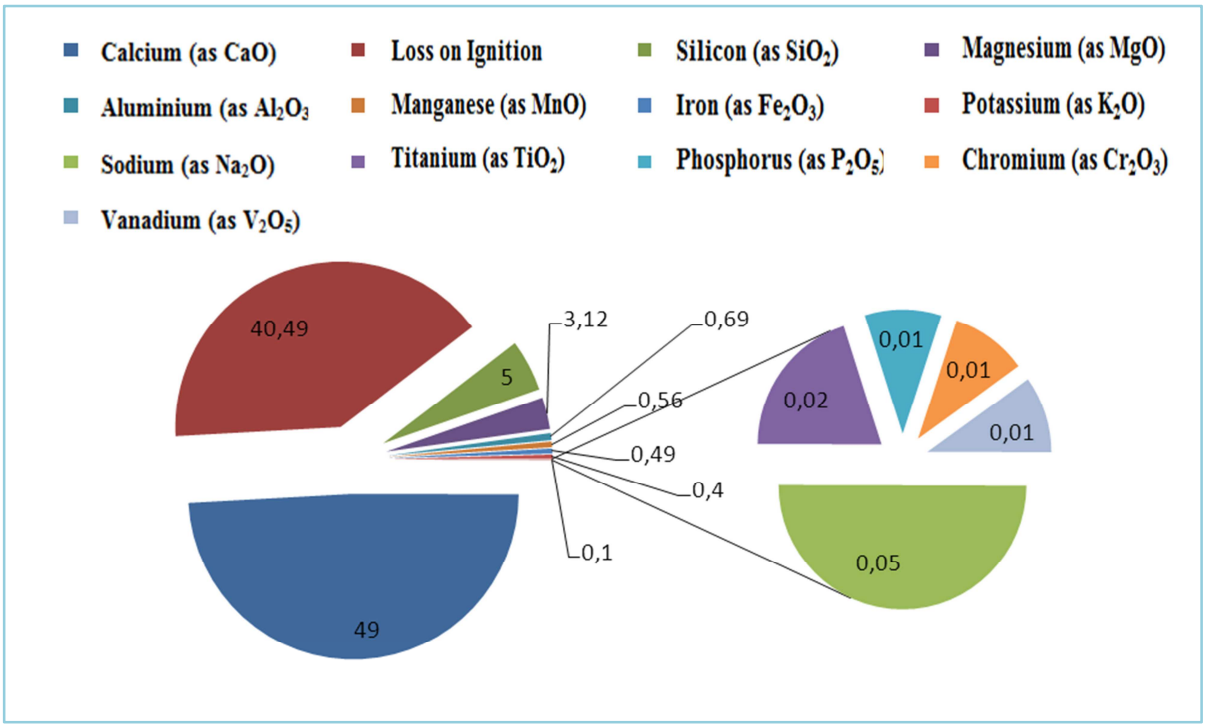


Figure 4-3: Sorbent Ash Elemental Analysis

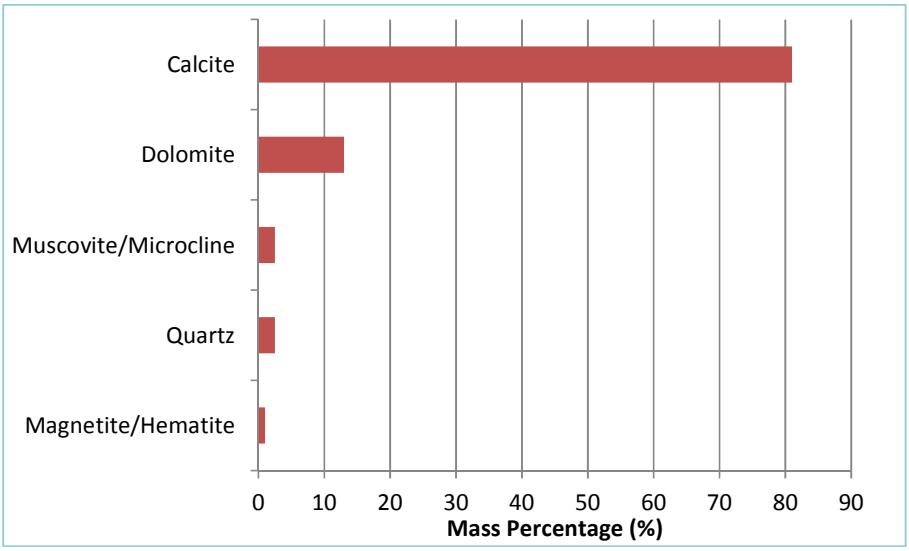


Figure 4-4: Sorbent Mineral Proportion Analysis

The ash elemental analysis as shown in Figure 4-3 indicates that sorbent has 49% of calcium and 3.12% of magnesium, whereas the mineral proportion analysis as shown in Figure 4-4 indicates that 82% of the sorbent is calcite and 13% is dolomite. The ash elemental analysis

detected other elements and these are quantified by the mineralogy assessment which shows quartz, muscovite/microcline and magnetite/hematite as the 'other elements'.

4.3 Pilot Scale Test Results

The raw data obtained during the FBC coal firing tests (test matrix in Table 3-1, Appendix B, C and D) and the related calculations (Appendix E) are attached. The results presented in this section cover the reactor temperature profile comparisons for the different tests, carbon efficiency, gaseous emissions and fly-ash analysis.

4.3.1 Reactor Temperature Profiles

The reactor temperature profile is an indication of the heat dissipation within the pilot BFBC furnace during the experimental tests. In a commercial FBC plant the higher temperature areas represent the area where heat transfer occurs largely by conduction, and the lower temperature areas represent heat transfer by convection. These temperature values at the different points (see Figure 3-1 for the illustration of the points) are shown in Table 4-2.

Table 4-2: Temperature reading across the bed and the free-board

	Bed Temp	Temp 01	Temp 02	Temp 03	Temp 04	Temp 05	Temp 06	Temp 07	Temp 08	Temp 09	Temp 10	Temp 11
Coal A	*830*	833	833	838	835	837	831	819	690	631	547	500
	850	851	851	857	853	854	848	824	686	626	545	499
	870	871	871	877	874	873	866	832	682	622	542	496
Coal B	*830*	819	819	826	823	823	817	797	669	610	528	488
	850	857	857	863	860	857	846	810	673	611	527	491
	870	872	872	877	874	869	856	819	674	611	527	491
Coal C	*830*	830	830	836	833	834	830	829	712	652	559	503
	850	845	845	850	848	848	843	842	719	657	561	505
	870	867	867	872	869	871	865	865	729	666	568	509

To present a trend of the temperature profiles, the temperature reading for the test at each specific bed temperature (830 °C, 850 °C and 870 °C) were averaged. The reactor temperature profile trends are presented in Figure 4-5.

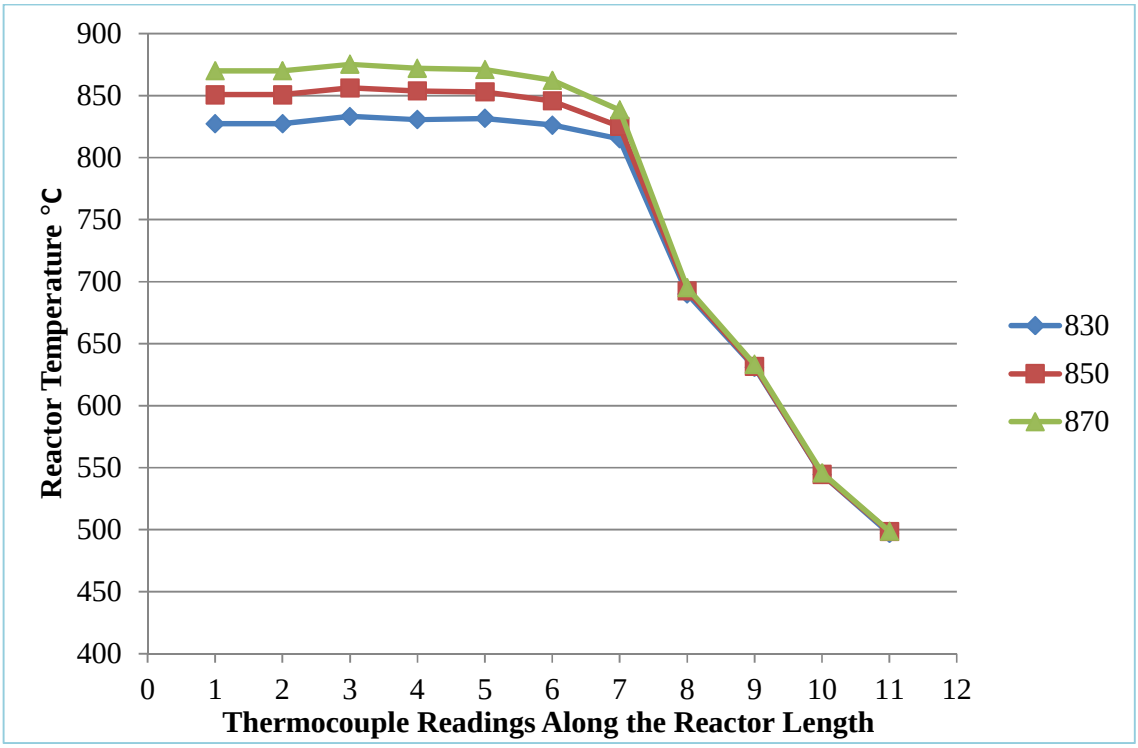


Figure 4-5: Reactor temperature profiles averaged for the three coals

These profiles are averages of the test temperature setting (830 °C, 850 °C, and 870 °C) for all tests associated with the three coals. When the reactor is warmed-up properly, the over-board temperature readings (TE 7 to 11, Figure 3-1) will be similar if not the same throughout the tests, whereas bed temperature will change as per requirement. The consistency of the temperatures across the bed (thermocouples 1 to 6) for each temperature setting is relevant to eliminate discrepancies in the results. The profile in figure 4-5 shows that the tests were conducted according to the pre-described methodology.

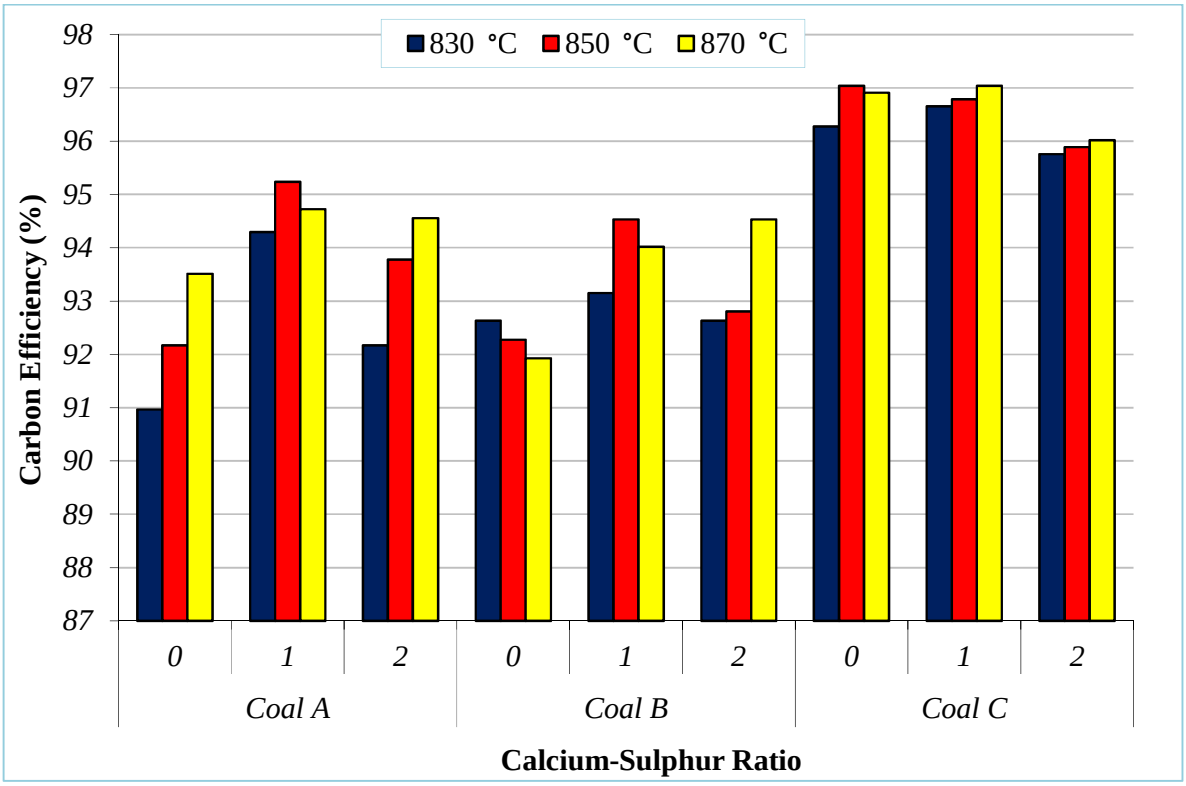
4.3.2 Carbon Efficiency

Carbon efficiency is a measure of the conversion of carbon in the coal and represents the effectiveness of the reactor. Efficiency is calculated by analytically determining the amount of unburnt carbon in fly-ash and it is calculated by the following equation;

$$a = \frac{Coal\ mass\ flow \times carbon\ in\ ash \times Ash\ content}{100 * (100 - carbon\ in\ ash)} \qquad \text{Equation 4-1}$$

$$Carbon\ Efficiency = 100 - \left(\frac{100 - a}{coal\ mass\ flow \times Carbon\ content}\right) \qquad \text{Equation 4-2}$$

Figure 4-6 shows the combustion efficiencies for the 27 coal firing tests conducted (nine per coal).



Key: 0 – No Sorbent; 1 – Ca/S of 1; 2 – Ca/S of 2

Figure 4-6: Combustion Efficiency graph

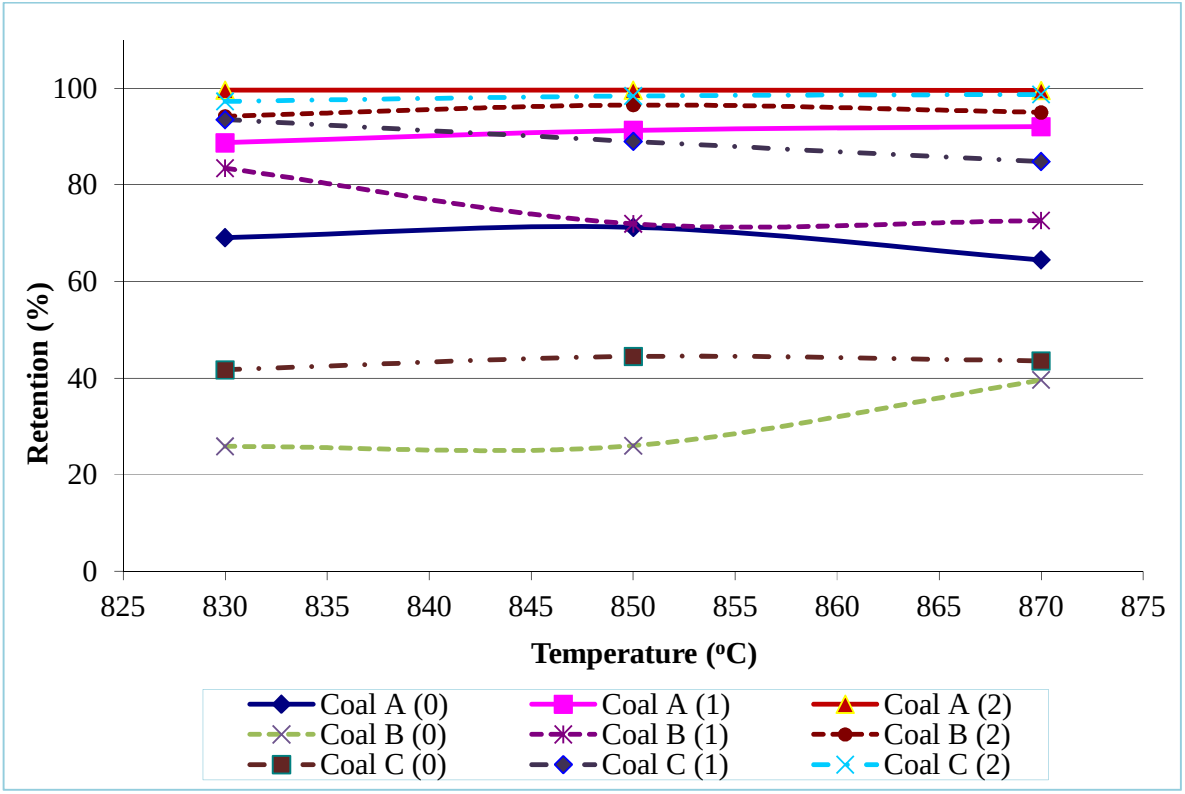
Coal C has an overall higher carbon efficiency as compared to Coal A & B. A constant trend with the results is seen in Figure 4-6 where the combustion efficiency increased at the initial introduction of sorbent and dropped as the Ca/S ratio is increased to two. This is an indication that unconverted reactants (C, S, Ca, N, etc. and CaO, CaMgO) will be found in the coarse ash and the fly ash.

The tests were conducted at similar total combustion air (i.e. keeping the coal/air ratio the same), when limestone was injected no adjustments were made to the total air. During the sulphation of lime (Equation 2-25) oxygen is consumed and this leads to a decreased availability of oxygen for carbon conversion. Hence the carbon efficiency at Ca/S=2 decreases because of limited oxygen available for further carbon conversion.

4.3.3 Sulphur Retention

Sulphur dioxide emission has an effect on human health (respiratory problems) and the ecosystem (acid rain). Sulphur retention is a mechanism of reducing the amount of SO_2 emission through the reaction of the SO_2 with calcium oxides.

Sulphur in coal is present as organic-sulphur and as pyrite. The latter is found in the mineral matter and the former dissipated in the coal matrix. Calcium in coal is present as either organic or non-organic. The reactivity of calcium depends on the form in which at it is mostly present in the coal. The level of sulphur retention observed during the tests is shown in Figure 4-7.



Key: 0 – No Sorbent; 1 – Ca/S of 1; 2 – Ca/S of 2

Figure 4-7: Sulphur Retention Trends

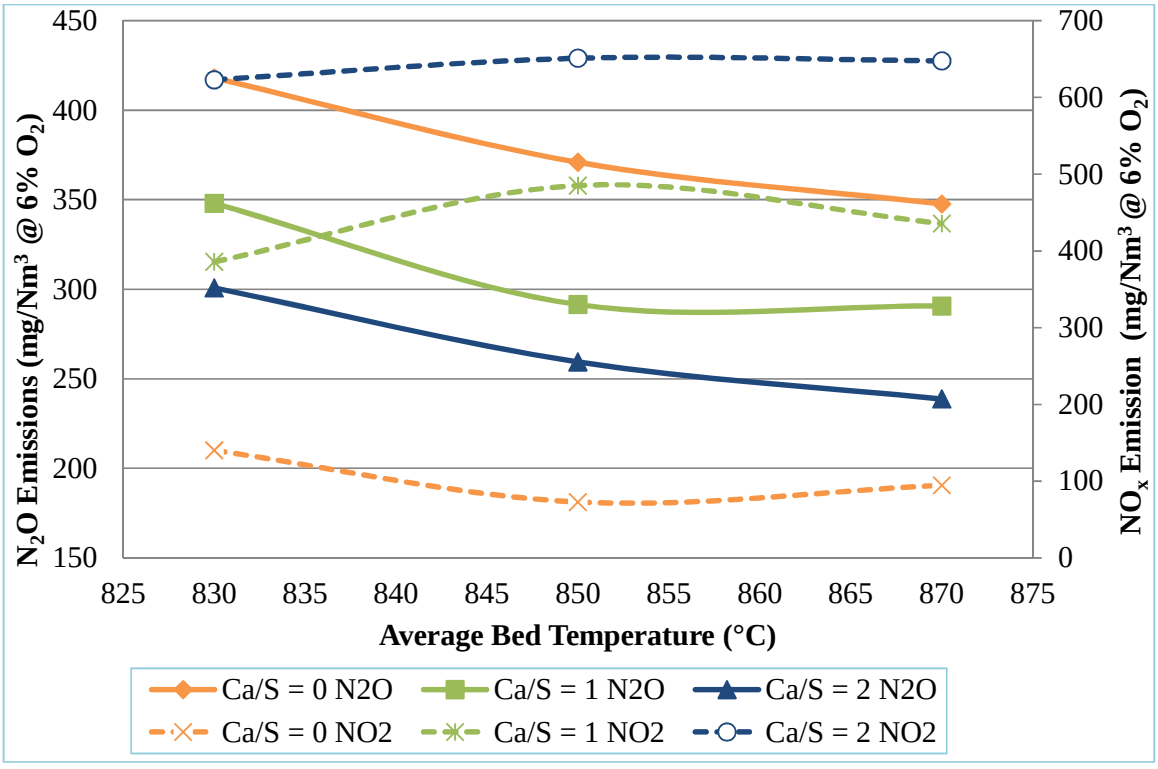
Figure 4-7 shows that sulphur self-retention for coal A is higher and that coal B has the lowest retention. The higher sulphur self-retention for coal A is attributed to the higher calcium content as shown in Figure 4-1. The reactivity of the coal-based calcium was not validated; however Figure 4-2 gives an indication of available calcite in the coal to react with SO_2. The calcite amount could infer the reactivity of calcium in coal to capture sulphur.

Addition of limestone to the BFBC reactor during coal combustion contributed to an increase in sulphur retention. The rate of sulphur capture is proportional to the feedrate of limestone, i.e. the molar ratio of calcium in limestone to sulphur in coal, as shows by the trends in Figure 4-7. The highest sulphur retention observed during the course of the test-work was 99% for coal A.

4.3.4 Nitrogen Oxides Formation

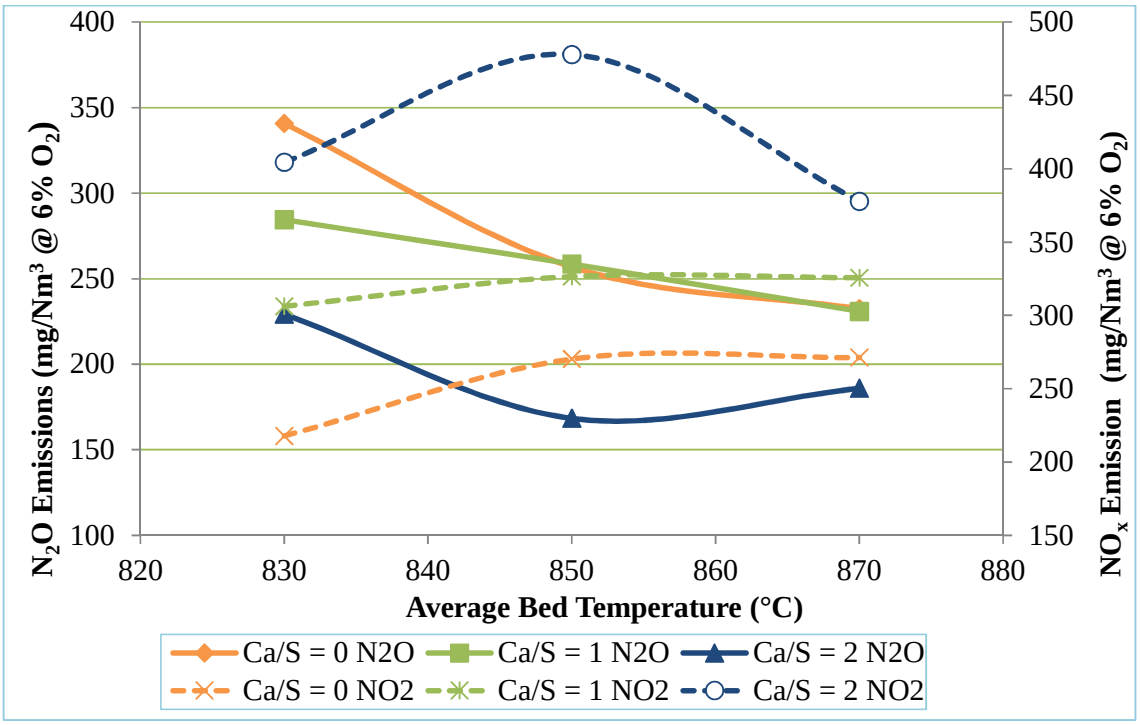
The production of NO_x and N_2O is a complex process that involves coal devolatilisation, volatile species oxidation, char oxidation, and partial reduction to N_2 (Zhangfa Wu, 2003). The operating temperature (800 °C to 900 °C) in BFBC obviate the formation of thermal NO_x, however the coal-bound nitrogen will react with O_2 to form NO_x and the more greenhouse gas potent N_2O.

The results for the three coals are presented in the following figures and placed in the order of Coal A (Figure 4-8), Coal B (Figure 4-9) and Coal C (Figure 4-10).



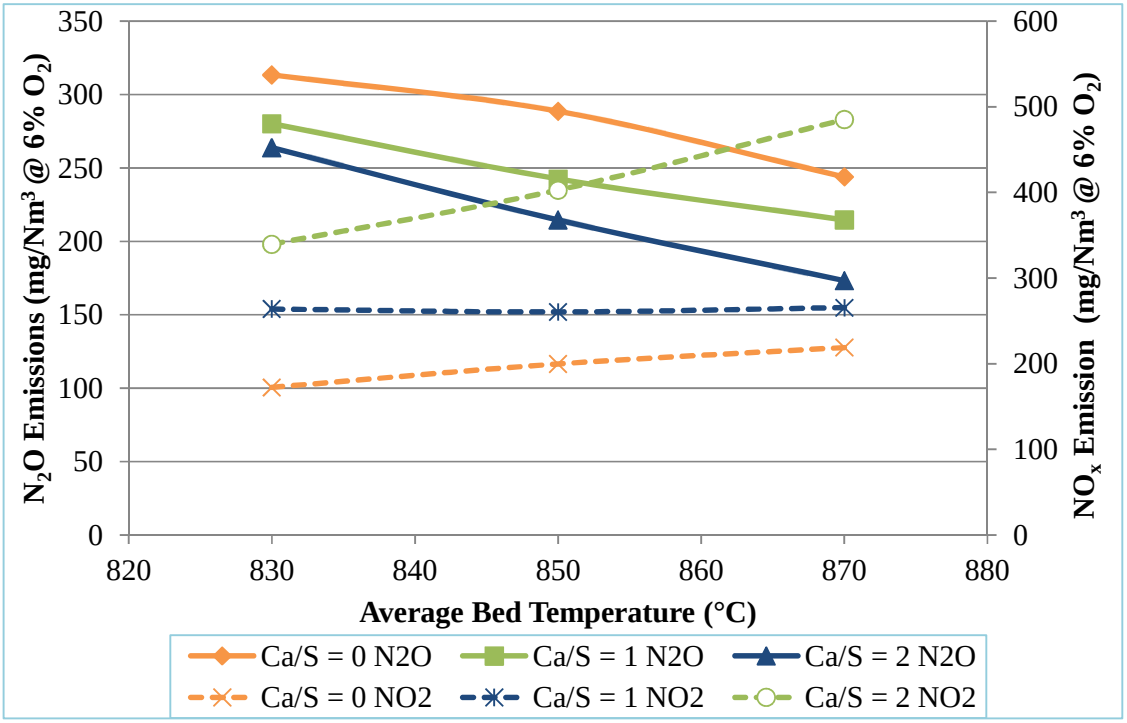
Key: 0 – No Sorbent; 1 – Ca/S of 1; 2 – Ca/S of 2)

Figure 4-8: Coal A - NO_x and N_2O Gaseous Emissions



Key: 0 – No Sorbent; 1 – Ca/S of 1; 2 – Ca/S of 2)

Figure 4-9: Coal B - NO_x and N_2O Gaseous Emission



Key: 0 – No Sorbent; 1 – Ca/S of 1; 2 – Ca/S of 2)

Figure 4-10: Coal C - NO_x and N_2O Gaseous Emission

A similarity in the trends in Figure 4-8, 4-9 and 4-10 was observed as explained below;

- NO_x production increased with increasing temperature whereas N_2O production decreased with increasing temperature in all three coals, and
- The introduction of limestone into the BFBC increased the production of NO_x and decreased that of N_2O.

Hence the average bed temperature and Ca/S ratio is proportional to NO_x emission and indirectly proportional to N_2O emission.

4.3.5 Fly Ash Analysis

Fly ash consists mainly of stone (alumina-silicate and quartz), pyrite cleats (iron oxide), calcite/dolomite cleats (calcium oxide and calcium magnesium oxide), and molten ash spheres. Fly ash samples obtained during the tests for the 850 °C experiments were submitted for ash elemental and mineralogy assessment. Ash elemental analyses for these tests are presented in Tables 4-3, 4-4 and 4-5.

Table 4-3: Coal A - Ash Elemental Results for the Tests at 850 ˚C

		Test 0.2	Test 0.4	Test 0.8
Silicon (as SiO_2)	%	48,1	43,1	34
Aluminium (as Al_2O_3)	%	26,2	27,5	22,2
Calcium (as CaO)	***%***	***4,59***	***5,27***	***21***
Magnesium (as MgO)	%	1,25	1,14	1,12
Iron (as Fe_2O_3)	%	6,09	6,34	5,15
Potassium (as K_2O)	%	0,65	0,5	0,39
Manganese (as MnO)	%	0,03	0,03	0,21
Sodium (as Na_2O)	%	0,09	0,05	0,05
Phosphorus (as P_2O_5)	%	0,62	0,82	0,66
Titanium (as TiO_2)	%	1,36	1,34	1,06
Chromium (as Cr_2O_3)	%	0,01	0,03	0,09
Vanadium (as V_2O_5)	%	0,01	0,01	0,01
Loss on Ignition	%	8,49	10,38	10,94

Key: Test 0.2 – No Sorbent; Test 0.4 – Ca/S of 1; Test 0.8 – Ca/S of 2; all at 850 °C

Table 4-4: Coal B - Ash Elemental Results for the Tests at 850 ˚C

		Test 1.2	Test 1.5	Test 1.8
Silicon (as SiO_2)	%	60,90	56,70	46,30
Aluminium (as Al_2O_3)	%	24,80	21,50	12,50
Calcium (as CaO)	***%***	***1,60***	***7,87***	***20,80***
Magnesium (as MgO)	%	0,72	0,75	0,72
Iron (as Fe_2O_3)	%	4,56	4,13	3,15
Potassium (as K_2O)	%	1,34	1,30	1,10
Manganese (as MnO)	%	0,01	0,08	0,23
Sodium (as Na_2O)	%	0,09	0,08	0,06
Phosphorus (as P_2O_5)	%	0,14	0,10	0,09
Titanium (as TiO_2)	%	1,00	0,84	0,60
Chromium (as Cr_2O_3)	%	0,01	0,01	0,01
Vanadium (as V_2O_5)	%	0,01	0,02	0,01
Loss on Ignition	%	4,25	4,05	6,10

Key: Test 1.2 – No Sorbent; Test 1.5 – Ca/S of 1; Test 1.8 – Ca/S of 2; all at 850 °C

Table 4-5: Coal C - Ash Elemental Results for the Tests at 850 ˚C

		Test 2.2	Test 2.5	Test 2.8
Silicon (as SiO_2)	%	53	44,9	37,4
Aluminium (as Al_2O_3)	%	31,5	28,1	24,2
Calcium (as CaO)	***%***	***3,07***	***10,6***	***20,3***
Magnesium (as MgO)	%	0,8	0,82	0,96
Iron (as Fe_2O_3)	%	4,44	4,16	3,75
Potassium (as K_2O)	%	0,76	0,59	0,43
Manganese (as MnO)	%	0,03	0,12	0,22
Sodium (as Na_2O)	%	0,05	0,05	0,5
Phosphorus (as P_2O_5)	%	0,28	0,26	0,22
Titanium (as TiO_2)	%	1,7	1,56	1,37
Chromium (as Cr_2O_3)	%	0,01	0,01	0,01
Vanadium (as V_2O_5)	%	0,01	0,01	0,03
Loss on Ignition	%	2,61	3,37	5,32

Key: Test 2.2 – No Sorbent; Test 2.5 – Ca/S of 1; Test 2.8 – Ca/S of 2; all at 850 °C

Literature (Anthony and Granatstein, 2001 and Zhangfa Wu, 2003) states that utilisation of limestone in FBC reactors is less than 50 %. This is shown by an increase in CaO in the fly ash samples obtained during the tests when the ratio of Ca/S is increased.

A mineralogy assessment by QEMSCAN was also performed on the same fly ash samples. The full QEMSCAN analysis data is presented in Appendix E. A synopsis of the mineralogical data highlighting calcium and sulphate compounds involved in the sulphur capture reactions is presented in Figure 4-11.

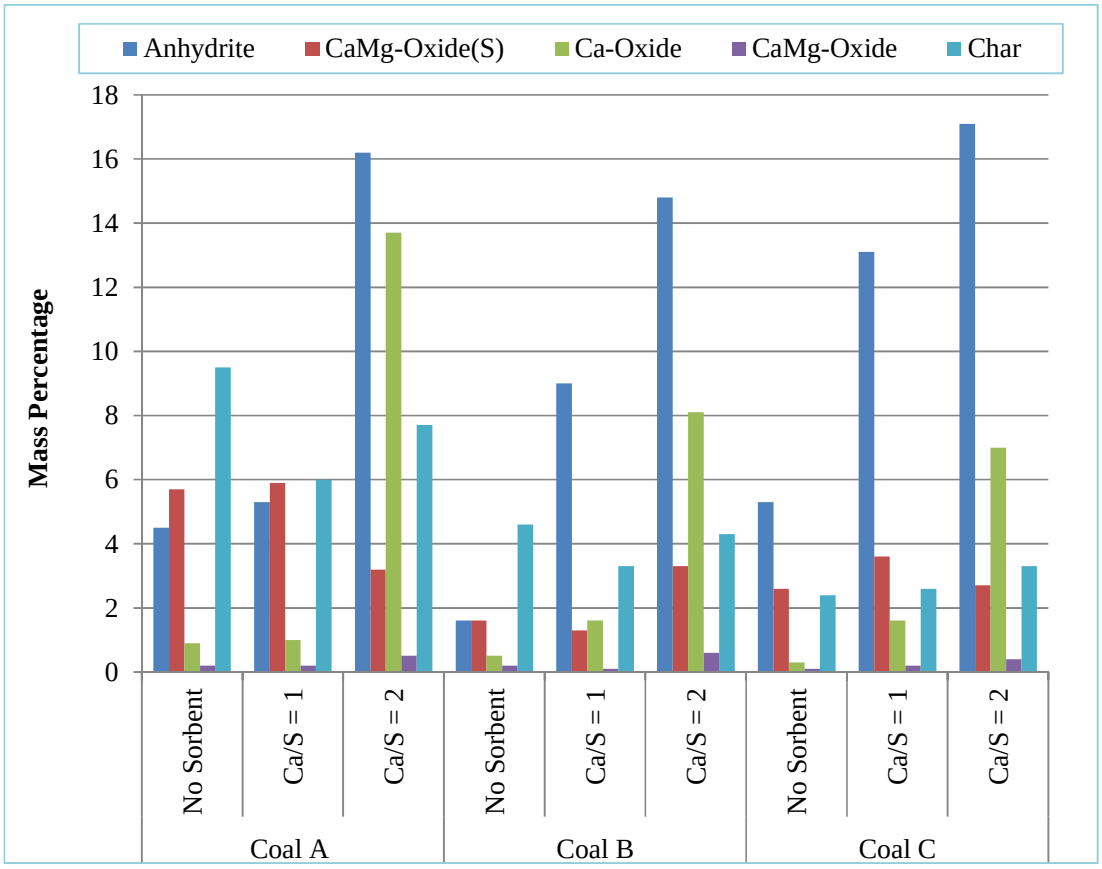


Figure 4-11: Mass Fractions Anhydrite, Calcite, dolomite, CaMg-Sulphate and Char

Calcium in fly ash was found in calcite ($CaCO_3$), dolomite ($CaMg(CO_3)_2$), anhydrite ($CaSO_4$), or CaMg-sulphate. Sulphur was found in anhydrite and the CaMg-sulphate compound. The mass fractions of anhydrite and CaMg-sulphate in each fly ash sample, correlates with the SO_2 measurements and the sulphur retention trends in Figure 4-7.

The mineralogical proportion of limestone showed that 80% of the sorbent was calcite, 10% dolomite, and the rest impurities. This indicates that at the highest limestone feedrate of

1.5 kg/h, the proportion of dolomite introduced into the FBC is 0.15 kg/h. Some of the dolomite will react with SO_2 and hence only a small fraction will be present in the fly ash as shown by Figure 4-11. However calcite in the fly ash increased with the increase in limestone feedrate.

Calcination stoichiometric reactions indicated that a higher proportion of sulphate compounds are expected and this was shown by the higher amount of anhydrite and the presence of CaMg-sulphate (Figure 4-11). Literature (Anthony and Granatstein, 2001 and Zhangfa Wu, 2003) also indicates that 50% or more of the calcite and dolomite in limestone will be found in ash (both fly ash and coarse ash). This is shown in Figure 4-12, where the proportion of the reacted and unreacted CaO and CaMgO is quantified.

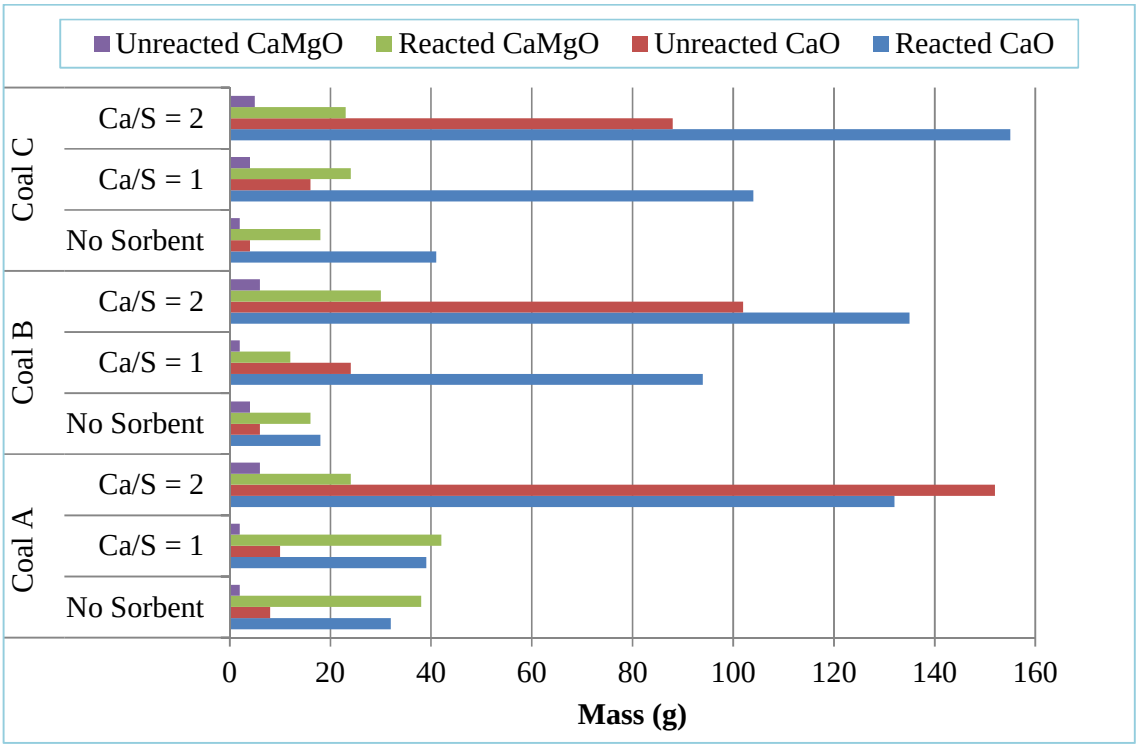


Figure 4-12: Proportion of the reacted and unreacted CaO and CaMgO

The proportion of the unreacted CaMgO remained low because the sorbent had a relatively low proportion of CaMgO. However the proportion of the unreacted CaO increased with the increment of Ca/S ratio. Evident in Figure 4-12 is that at a Ca/S ratio of 2, the amount of unreacted CaO is relatively high, even though Figure 4-7 indicates a sulphur retention of approximately 99%. The reaction between the sorbent and the coal at this ratio appears to be ineffective in terms of calcite conversion.

4.4 Discussion of the Results

The previous section presented the experimental test results and the analysis of fly ash. This section discusses these results with a focus on the main research question "Can South African coal be effectively combusted in a bubbling fluidised bed combustion technology?" and the sub-questions.

Answers to specific sub-questions are presented sequentially in section 4.4.1, 4.4.2, 4.4.3 & 4.4.4.

4.4.1 Differences in Carbon-in-Ash

"How does the carbon-in-ash differ for the coals at the different temperatures?"

The results are displayed by the carbon in ash trends for the different coals in Figure 4-13.

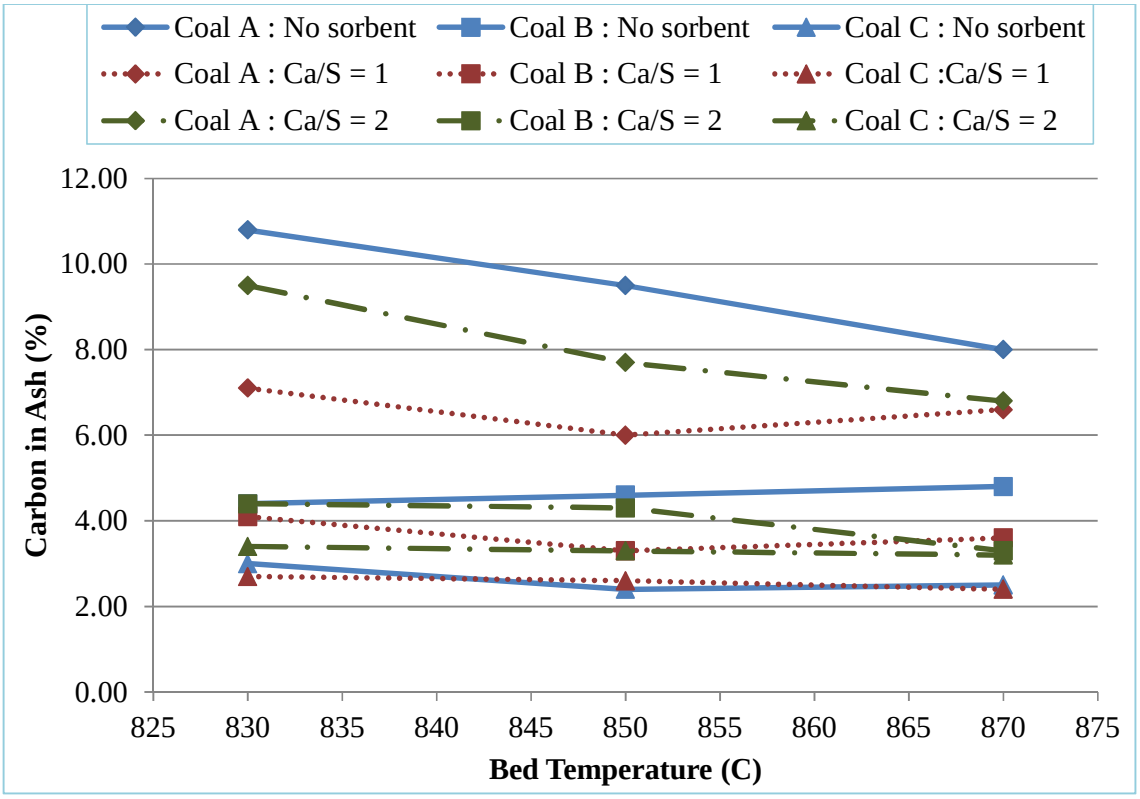


Figure 4-13: Carbon-in-ash at the different temperatures and calcium sulphur ratios

Ash produced from the combustion of coal A♦ has the highest carbon in ash at the different testing conditions. Coal C▲ combusts better with the lowest carbon-in-ash than the other two coals at all conditions, this translates to the highest combustion efficiency (Figure 4-6).

Carbon-in-ash for these coals range from 2.40% to 10.80%, this indicates that the organic material in these high ash coals does burn in the BFBC, with some minor variations between them. The overall trend shows reduction in carbon-in-ash with increasing temperature, especially in coal A. The initial injection of sorbent (Ca/S ratio of 1) improved carbon conversion for all three coals, however further increasing the ratio to 2 increased the carbon-in-ash percentage in the fly ash. The total combustion air for each coal was kept constant during the test; hence the introduction of limestone, and the resultant reaction of lime with SO_2 which utilises O_2, reduced the amount of oxygen available for char and carbon reactions. Mohamed *et al* (2008) showed in their study that altering the air-fuel ratio increased the combustion efficiency, bed temperature and total heat transfer. Hence keeping the total combustion air and coal feed rate constant while injecting limestone, will lead to reduced combustion efficiency as observed in Figure 4-6 an d Figure 4-14.

However, the introduction of fluidised bed combustion for the production of electricity in South Africa will have to compete with the conventional pulverised coal-fired boilers currently employed locally. Chapter 2 covers the factors that affect the implementation of FBC over the conventional coal-fired technology. Amongst these factors is combustion efficiency (alternatively carbon in ash). Figure 4-14 shows typical power station carbon in ash compared to the average carbon in ash for the three coals in BFBC.

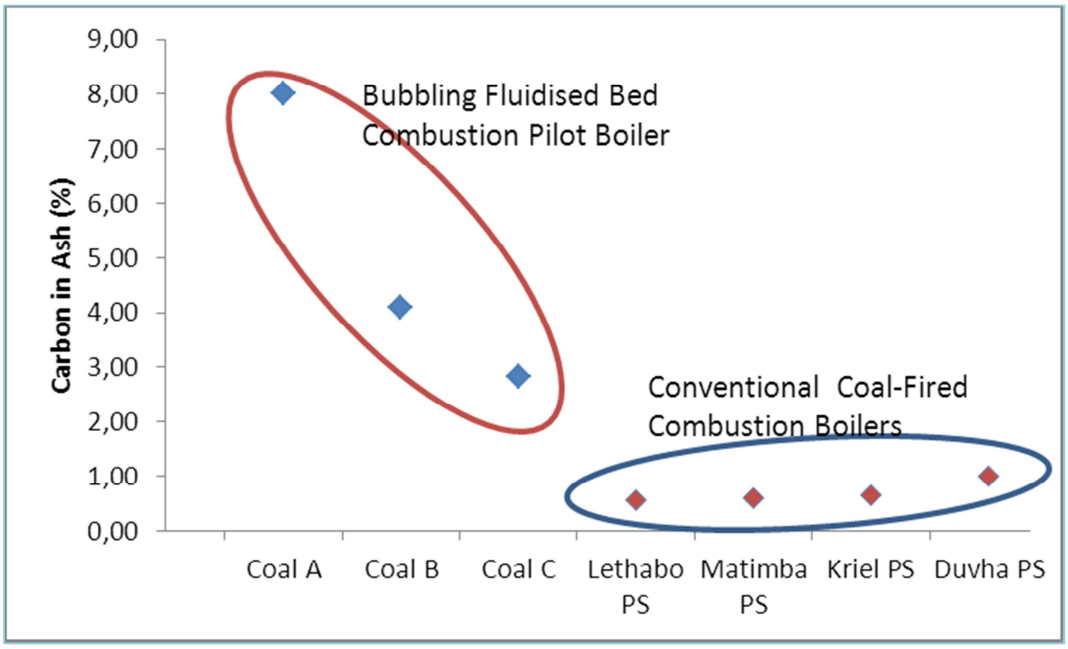


Figure 4-14: Typical power station carbon-in-ash compared to that in BFBC

A disadvantage of the FBC technology is the lower combustion efficiency relative to the conventional pulverised coal-fired boilers. This point is seen in Figure 4-14 where the carbon-in-ash portion of BFBC fly-ash is higher than the carbon-in-ash of the conventional pulverised coal-fired boilers. Eskom's boilers produce ash with carbon in the range of 1% and less. The pilot scale BFBC produces ash with carbon above 2% and as high as 8% on average. However, CFBC has been found to have lower carbon-in-ash as opposed to BFBC. The Overall plant efficiency of CFBC is similar to those of the conventional pulverised coal-fired boilers (Utt and Giglio, 2011).

In summation:

- Carbon-in-ash from BFBC fly ash samples, in general, reduces with increase in combustion temperature, indicating that combustion reactions improve with temperatures. However there is an exception with Coal B
- The tests show that adding limestone into the BFBC reactor can improve the conversion of carbon; however, the air-fuel ratio must be adjusted to keep the excess air the same for all tests.
- The BFBC appears to produces higher carbon-in-ash than conventional pulverised coal-fired boilers. This disadvantage, as reported in literature, indicate that BFBC technology has a lower combustion efficiency.
- However the overall findings from this study with respect to carbon-in-ash, indicates that BFBC is capable of burning SA coals effectively.

4.4.2 Local Impact of BFBC SO_2 Emission

"How are the gaseous emissions impacted by utilising the BFBC technology?"

The National Environmental Management: Air Quality Act, 2004 (ACT no. 39 of 2004) notice no. 284, states that existing and new plants must comply with the minimum emission standards as stipulated in the act from the date it was issued. An extract of the act (notice no. 284) showing the required minimum emission standards is shown in Table 4-6.

Table 4-6: Minimum Emission Standards for Solid Fuel Combustion Installations

Description:	Solid fuels (excluding biomass) combustion installations used primarily for steam raising or electricity generation		
Application:	All installations with design capacity equal to or greater than 50 MW heat input per unit, based on lower calorific value of the fuel used		
Substance or mixture of substances		plant status	mg/Nm^3 under normal conditions of 10% O_2, 273 K and 101.3 kPa
common name	chemical symbol		
Particulate matter	N/A	New	50
		Existing	100
Sulphur dioxide	SO_2	New	500
		Existing	3500
Oxides of nitrogen	NO_x expressed as NO_2	New	750
		Existing	1100

The SO_2 emissions from the tests conducted were normalised at 10% O_2 so that they could be compared to the minimum emission standards. Figure 4-16 compares the emissions from the pilot scale combustor to the AQA 2004 minimum standard emissions.

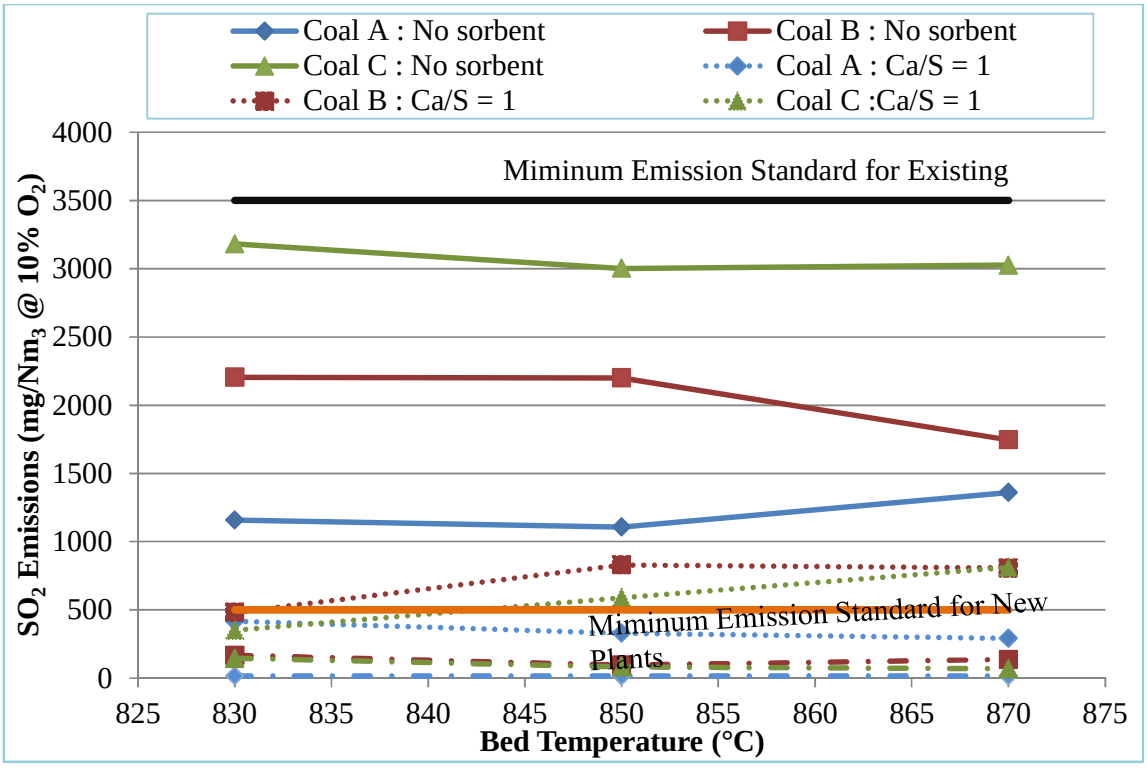


Figure 4-15: BFBC SO_2 Emission Compliancy to NEM: AQA 2004

SO_2 emissions for coal combustion tests without limestone reached a high of 3100 mg/Nm^3 (10%O_2) for coal C▲. This came just below minimum emission standard for existing plants (3500 mg/Nm^3 at 10% O_2). The coals displayed SO_2 emissions higher than the minimum emission standard for new plants (500 mg/Nm^3 at 10% O_2) when combusted without limestone. This is a concern for South African utilisation as any new built BFBC power plant will be required to meet the standard for new plants.

The addition of limestone at a Ca/S ratio of 1 decreased SO_2 emissions for all three with the least amount of emission at 290 mg/Nm^3 (10% O_2) for coal A♦. Coal C emitted the highest with 811 mg/Nm^3 (10% O_2) and higher than the new plant standard. Some coals at this rate of limestone addition will still not meet the standard for new plants.

Further addition of limestone at Ca/S ratio of 2 decreased the SO_2 emissions to lower amounts. Under these conditions, all three coals displayed emissions (maximum of 145 mg/Nm^3 at 10% O_2 for coal C) lower than the new plant minimum emission standards. This is an indication that the BFBC plant is capable of burning SA coals in the presence of limestone with reduced SO_2 emissions.

International emission standards are relatively more stringent than those in South African. In order to compare them, SO_2 emissions from the BFBC tests were compared to SA emission regulations, some of the international standards and emissions from Eskom's conventional coal-fired boilers. To give a realistic indication of BFBC results, SO_2 emissions at the Ca/S ratios (0, 1 & 2) where averaged to give single values for the different ratios. This comparison is shown in Figure 4-16 below.

It is noted that to meet the local and international emission regulations (WRI, 2012), a Ca/S ratio higher than 1 will have to be implemented in SA FBC coal combustion. However, the emissions from the BFBC are relatively lower than the emissions from the conventional coal-fired boilers at Eskom (Eskom Holdings, 2012). For conventional coal-fired boilers to meet the required emission limit for new plants, the implementation of the high CAPEX and OPEX flue gas desulphurisation plant will have to be undertaken

These results also complement the remarks made by Anthony and Granatstein (2001) and Zhangfa Wu (2003) which states that limestone/dolomite utilisation in FBC applications is lower than 50%. This observation is illustrated in Figure 4-12 where the amount of reacted CaO and MgO.Ca was compared to their unreacted counterparts.

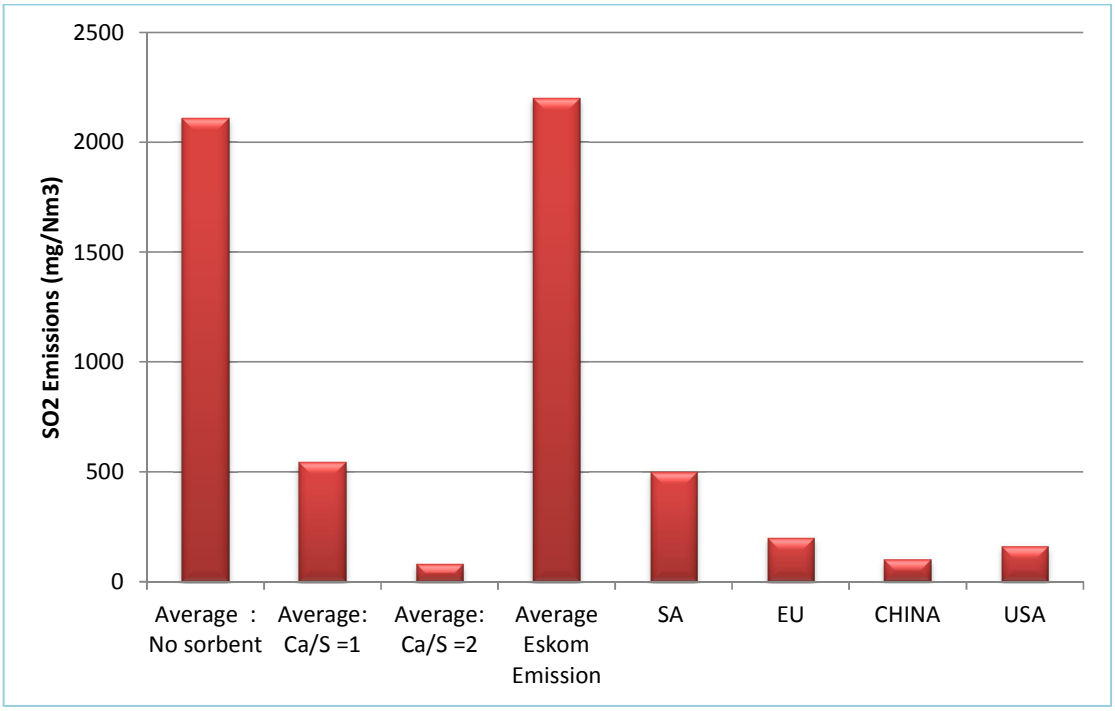


Figure 4-16: Equivalence BFBC SO_2 to Eskom and various regulators

In summation;

- A reduction in SO_2 emissions was apparent when coal was combusted in the pilot BFBC in the presence of limestone. Without limestone, a lower reduction in SO_2 was observed, however the addition of limestone was able to reduce the emission to values lower than 400 mg/Nm^3.
- Upon comparison with Eskom's conventional coal-fired boiler and the minimum emission standards for SO_2 emissions, the BFBC displayed the potential to emit fewer emissions than currently experienced by Eskom and also the potential to meet the standard for new plant when limestone was added into the reactor.
- Therefore the use of BFBC for coal combustion in generating electricity has a beneficial impact on the emissions, and it emits less SO_2 at a lower cost. It also has less impact on the environment as SO_x emission is detrimental to particulate aggregation in the atmosphere and leads to acid rains.

4.4.3 Local Impact of NO_x Emissions

"How are the gaseous emissions impacted by utilising the BFBC technology?"

A study conducted by Valentim et al (2006) showed that SA coals produce higher NO and N_2O than their Columbian and USA counterparts. In their study, the authors showed that increasing the combustion temperature, decreased the formation of NO for the vitrinite-rich coals (Columbian and USA) and increased the formation of NO for the inertinite-rich coals (SA). N_2O formation decreased with an increase in combustion temperature for both types of coal.

Konttinen et al (2013) evaluated the tendency of NO formation and concluded that the standard fuel analysis is not enough to provide the required inputs for NO emission predictions in large scale fluidized bed combustion. Their combustion test results showed that the maximum cumulative conversion of fuel nitrogen to NO under non-staged fluidized bed combustion is 20–50% (850 °C with O_2 in excess). Zhangfa Wu (2003) stated that the coal-bound N_2 converted to NO_x is between 5% and 40%, whereas less than 10% is converted to N_2O and the rest is emitted as N_2. Figure 4-17 shows the NO_x emissions from the BFBC tests as compared to the SA AQA 2004 minimum emission standard for NO_x in existing and new plants.

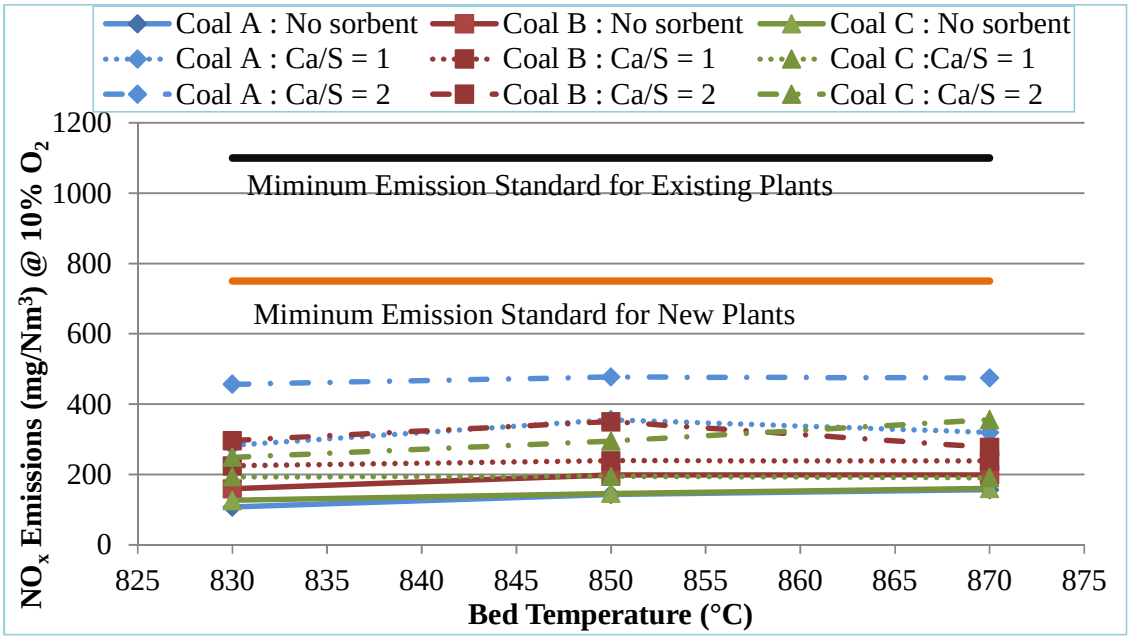


Figure 4-17: BFBC NO_x Emission Compliancy to NEM: AQA 2004

The values reported in the BFBC tests and as illustrated by Figure 4-17 indicate that all results are lower than the minimum emission standard for new plants of 750 mg/Nm^3 at 10 % O_2 (Table 4-6). The production of NO_x increases with increasing bed temperature, the addition of limestone also increases the production of NO_x as shown by Figure 4-18. These trends are similar to the findings by Valentim et al (2006). A stoichiometric calculation that takes into consideration comments by Zhangfa Wu (2003) and Konttinen et al (2013), estimates the range of NO_x emissions for these coals between 30 and 620 mg/Nm^3 (5 % to 50 % conversion of N_2 into NO_x). The actual emissions of NO_x fall within this range when coal was combusted in the pilot BFBC, even with the addition of limestone, the highest NO_x emission was detected at 487 mg/Nm^3 at 10 % O_2.

To further assess the impact of using the BFBC on the emissions, NO_x emissions were compared to international emission limits (WRI, 2012), and the average NO_x emissions from Eskom's coal-fired boilers (Eskom Holding SOC, 2012). NO_x emissions at the different Ca/S ratios (0, 1 & 2) where averaged to give a realistic estimate of the expected emissions from BFBC coal combustion. This is shown in Figure 4-18 below.

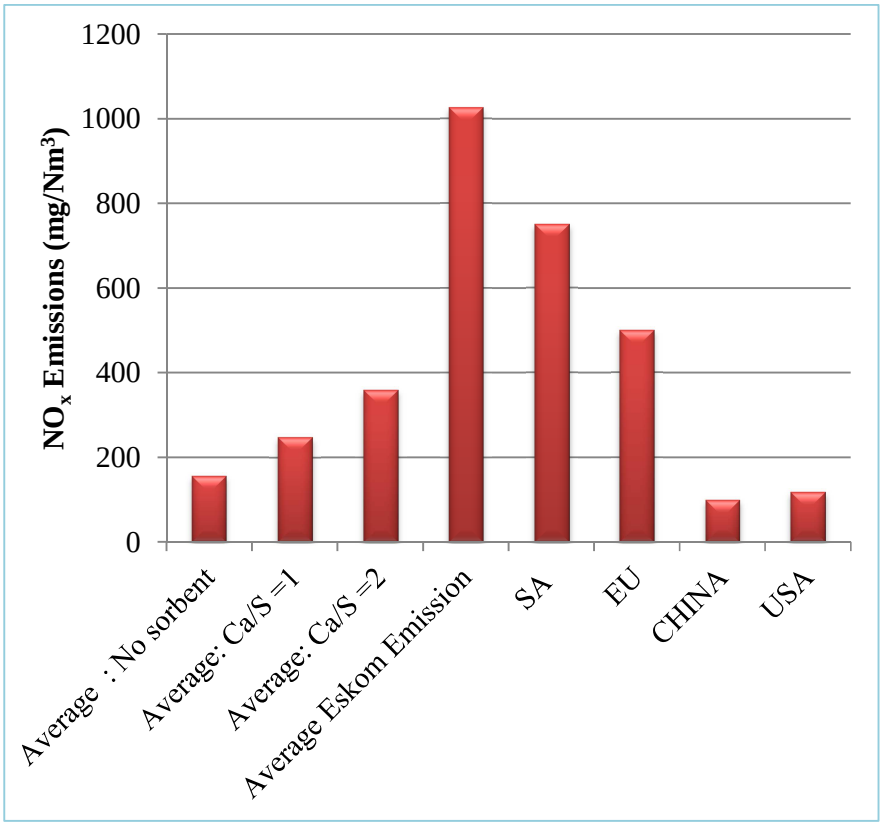


Figure 4-18: Equivalence of BFBC NO_x emissions to Eskom and various regulators

The Chinese and USA NO_x emission standards are more stringent than the EU and SA standards. It has become a norm than any new built BFBC, CFBC and conventional PF plants in the USA and China must consider a $DeNO_x$ unit to be able to meet these stringent limits. The cost implication has in some instance taken away the advantage that a FBC plant has over the conventional coal-fired boiler due to its non-thermal NO_x formation.

Figure 4-18 indicates that the BFBC produces less NO_x than the conventional pulverised coal-fired boilers and is below the local and the EU emission standards for all Ca/S ratios. NO_x emission results obtained during the tests indicate that the pilot scale BFBC has a positive impact on the emission of NO_x.

In summation:

- The production of NO_x increases with temperature and also with limestone addition. The production of N_2O decreases with increasing temperature and also with limestone addition.
- There are currently no emission limits for N_2O; however this is a more potent greenhouse gas than CO_2 and its production from BFBC reactors should be minimised. Conventional coal-fired boilers produce negligible N_2O and hence have an advantage over the BFBC in this regard.
- The NO_x produced from the BFBC coal combustion tests are lower than the SA minimum emission standard for NO_x and 25% lower than those currently produced by Eskom's pulverised coal-fired boiler. From a NO_x emission perspective, the BFBC emits less due to its lower operating temperature.
- However, international standard are more stringent than SA standards and the BFBC is able to meets at least one of the standards, the EU standard. These means that DeNOx units might have to be installed should SA revise its standard to follow the USA and Chinese. Air staging is able to achieve further NO_x reduction; it is a less expensive option than the $DeNO_x$ units.
- These tests have shown that NO_x production from the BFBC testing facility is low and that it falls within the trends in FBC experienced world-wide. This infers that BFBC is capable of burning SA coals effectively, therefore inducing less environmental concerns, with respect to NO_x, as opposed to the conventional pulverised coal-fired plants.

4.4.4 Ash Depositions in BFBC

"How does the coal constituent affect ash deposition in BFBC?"

FBC ash consists mainly of anhydrite (CaSO4), lime (CaO), silica (SiO2), and related oxides of magnesium, iron, and dehydroxylated clays originating from coals (Yoon, Balunaini and Prezzi, 2007). Zevenhoven-Onderwater et al (2000) mentions that a number of empirically based slagging and fouling indices have been developed over the years and that these methods are based on the production of laboratory ashes, which have little in common with the ashes found in a boiler. Kovacs (2003) state that bed agglomeration are related to high content of alkali metals in the coal, combined with high sulphur content, chlorine, silica, and phosphorous. All these aspects form part of the inputs into the determination of slagging and fouling indices. Slagging propensities as shown in Table 4-6 were determined from the coal analysis of the coals tested.

Table 4-7: Slagging Propensity of the Coals

Properties	Unit	Coal A	Coal B	Coal C
SiO_2 - Ratio	%	84,45	91,52	80,25
Alkali Index	%	0,16	0,71	0,13
Base / Acid Ratio	%	0,13	0,09	0,15
Fouling Index	%	0,08	0,19	0,06
Slagging Index	%	0,23	0,13	0,40
Slagging Propensity	%	LOW	LOW	LOW

The agglomeration prediction ratios used in this research are based on the acid/base ratio, slagging index and the fouling index. As presented in Table 4-7, the three coals were found to have low slagging propensities. However, agglomeration and slagging can occur if the process experiences poor fluidisation and poor mixing due to low fluidisation velocity, excess bed material and coarse bed particles. Localised high temperature points within the BFBC could also lead to slagging through the decomposition and melting of minerals at those localised temperatures. Fly ash mineralogy assessment (QEMSCAN) was used to identify the different minerals in the fly ashes obtained during the tests. The mineralogy of fly ashes from coal A, B and C at 850 °C are shown in Figure 4-19, 4-20 & 4-21 respectively.

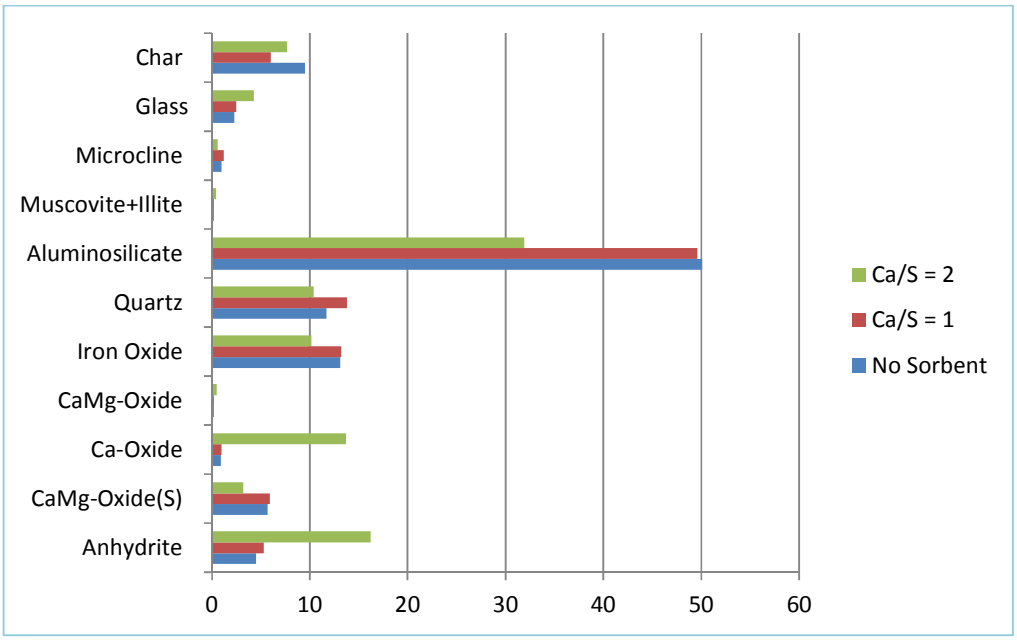


Figure 4-19: Fly Ash Mineralogy from Coal A

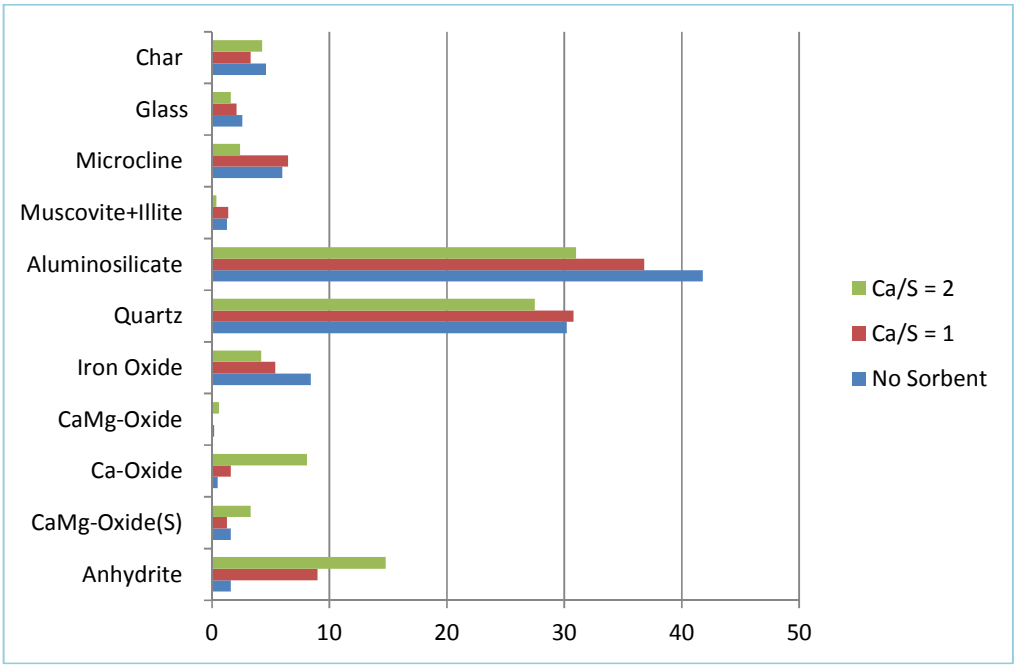


Figure 4-20: Fly Ash Mineralogy from Coal B

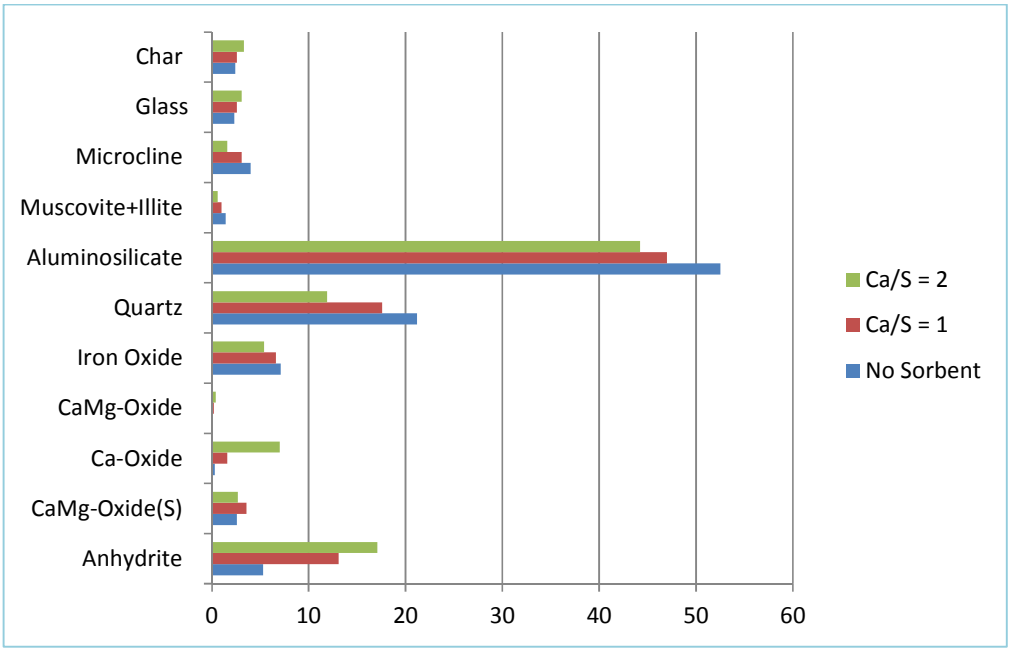


Figure 4-21: Fly Ash Mineralogy from Coal C

The predominant minerals found in the fly ashes are the mullite (aluminosilicate), quartz and anhydrite. These minerals have melting points (Table 2-4) higher than the operating temperatures of FBC boilers. A small fraction (<5%) of glass was found in the fly ashes, this might be an indication of some agglomeration during the tests. An observation of the coarse ash showed no sign of slagging or fouling. Therefore from an analytical and testing point of view, the ashes from the BFBC do not display any tendencies of ash deposition.

In summation:

- The BFBC operates at temperatures lower than the ash melting points of most coals. However particle temperature is higher than the overall bed temperature and in some cases ash melting point has been reached leading to severe ash agglomeration.
- From a pure analytical assessment, the coals display low slagging propensity.
- Physical inspection of the plant after the test showed no agglomeration or slagging.
- Therefore the current tests indicate that the BFBC can combust coal without slagging or fouling.

CHAPTER 5 : CONCLUSIONS AND RECOMMENDATIONS

4.5 Conclusion

The primary objective of this study was to establish the combustibility of high-ash coals (power station and discard coals) in Eskom's pilot BFBC facility. Coal combustion tests with and without limestone addition were conducted with the aim of computing carbon efficiency, gaseous emissions and the constituents' of fly ash at different bed temperatures. This section concludes on the findings of this dissertation.

- The amount of carbon-in-ash from the BFBC is higher than that experienced in conventional pulverised coal-fired boilers. This amount of carbon-in-ash is indirectly proportional to BFBC bed temperature. Fly ash from Coal C had the lowest carbon residue in ash for all test conditions.
- The carbon-in-ash percentage in the BFBC facility parallels with literature findings on the conversion of carbon in BFBC's.
- However excess air has an impact on carbon conversion, where if not adjusted to meet the stoichiometric requirements of both carbon and calcite, there will be less oxygen available for the reactions.
- The addition of limestone reduces the amount of SO_2 emitted. With the exception of coal A (SO_2 emission at a Ca/S molar ratio of 1 is below 500 mg/Nm^3 at 10 % O_2) Ca/S ratios higher than 1 are necessary to meet the minimum emission standard for new plants for coals B and C in South Africa.
- The fraction of anhydrite and CaO in the fly ash increased with the addition of limestone at 1 and 2 Ca/S ratios. The increase in CaO is indicative of the reaction limitation between the SO_2 gas and the CaO particles. This finding in the BFBC testing facility fly ash concurs with literature where less than 50 % of the limestone is utilised [Zhangfa (2003), Anthony and Granatstein (2001)].
- NO_x emission from the BFBC for all coals is lower than the minimum emission standard for new plants, but increases with bed temperature and with the addition of limestone. The highest emission was 487 mg/Nm^3 (at 10 % O_2) for coal A.
- The emission of N_2O is a concern for future application of FBC technology. However the addition of limestone and increases in bed temperature abate the emission of N_2O to acceptable levels. The highest was 418 mg/Nm^3 (at 10 % O_2) for Coal A.

- There was no agglomeration or slagging during the BFBC tests. This is due to the lower operating temperature of the BFBC and the low slagging propensity determined from ash composition.

Overall, this study has shown that low quality coals can be combusted in the BFBC with and without sorbent addition. The results showed that the considered coals can be combusted effectively with reduced emissions, without ash agglomeration, and with lower carbon-in-ash.

4.6 Recommendations

- Further research should be conducted using different sorbents (limestone and dolomites) to further assess the utilisation of sorbent in FBC plants.
- The mechanism of sulphur self-capture should be researched to develop a methodology of determining the reactivity of the calcium in coal.
- Future research on the utilisation of limestone should be undertaken; the aim would be to determine the possibility of maximising sorbent usage in FBC.
- A database of the different FBC fly ash mineralogy's using the QEMSCAN should be developed to understand the reaction of coal in FBC better.

REFERENCES

Anthony, E. J. and Granatstein, D. L. 2001. Sulfation Phenomena in Fluidized Bed Combustion Systems. *Progress in Energy and Combustion Science*. **27**, 215-236 (2001).

Alphen, C. 2005. *Factors Influencing Fly Ash Formation and Slag Deposit Formation (Slagging) on Combusting a South African Pulverised Fuel in a 200 MW_e Boiler* (Doctoral Thesis).University of the Witwatersrand, Johannesburg. South Africa

Avidan, A. A., Grace, J. R., Knowlton, T. M. 1997. *Circulating Fluidized Beds.* Chapman & Hall.

Aziz, T. Dittus, M.H. 2011. Kuyasa mine-mount coal-fired power project: Evaluation of circulating fluidised-bed technology. *Proceedings of the IFSA 2011 conference on fluidisation.* IFSA Johannesburg, South Africa pp 11- 26

Botha, M.F. Biyela, S.L. Fry, M.R. Paladh, R. 2011. Sewage-sludge incineration in South Africa using a fluidized-bed reactor. *Proceedings of the IFSA 2011 conference on fluidisation.* IFSA Johannesburg, South Africa pp 315 -323

Coal Technology. 2013. *Slagging and Fouling Indices.* [Accessed June 2013 http://www.coaltech.com.au/LinkedDocuments/Slagging%20&%20Fouling.pdf]

Eberhard, A. 2011. The Future of South African Coal: Market, Investment, and Policy Challenges. *Working Paper, Program on Energy and Sustainable Development*

Escudero, D. R. 2010. *Bed height and material density effects on fluidized bed hydrodynamics* (Graduate Theses and Dissertations). Iowa State University. Paper 11656.

Falcon, R.M.S. and Snyman, C.P. 1986. An introduction to coal petrography: Atlas of petrographic constituents in bituminous coals of Southern Africa. *The Geological Society of South Africa*, Review Paper Number 2.

Fueyo , N. Dopazo, C. 1995. Fluidization Fundamentals. *Pressurised Fluidized Bed Combustion* .

Hall, I. Eslait, J. den Hoed, P. 2011. Khanyisa IPP–a 450-MWe CFB project: Practical challenges. *A paper in the proceedings of a conference on fluidization 16–17 November 2011, Johannesburg, South Africa*. Pg 47-55

Holdich, R. G. 2002. *Fundamental of Particle Technology*. Midland Information Technology and Publishing, Loughborough, UK . Chapter 7

Howard, J.R. Elliot, D. 1983. *Fluidised Beds: Combustion and Applications.* Applied Science Publishers

French, D. Ward, C.R. 2009. The application of advanced mineralogical techniques to coal combustion product characterisation. *2009 World of Coal Ash (WOCA) Conference – May 4-7*. lexington, KY, USA.

Galbreath, K. Zygarlicke, C. Casuccio, G. Moore, T. Gottlieb, P. Agron-Olshina, N. Huffman, G. Shah, A. Vang, N. Vleeskens, J. Hamburg, G. 1996. Collaborative study of quantitative coal mineral analysis using Computer-Controlled Scanning Electron Microscopy. *Fuel. vol. 75*. 4. pp. 424-430.

IEA Clean Coal Center. June 2006. *Profiles: Development in Fluidised Bed Combustion Technology*. CCC/110, ISBN 92-9029-426-4,

IEA Clean Coal Center. November 2013. *Profiles: Techno-economic analysis of PC versus CFB combustion technology.* CCC/226, ISBN 978-92-9029-546-4,

Johnsson, F. 2007. Fluidized Bed Combustion for Clean Energy. *2007 ECI Conference on the 12th International Conference on Fluidization - New Horizons in Fluidization Engineering.*

Konttinen, J. Kallio, S. Hupa, M. Winter, F. 2013. NO formation tendency characterization for solid fuels in fluidized beds. *Fuel 108.* Pg 238-246

Kovacs, J. 2001. *What are the main characters of fluidised bed combustors?* [Accessed February 2012 http://www.handbook.ifrf.net/handbook/cf.html?id=87]

Kovacs, J. 2003. *What is fluidised bed agglomeration?* [Accessed June 2013 http://www.handbook.ifrf.net/handbook/]

Lloyd, P. J. 2000. The potential of coal wastes in South Africa. *The Journal of The South African Institute of Mining and Metallurgy.*

Mladenovic, M. R. Dakic, D. V. Nemoda, S. D. Mladenovic, R. V. Eric, A. M. Repic, B. S. Komatina, M. S. 2012. Combustion of Low Grade Fractions of Lubnica Coal in Fluidized Bed. *Thermal Science. Vol. 16, No. 1*, pp. 297-311

Matjie, R. H. 2008. *Sintering and Slagging Mineral Matter of South African Coals during the Coal Gasification Process* (Doctoral Thesis). University of Pretoria, South Africa

Moodley, L. *The evaluation of the Fluidised Bed Combustion performance of South African coals in the presence of sorbents (*Masters Dissertation). University of Kwa-Zulu Natal. Durban

North, B. 2010. Utilisation of low grade fuels in Fluidised Bed Combustors. *Proceeding at the Clean Coal to Clean Energy Research and Development to meet Supply and Demand for Africa. 17 and 18 November*. CD Fossil Fuel Foundation of Africa. Johannesburg, South Africa

North, B.C. 2012. *Utilization of low grade fuels in fluidised bed combustors.* Vol 1. (Doctoral Thesis) University of Witwatersrand, Johannesburg. South Africa

Olsson, J. 2008. *Modelling of Bubble Flow in Fluidized Bed Combustion Units* (Dissertation*)* Chalmers University of Technology, Goteborg. Sweden

Pando, M. Hwang, S. Guadalupe, Y. Reyes, A. Rossi, L. Ruiz, E. 2006. Possible Applications for Circulating Fluidized Bed Coal Combustion By-Products from the Guayama Aes Power Plant. University of Puerto Rico. Mayagüez. PR, 00681-9041

Perry, R. H. Green, D.W. Maloney, J. O. 2007. *Perry's Chemical Engineers' Handbook*. 7th Edition. McGraw-Hill

Petrie, J. G. 1985. Fluidised Bed Combustion of S. A. Coals – Final Report. *Energy Research Institute*. Report No. 83

Shindell, D. Faluvegi, G. 2010. The net climate impact of coal-fired power plant emissions. *Atmos. Chem. Phys., 10, 3247–3260, 2010*

Shen, X. 2009. Coal Combustion and Combustion Products. *Coal, Oil Shale, Natural Bitumen, Heavy Oil and Peat*. Vol. 1. EOLSS Publishers Co Ltd

Singh, S. 2011. Maceral identification and quantification by QEMSCAN/Determination of washability curves using QEMSCAN. *Presentation to the CoalTech Research Association Annual Colloquium 22 July*.

Suksankraisorn, K. Patumsawad, S. Fungtammasa, B. 2001. Prediction of Minimum Fluidisation Velocity from Correlations: An Observation. *Asian J. Energy Environ.* Vol 2. Issue 2 pp. 145-154

Sulovsky, P. 2002. Mineralogy and chemistry of conventional and fluidised bed coal ashes. *Bulletin of the Czech Geological Survey*, Vol. 77, No. 1, 1–11. Czech Geological Survey, ISSN 1210-3527

Utt, J. Giglio, R. 2011. Technology comparison of CFB versus pulverized-fired firing for utility power generation. *A paper in the proceedings of a conference on fluidization 16–17 November 2011, Johannesburg, South Africa.* Pg 91 -99

Valentim, B. Lemos de Sousa, M. J. Abelha, P. Gulyurtlu, I. 2006. Combustion of studies in a fluidised bed – The link between temperature, NOxs and N2O formation, char morphology and coal type. *International Journal of Coal Geology 67.* pp 191 -201

Yoon, S. Balunaini, U. Prezzi, M. 2007. Forensic examination of the severe heaving of an embarkment constructed with fluidized-bed-combustion (FBC) ash. *Transportation Research Record: Journal of the Transportation Research Board.* Pg 9 - 17

Zenenhoven-Onderwater, M. Blomquist, J, P. Skrifvars, B. J. Backman, R. Hupa, M. 2000. The prediction fo behaviour of ashes from five different solid fuels in fluidised bed combustion. *Fuel 79.* Pg 1353 - 1361

Zhangfa Wu. 2003. *Understanding Fluidised Bed Combustion*. IEA Clean Coal Center. CCC/76

APPENDIX A: COAL AND SORBENT ANALYSIS DATA

Table A-1: Chemical Analysis Data for Coal A

Ultimate and Proximate Analysis		
Inherent Moisture	%	2.1
Volatile Matter	%	19.8
Ash	%	36.3
Carbon (by difference)	%	41.8
Total Carbon (Instrument)	%	48.65
Nitrogen	%	2.34
Hydrogen	%	1.11
Total sulphur	%	1.79
Carbonate (as CO_2)	%	1.81
Oxygen (difference)	%	5.9
Gross Caloric Value (HHV)	MJ/kg	18.63
Net Caloric Value (LHV)	MJ/kg	18.39
Total Moisture	%	5.2
Ash Analysis		
Silicon (as SiO_2)	%	54.3
Aluminium (as Al_2O_3)	%	26.5
Calcium (as CaO)	%	6.1
Magnesium (as MgO)	%	1.3
Iron (as Fe_2O_3)	%	2.6
Potassium (as K_2O)	%	0.5
Manganese (as MnO)	%	0.01
Sodium (as Na_2O)	%	0.1
Phosphorus (as P_2O_5)	%	1.04
Titanium (as TiO_2)	%	1.7
Chromium (as Cr_2O_3)	%	0.01
Vanadium (as V_2O_5)	%	0.01
Loss on Ignition	%	3.87

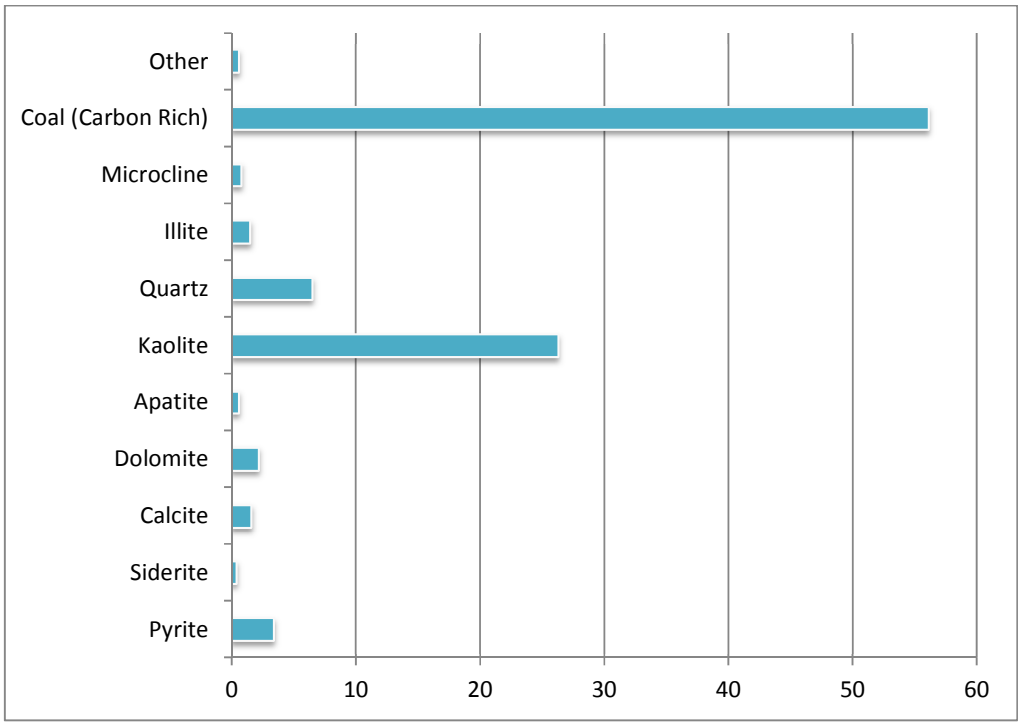


Figure A-1: Mineralogy Assessment Graph for Coal A

Table A-2: Chemical Analysis Data for Coal B

Ultimate and Proximate Analysis		
Inherent Moisture	%	2.7
Volatile Matter	%	19.7
Ash	%	52.5
Carbon (by difference)	%	25.1
Total Carbon (Instrument)	%	32.78
Nitrogen	%	2.12
Hydrogen	%	0.58
Total sulphur	%	1.41
Carbonate (as CO_2)	%	1.45
Oxygen (difference)	%	6.46
Gross Caloric Value (HHV)	MJ/kg	13.6
Net Caloric Value (LHV)	MJ/kg	12.68
Total Moisture	%	2.7
Ash Analysis		
Silicon (as SiO_2)	%	67.2
Aluminium (as Al_2O_3)	%	20.1
Calcium (as CaO)	%	1.23
Magnesium (as MgO)	%	0.63
Iron (as Fe_2O_3)	%	4.37
Potassium (as K_2O)	%	1.85
Manganese (as MnO)	%	0.01
Sodium (as Na_2O)	%	0.09
Phosphorus (as P_2O_5)	%	0.07
Titanium (as TiO_2)	%	0.88
Chromium (as Cr_2O_3)	%	0.01
Vanadium (as V_2O_5)	%	0.01
Loss on Ignition	%	2.74

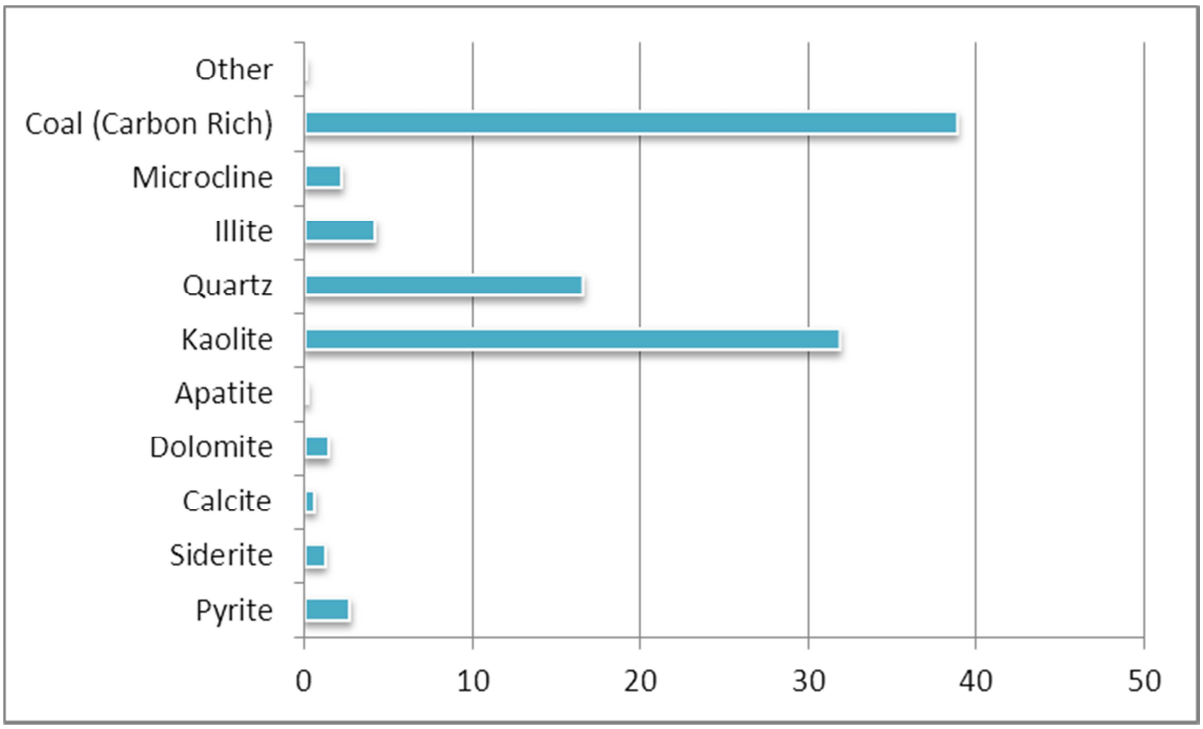


Figure A-2: Mineralogy Assessment Graph for Coal B

Table A-3: Chemical Analysis Data for Coal C

Ultimate and Proximate Analysis		
Inherent Moisture	%	2.8
Volatile Matter	%	18.1
Ash	%	45.2
Carbon (by difference)	%	33.9
Total Carbon (Instrument)	%	37.52
Nitrogen	%	1.92
Hydrogen	%	0.76
Total sulphur	%	2.67
Carbonate (as CO_2)	%	2.35
Oxygen (difference)	%	6.78
Gross Caloric Value (HHV)	MJ/kg	14.54
Net Caloric Value (LHV)	MJ/kg	14.12
Total Moisture	%	2.8
Ash Analysis		
Silicon (as SiO_2)	%	47.3
Aluminium (as Al_2O_3)	%	32.4
Calcium (as CaO)	%	3.05
Magnesium (as MgO)	%	0.78
Iron (as Fe_2O_3)	%	7.81
Potassium (as K_2O)	%	0.33
Manganese (as MnO)	%	0.08
Sodium (as Na_2O)	%	0.05
Phosphorus (as P_2O_5)	%	0.02
Titanium (as TiO_2)	%	2.08
Chromium (as Cr_2O_3)	%	0.02
Vanadium (as V_2O_5)	%	0.01
Loss on Ignition	%	4.93

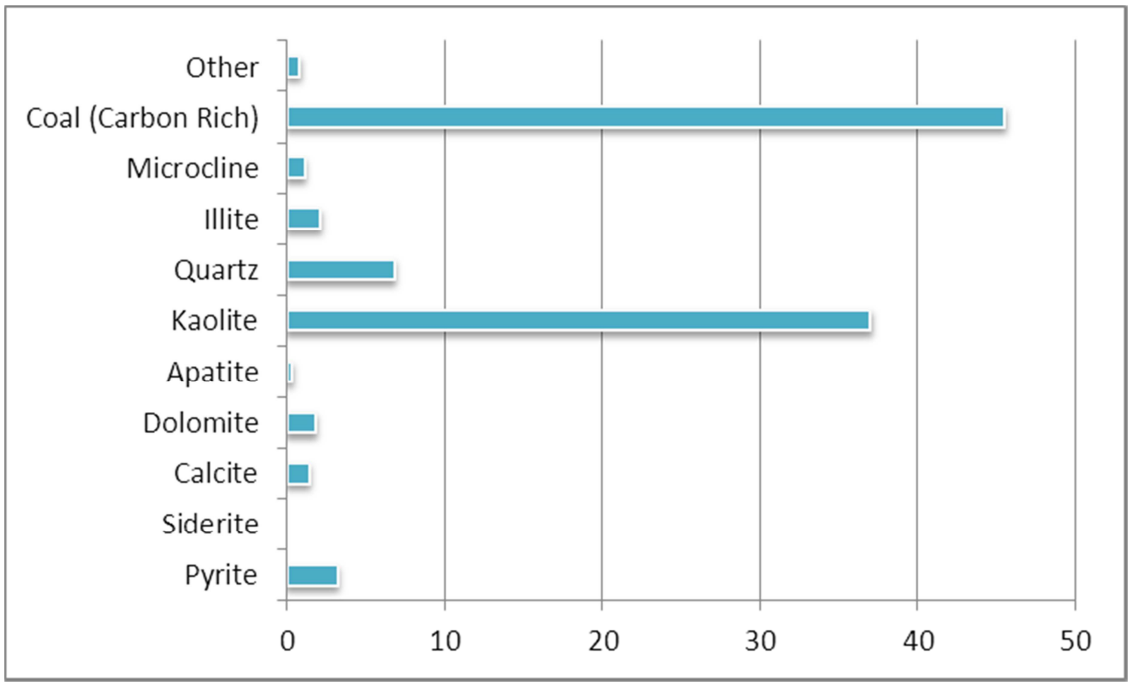


Figure A-3: Mineralogy Assessment Graph for Coal C

Table A-4: Chemical Analysis of Limestone

	Unit	Value
Silicon (as SiO_2)	%	5.00
Aluminium (as Al_2O_3)	%	0.69
Calcium (as CaO)	%	49.00
Magnesium (as MgO)	%	3.12
Iron (as Fe_2O_3)	%	0.49
Potassium (as K_2O)	%	0.40
Manganese (as MnO)	%	0.56
Sodium (as Na_2O)	%	0.05
Phosphorus (as P_2O_5)	%	0.01
Titanium (as TiO_2)	%	0.02
Chromium (as Cr_2O_3)	%	0.01
Vanadium (as V_2O_5)	%	0.01
Loss on Ignition	%	40.49

APPENDIX B: COAL A TEST RESULTS

Table B-1: Experimental Test Data for Coal A

	Units	Test 0.1	Test 0.2	Test 0.3	Test 0.4	Test 0.5	Test 0.6	Test 0.7	Test 0.8	Test 0.9
Molar Ratio										
Ca/S = 0		X	X	X						
Ca/S = 1					X	X	X			
Ca/S = 2								X	X	X
Bed Temperature										
830	˚C	X			X			X		
850	˚C		X			X			X	
870	˚C			X			X			X
Air										
Total air	kg/hr	74.70	74.74	75.00	76.92	76.00	75.90	76.10	76.50	76.30
Combustion/Primary		3.80	3.80	3.90	3.70	3.70	3.70	3.80	3.80	3.80
Excess Air		36.67	40.74	40.57	38.19	39.95	36.57	53.71	50.50	45.59
Fuel										
Coal Flow	kg/hr	8.50	8.50	8.50	8.50	8.50	8.50	8.50	8.50	8.50
Thermal Input	kW	43.99	43.99	43.99	43.99	43.99	43.99	43.99	43.99	43.99
Sorbent										
Flow	kg/hr	0.00	0.00	0.00	0.59	0.59	0.59	1.18	1.18	1.18
Reactor										
Fludising Velocity	m/s	1.10	1.12	1.14	1.22	1.26	1.25	1.22	1.23	1.23
Pressure	kPa	55.00	55.00	55.00	55.00	55.00	55.00	55.00	55.00	55.00
Gaseous Emission										
O2	%	5.62	6.06	6.05	5.79	5.98	5.61	7.32	7.03	6.56
CO	ppm	173.73	164.13	168.55	219.95	193.11	210.84	213.14	171.11	161.54
CO (6% O2)	mg/m^3	175.03	170.28	174.66	224.07	199.22	212.27	241.50	189.85	173.38
CO (6% O2) STP	mg/Nm^3	211.62	205.88	211.16	270.91	240.87	256.64	291.98	229.53	209.62
CO2	%	12.30	11.94	12.01	13.19	13.00	12.84	11.81	12.12	12.67
CO2 (6% O2)	g/m^3	194.72	194.68	195.54	211.14	210.74	203.12	210.31	211.37	213.62
CO2 (6% O2) STP	g/Nm^3	235.42	235.37	236.41	255.27	254.79	245.58	254.27	255.55	258.27
NOx	ppm	112.31	145.45	159.08	292.34	363.06	334.09	424.61	453.16	465.95
NOx (6% O2)	mg/m^3	121.23	161.68	176.62	319.09	401.32	360.39	515.49	538.69	535.80
NOx (6% O2) STP	mg/Nm^3	146.58	195.47	213.53	385.78	485.20	435.72	623.24	651.29	647.80
N2O	ppm	218.42	188.18	176.61	179.82	148.71	151.98	139.71	123.06	117.06
N2O (6% O2)	mg/m^3	345.81	306.79	287.58	287.87	241.09	240.45	248.76	214.55	197.43
N2O (6% O2) STP	mg/Nm^3	418.10	370.92	347.69	348.04	291.48	290.71	300.75	259.40	238.69
SO2	ppm	554.77	515.20	634.21	197.49	154.06	140.00	6.79	6.49	7.50
SO2 (6% O2)	mg/m^3	1277.57	1221.76	1502.16	270.01	889.62	531.21	185.03	106.10	150.83
SO2 (6% O2) STP	mg/Nm^3	1544.62	1477.14	1816.15	555.98	439.23	389.51	21.26	19.90	22.24
SO2 Retention		69.06	71.22	64.47	88.73	91.30	92.09	99.61	99.63	99.57
N2	%	81.97	81.89	81.83	80.93	80.94	81.47	80.79	80.77	80.70
Combustion matter in fly-ash	%	10.80	9.50	8.00	7.10	6.00	6.60	9.50	7.70	6.80
Combustion Efficiency	%	90.97	92.17	93.51	94.30	95.24	94.73	92.17	93.78	94.56

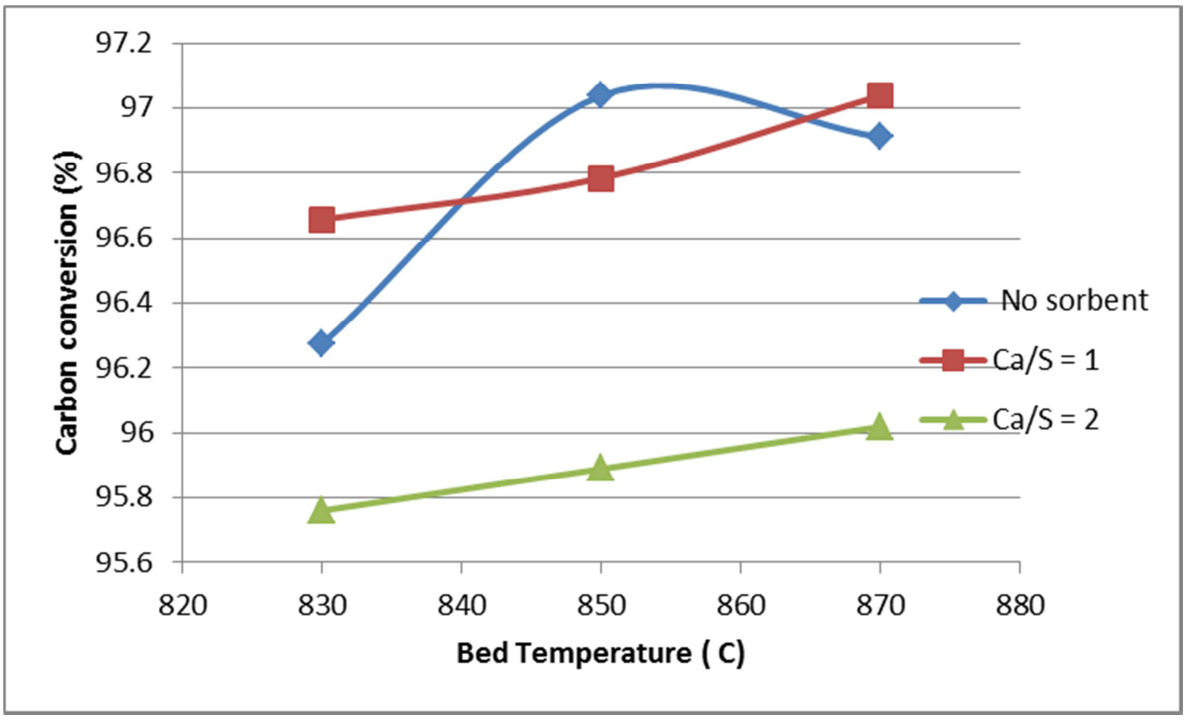


Figure B-1: Carbon Conversion for Coal A

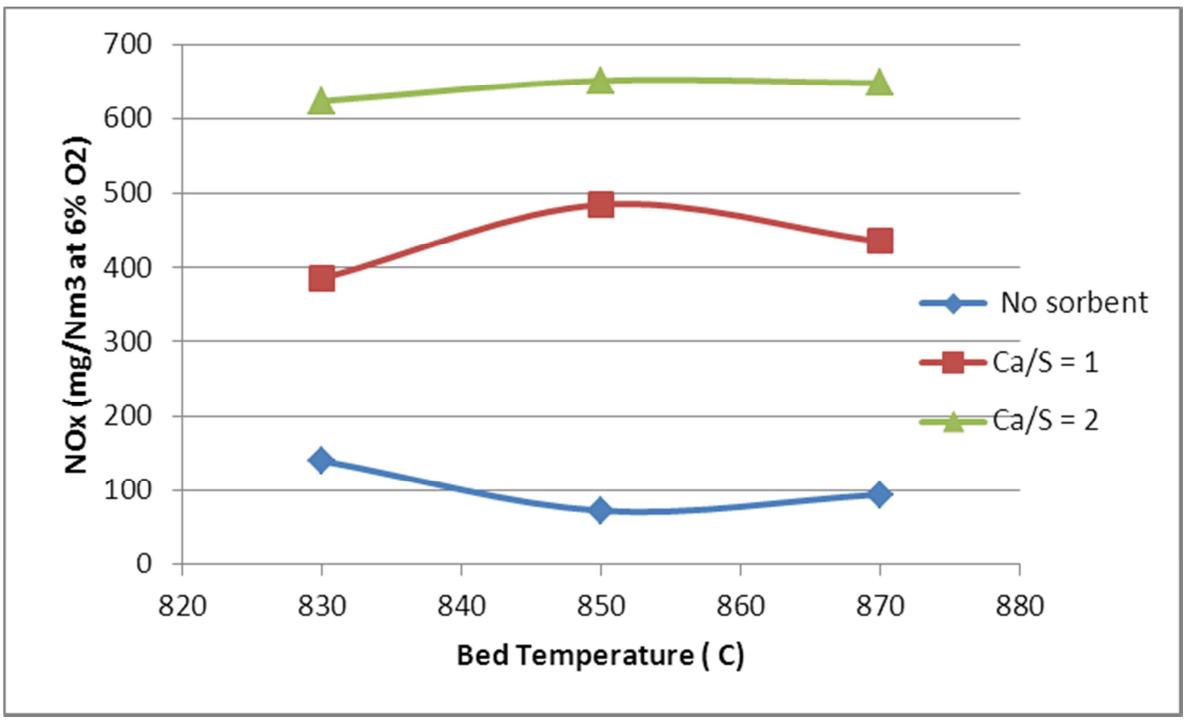


Figure B-2: NO_x Emissions for Coal A

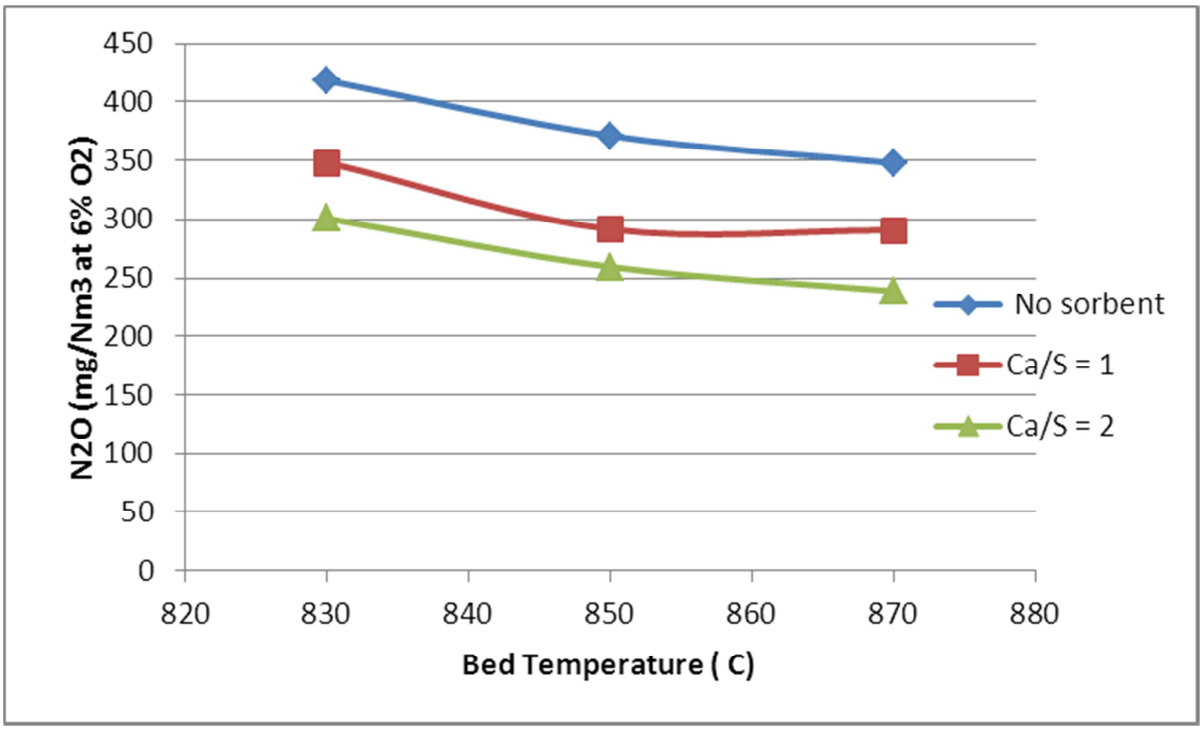


Figure B-3: N_2O Emissions for Coal A

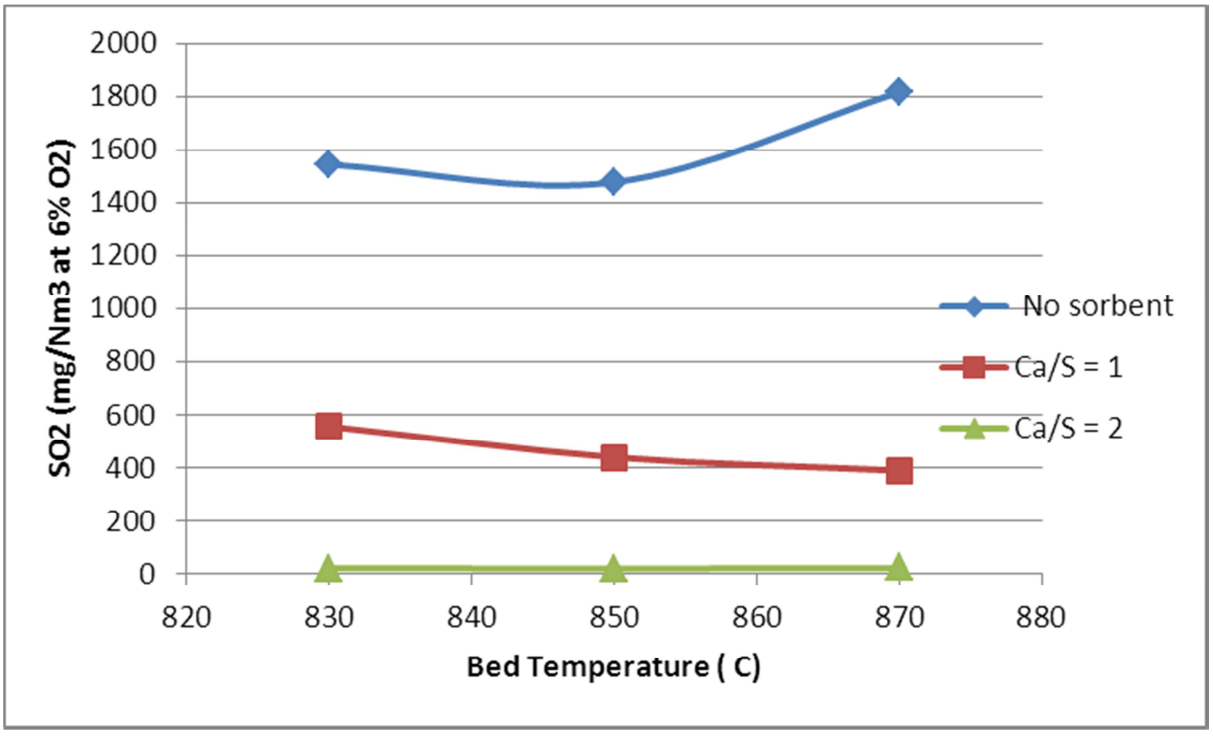


Figure B-4: SO_2 Emissions for Coal A

APPENDIX C: COAL B TEST RESULTS

Table C-1: Testing Results for Coal B with and without Limestone

	Units	Test 1.1	Test 1.2	Test 1.3	Test 1.4	Test 1.5	Test 1.6	Test 1.7	Test 1.8	Test 1.9
Molar Ratio										
Ca/S = 0		X	X	X						
Ca/S = 1					X	X	X			
Ca/S = 2								X	X	X
Bed Temperature										
830	^{0}C			X			X	X		
850	^{0}C		X		X				X	
870	^{0}C	X				X				X
Air										
Total air	kg/hr	72,00	71,24	71,59	71,87	71,48	72,06	71,92	71,38	71,91
Combustion/Primary		2,95	3,07	3,05	3,12	3,13	3,08	3,00	2,92	2,82
Excess Air		34,84	37,14	37,88	37,50	36,04	35,63	33,88	27,70	26,95
Fuel										
Coal Flow	kg/hr	8,00	8,00	8,00	8,00	8,00	8,00	8,00	8,00	8,00
Thermal Input	kW	30,22	30,22	30,22	30,22	30,22	30,22	30,22	30,22	30,22
Sorbent										
Flow	kg/hr	0,00	0,00	0,00	0,40	0,40	0,40	0,79	0,79	0,79
Reactor										
Fludising Velocity	m/s	0,99	0,95	0,98	1,01	1,04	1,00	0,98	0,97	0,96
Pressure	kPa	55,00	55,00	55,00	55,00	55,00	55,00	55,00	55,00	55,00
Gaseous Emission										
O2	%	5,41	5,67	5,76	5,71	5,55	5,50	5,30	4,55	4,45
CO	ppm	116,09	83,19	110,90	86,41	82,21	97,15	90,66	84,37	78,84
CO (6% O2)	mg/m^3	115,40	84,11	115,40	115,40	115,40	115,40	115,40	115,40	115,40
CO (6% O2) STP	mg/Nm^3	139,52	99,98	133,29	103,85	98,81	116,76	108,96	101,40	94,76
CO2	%	12,24	12,27	12,16	12,48	12,61	12,69	13,08	13,77	13,49
CO2 (6% O2)	g/m^3	191,21	194,86	194,19	198,71	198,68	199,45	202,88	203,77	198,44
CO2 (6% O2) STP	g/Nm^3	231,17	235,59	234,78	240,25	240,21	241,14	245,29	246,37	239,92
NOx	ppm	210,62	206,31	165,43	248,63	250,69	236,43	316,36	391,87	311,66
NOx (6% O2)	mg/m^3	224,32	223,47	180,17	270,01	269,38	253,27	334,54	395,27	312,50
NOx (6% O2) STP	mg/Nm^3	271,21	270,18	217,83	326,45	325,69	306,21	404,47	477,89	377,82
N2O	ppm	123,08	133,77	176,48	134,29	121,20	149,76	122,30	94,12	104,57
N2O (6% O2)	mg/m^3	192,26	212,51	281,89	213,90	191,01	235,30	189,68	139,24	153,79
N2O (6% O2) STP	mg/Nm^3	232,45	256,93	340,81	258,61	230,93	284,48	229,33	168,35	185,93
SO2	ppm	848,36	1050,64	1047,45	395,34	388,08	232,45	82,02	49,31	70,51
SO2 (6% O2)	mg/m^3	1927,60	2427,84	2433,55	915,93	889,62	531,21	185,03	106,10	150,83
SO2 (6% O2) STP	mg/Nm^3	2330,51	2935,32	2942,23	1107,39	1075,57	642,24	223,70	128,28	182,35
SO2 Retension	%	39,61	26,01	25,86	71,94	72,61	83,47	94,19	96,54	95,01
N2		82,22	81,91	81,94	81,72	81,76	81,73	81,56	81,62	82,00
Combustion matter in fly-ash	%	4,80	4,60	4,40	3,30	3,60	4,10	4,40	4,30	3,30
Combustion Efficiency	%	91,92	92,28	92,63	94,53	94,02	93,15	92,63	92,80	94,53

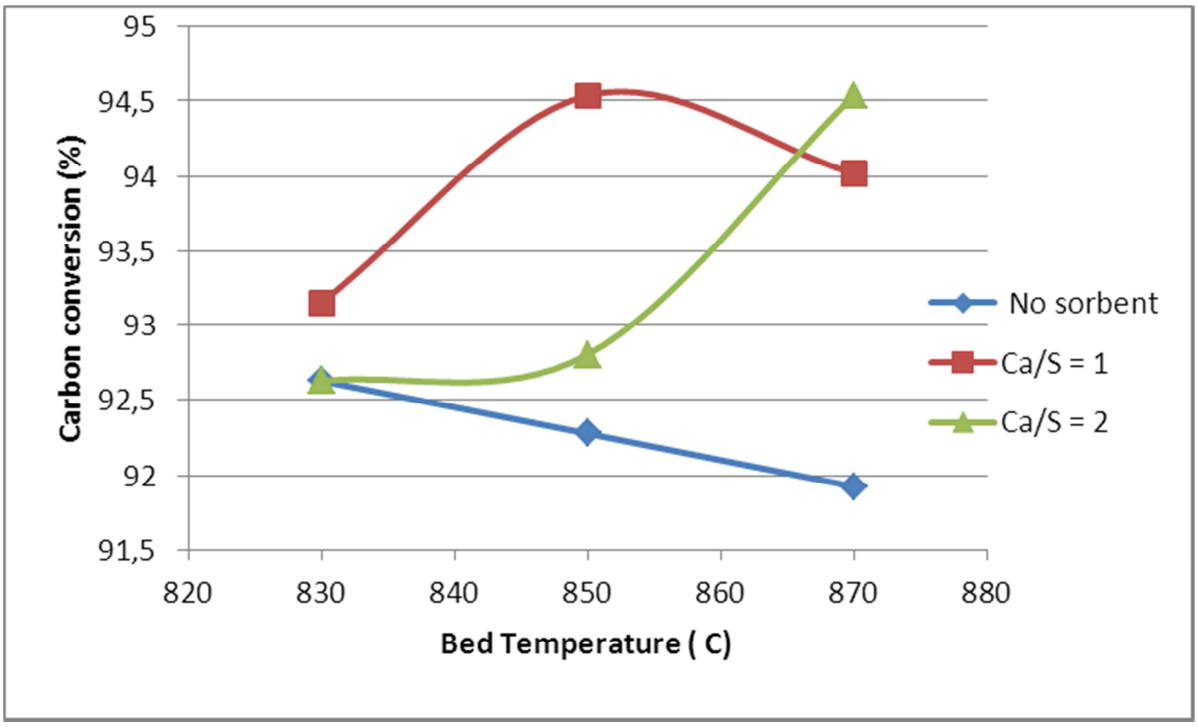


Figure C-1: Carbon Conversion for Coal B

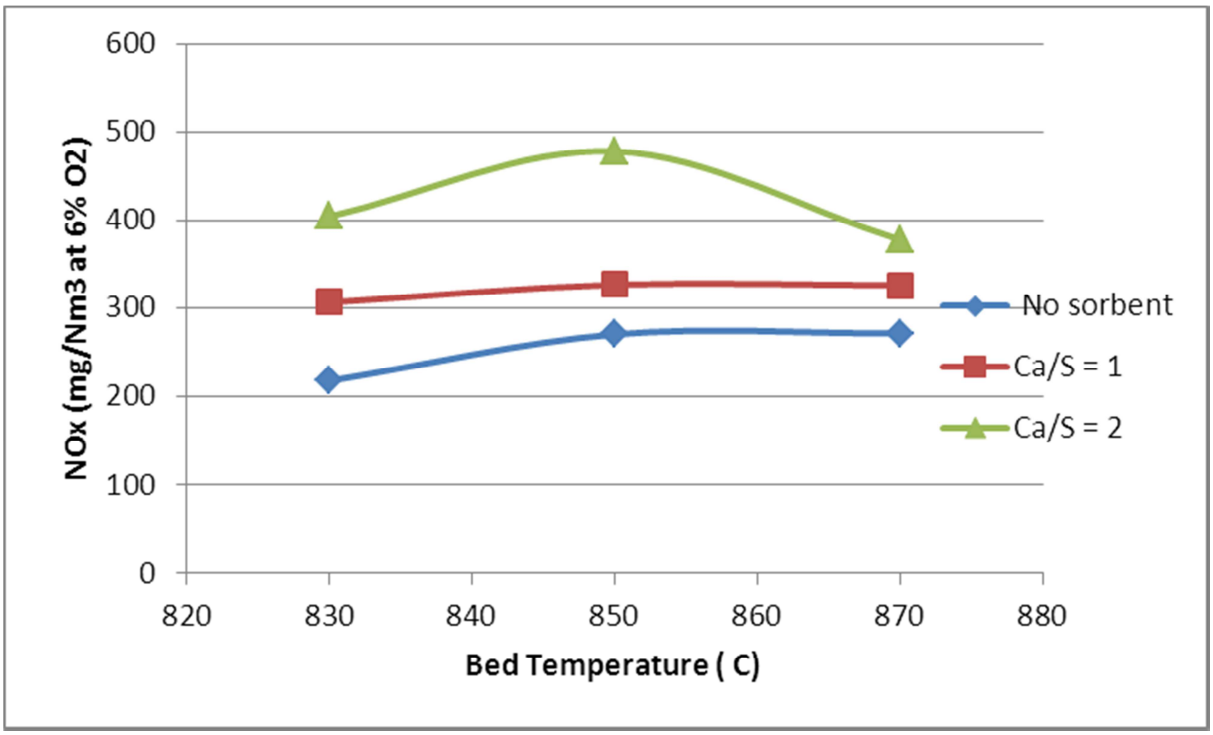


Figure C-2: NOx Emissions for Coal B

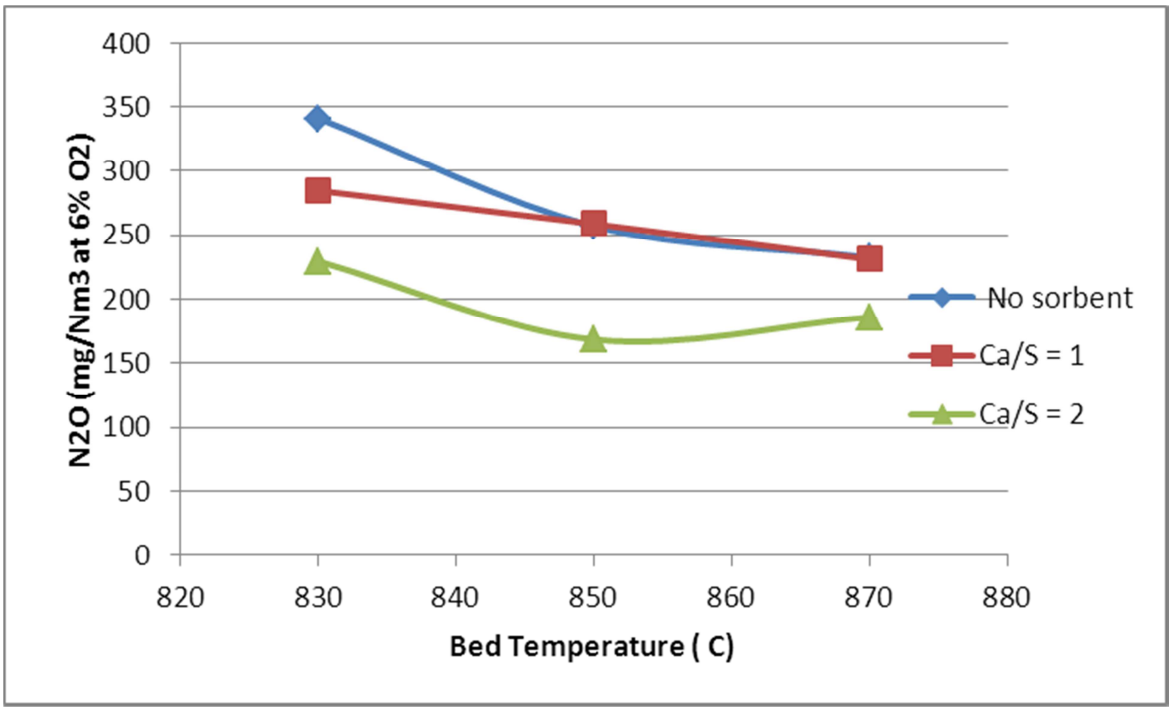


Figure C-3: N_2O Emissions for Coal B

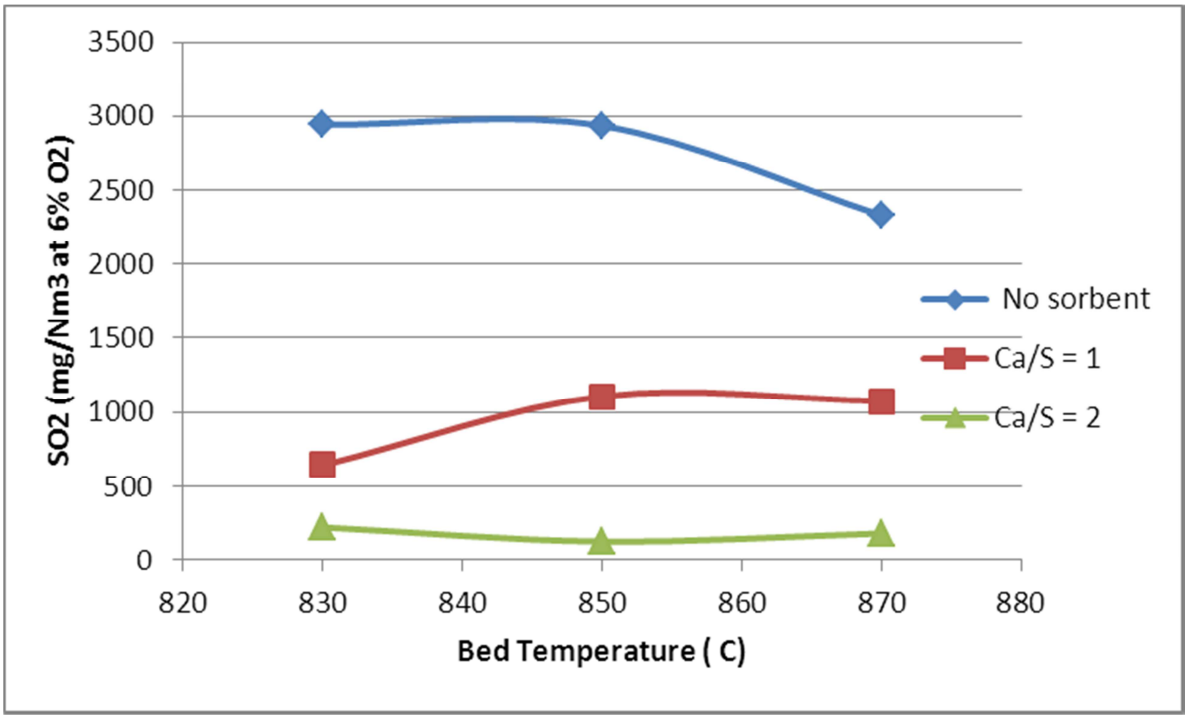


Figure C-4: SO_2 Emissions for Coal B

APPENDIX D: COAL C TEST RESULTS

Table D-1: Table Results for Coal C with and without Limestone

	Units	Test 2.1	Test 2.2	Test 2.3	Test 2.4	Test 2.5	Test 2.6	Test 2.7	Test 2.8	Test 2.9
Molar Ratio										
Ca/S = 0		X	X	X						
Ca/S = 1					X	X	X			
Ca/S = 2								X	X	X
Bed Temperature										
830	˚C	X					X	X		
850	˚C		X			X			X	
870	˚C			X	X					
Air										X
Total air	kg/hr	70,17	69,96	69,44	69,58	69,73	69,67	69,80	70,02	69,93
Combustion/Primary		3,20	3,19	3,17	3,15	3,20	3,15	3,12	3,08	3,07
Excess Air		31,60	30,09	28,00	27,64	28,15	29,48	28,20	25,65	26,84
Fuel										
Coal Flow	kg/hr	8,00	8,00	8,00	8,00	8,00	8,00	8,00	8,00	8,00
Thermal Input	kW	32,31	32,31	32,31	32,31	32,31	32,31	32,31	32,31	32,31
Sorbent										
Flow	kg/hr	0,00	0,00	0,00	0,70	0,70	0,70	1,50	1,50	1,50
Reactor										
Fludising Velocity	m/s	1,02	1,03	1,05	1,05	1,04	1,01	1,00	1,01	1,01
Pressure	kPa	55,00	55,00	55,00	55,00	55,00	55,00	55,00	55,00	55,00
Gaseous Emission										
O2	%	5,03	4,85	4,58	4,54	4,60	4,77	4,61	4,28	4,43
CO	ppm	122,05	102,63	94,49	84,27	90,05	103,78	113,01	101,94	92,31
CO (6% O2)	mg/m^3	118,40	98,43	89,17	79,30	85,07	99,06	106,80	94,43	86,31
CO (6% O2) STP	mg/Nm^3	143,15	119,00	107,80	95,87	102,85	119,76	129,13	114,16	104,35
CO2	%	13,03	12,97	13,10	13,55	13,46	13,37	13,75	14,14	14,23
CO2 (6% O2)	g/m^3	198,64	195,39	194,31	200,38	199,84	200,51	204,14	205,83	209,16
CO2 (6% O2) STP	g/Nm^3	240,16	236,23	234,92	242,26	241,61	242,42	246,81	248,85	252,88
NOx	ppm	137,16	160,75	179,04	217,84	212,78	213,39	277,34	335,70	400,55
NOx (6% O2)	mg/m^3	142,56	165,18	181,01	219,62	215,37	218,23	280,84	333,17	401,30
NOx (6% O2) STP	mg/Nm^3	172,36	199,71	218,85	265,53	260,39	263,84	339,54	402,81	485,18
N2O	ppm	170,06	158,43	136,05	120,04	135,15	154,53	146,95	121,91	97,55
N2O (6% O2)	mg/m^3	259,25	238,76	201,75	177,50	200,63	231,78	218,24	177,45	143,34
N2O (6% O2) STP	mg/Nm^3	313,44	288,66	243,92	214,60	242,56	280,22	263,86	214,54	173,30
SO2	ppm	1583,72	1511,79	1548,21	416,14	300,97	176,89	74,08	43,16	35,37
SO2 (6% O2)	mg/m^3	3511,72	3313,98	3339,25	895,03	649,89	385,92	160,02	91,37	75,60
SO2 (6% O2) STP	mg/Nm^3	4245,75	4006,68	4037,24	1082,11	785,74	466,59	193,47	110,47	91,41
SO2 Retention		41,71	44,47	43,56	84,82	88,99	93,53	97,29	98,42	98,71
N2	%	81,74	82,00	82,12	81,83	81,86	81,80	81,58	81,52	81,27
Combustion matter in fly-ash	%	3,00	2,40	2,50	2,40	2,60	2,70	3,40	3,30	3,20
Combustion Efficiency	%	96,27	97,04	96,91	97,04	96,78	96,66	95,76	95,89	96,02

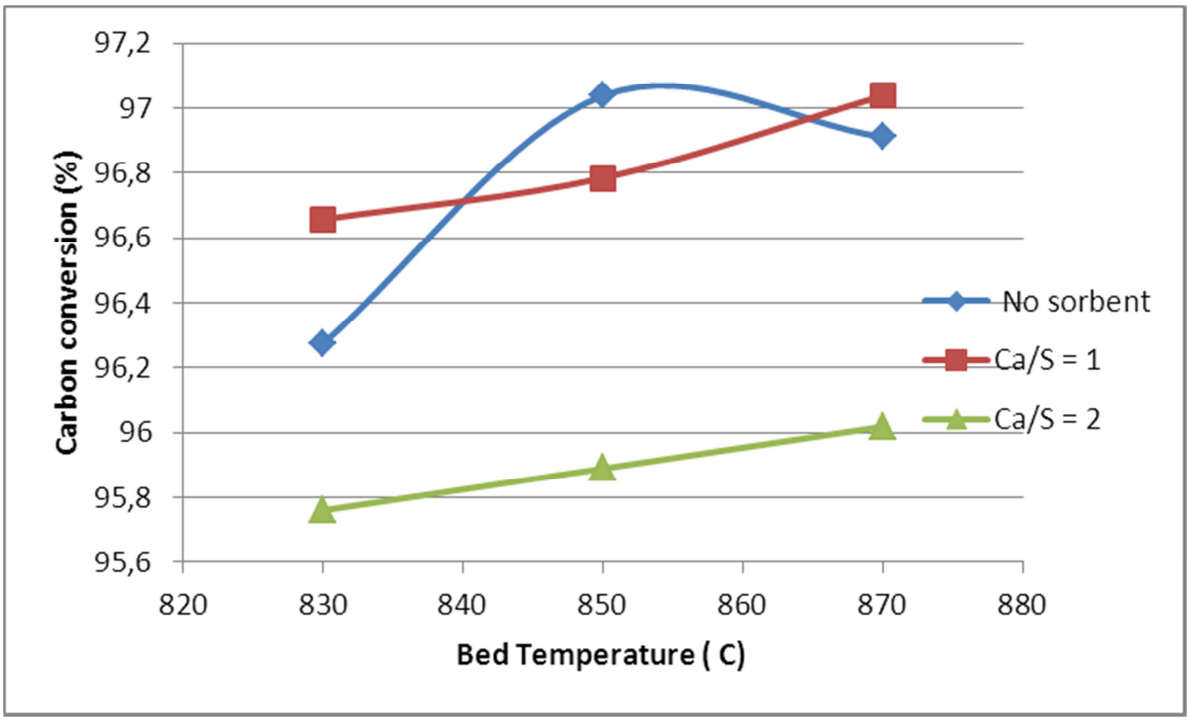


Figure D-1: Carbon Conversion for Coal C

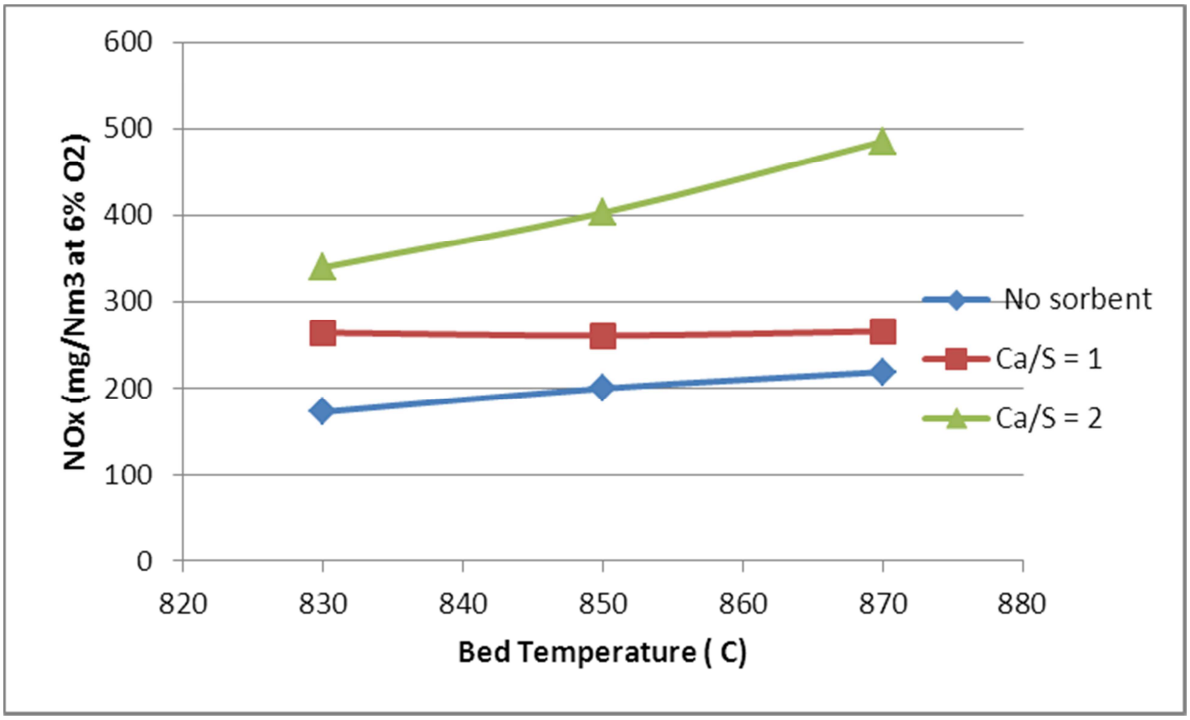


Figure D-2: NOx Emissions for Coal C

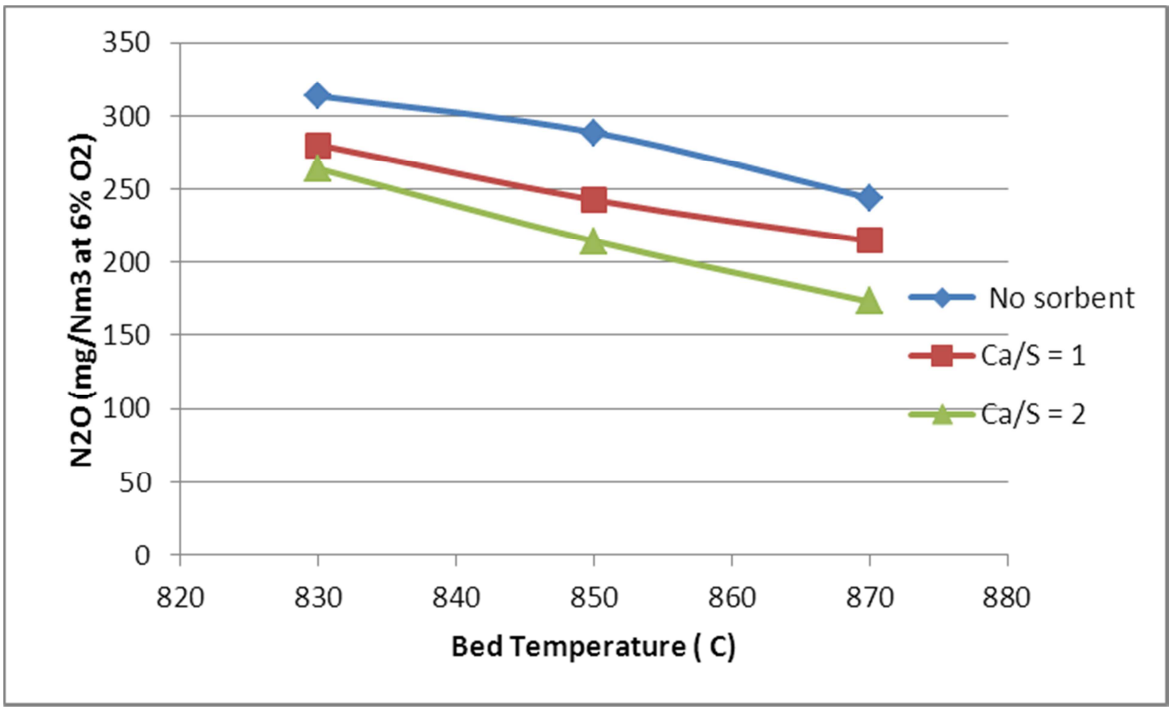


Figure D-3: N_2O Emissions for Coal C

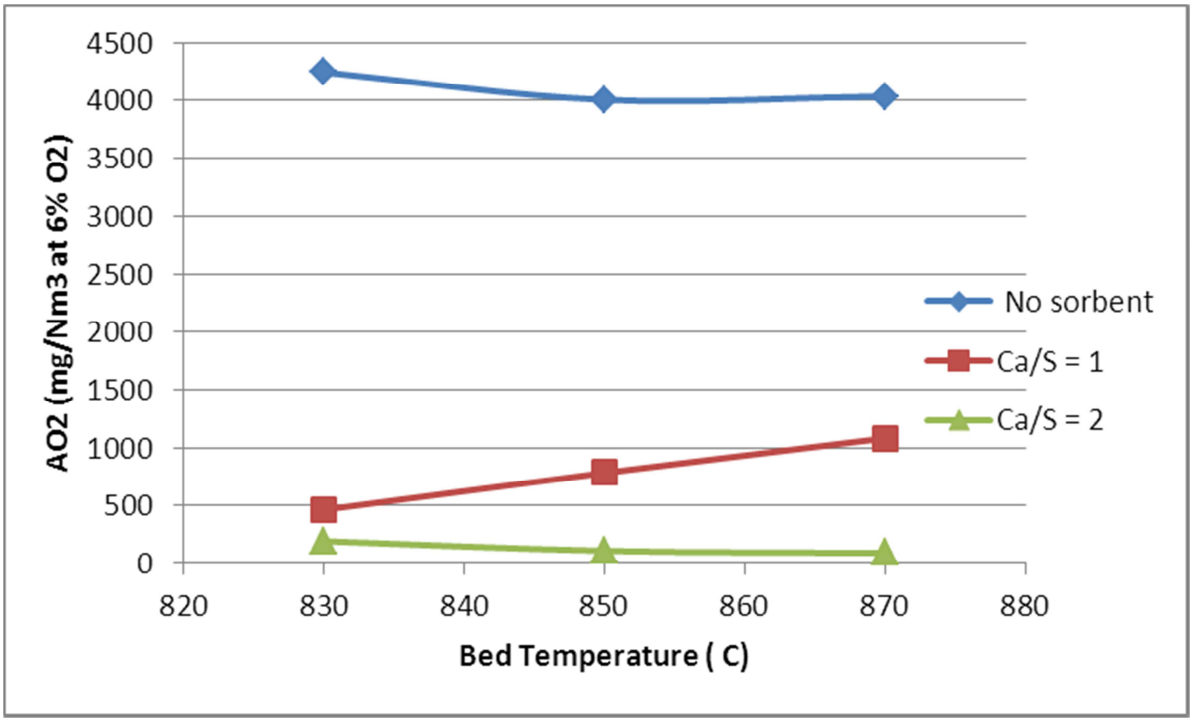


Figure D-4: SO_2 Emissions for Coal C

APPENDIX E: FLY ASH ANALYSIS DATA

The following figures represent the elemental fraction and mineralogy assessments of the fly ash samples submitted fot XRF analysis.

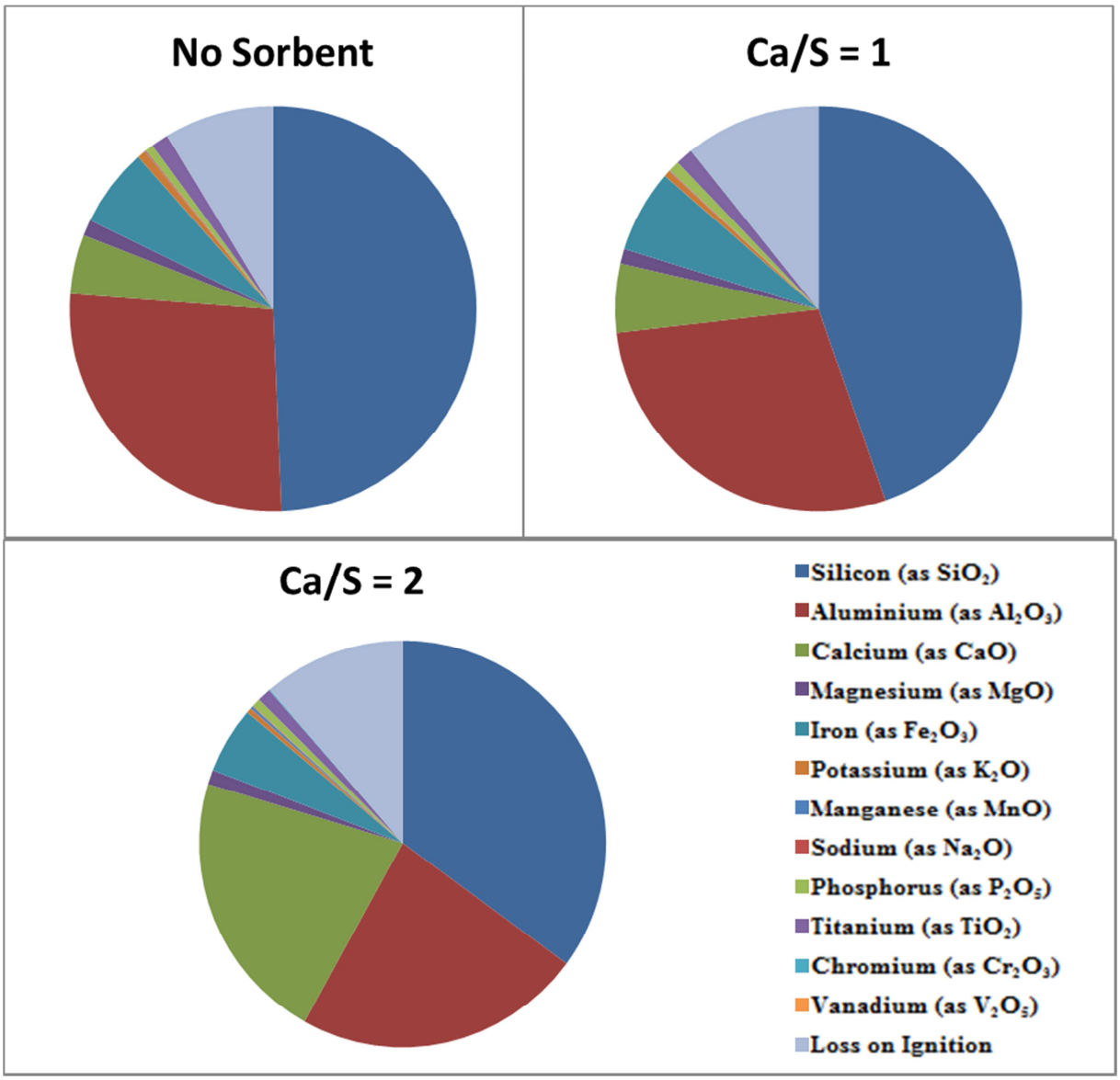


Figure E-1: Ash Elemental of fly ash from Coal A, 850 °C tests

Table E-1: Mineralogy Assessment of fly ash from Coal A, 850 °C tests

	No Sorbent	Ca/S = 1	Ca/S = 2
Anhydrite	4.5	5.3	16.2
CaMg-Oxide(S)	5.7	5.9	3.2
Ca-Oxide	0.9	1	13.7
CaMg-Oxide	0.2	0.2	0.5
Iron Oxide	13.1	13.2	10.2
Quartz	11.7	13.8	10.4
Aluminosilicate	50.1	49.6	31.9
Muscovite+Illite	0.2	0.2	0.4
Microcline	1	1.2	0.6
Glass	2.3	2.5	4.3
Char	9.5	6	7.7

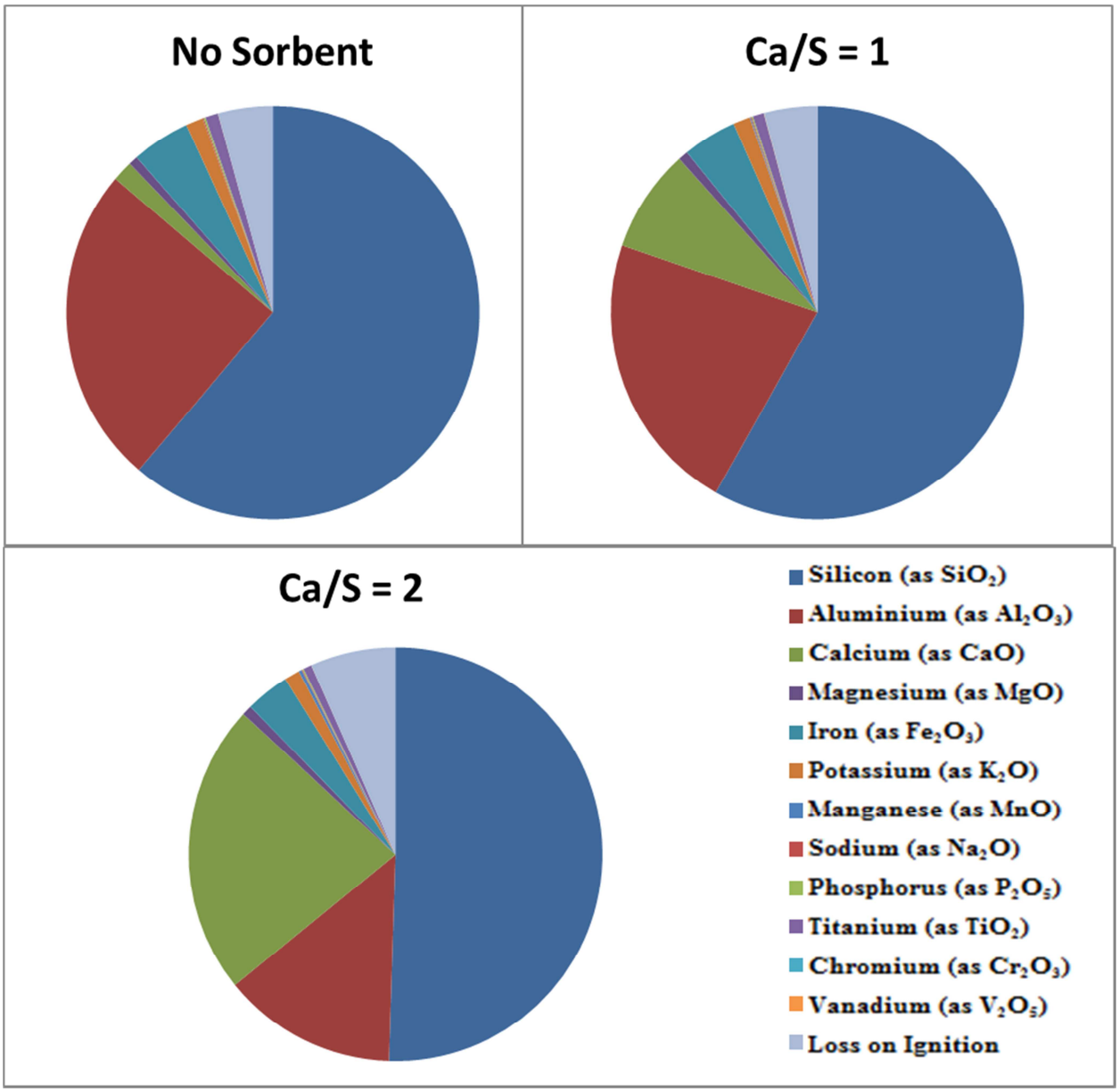


Figure E-2: Ash Elemental of fly ash from Coal B, 850 °C tests

Table E-2: Mineralogy Assessment of fly ash from Coal B, 850 °C tests

	No Sorbent	Ca/S = 1	Ca/S = 2
Anhydrite	1.6	9	14.8
CaMg-Oxide(S)	1.6	1.3	3.3
Ca-Oxide	0.5	1.6	8.1
CaMg-Oxide	0.2	0.1	0.6
Iron Oxide	8.4	5.4	4.2
Quartz	30.2	30.8	27.5
Aluminosilicate	41.8	36.8	31
Muscovite+Illite	1.3	1.4	0.4
Microcline	6	6.5	2.4
Glass	2.6	2.1	1.6
Char	4.6	3.3	4.3

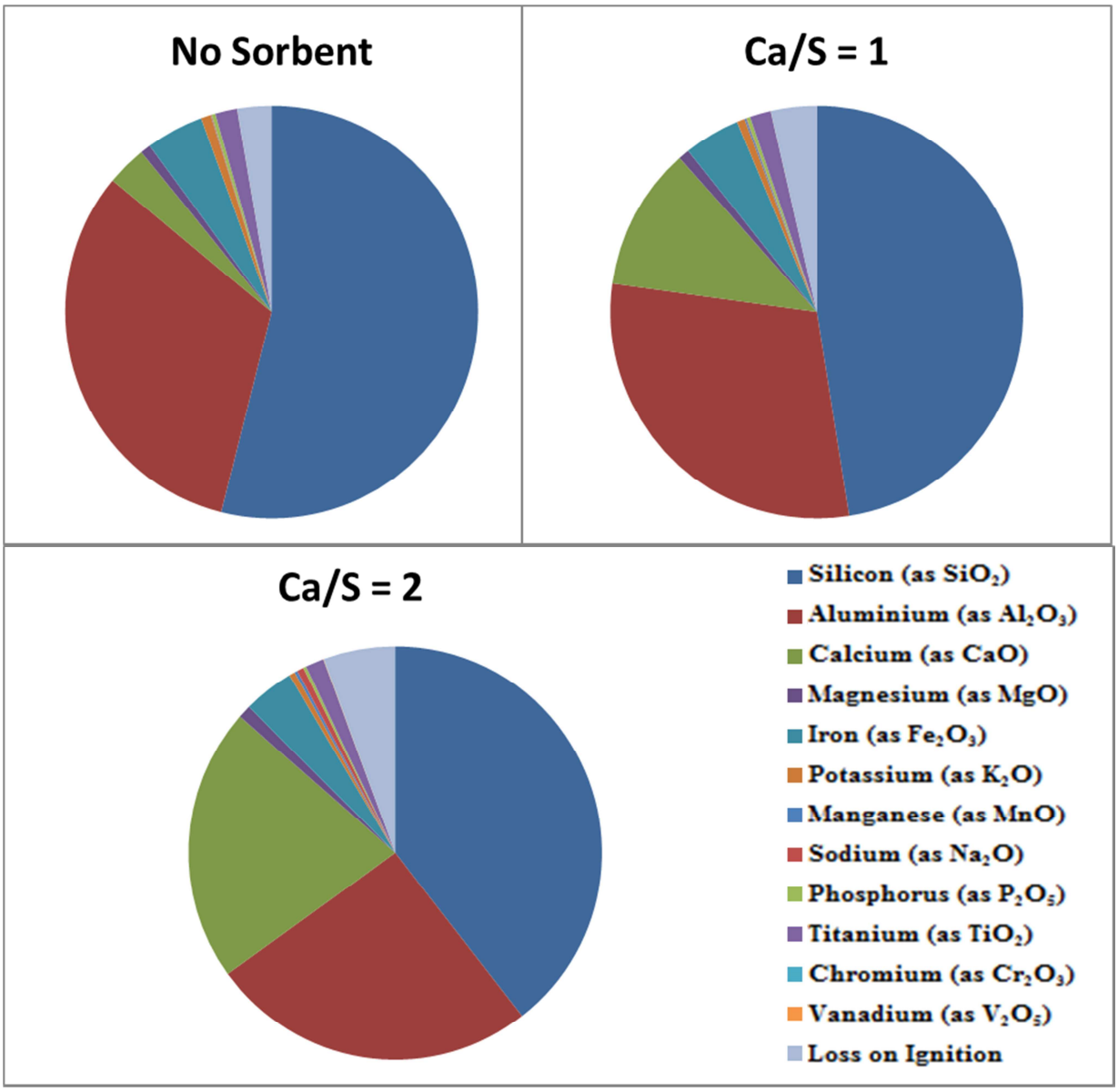


Figure E-3: Ash Elemental of fly ash from Coal C, 850 °C tests

Table E-3: Mineralogy Assessment of fly ash from Coal C, 850 °C tests

	No Sorbent	Ca/S = 1	Ca/S = 2
Anhydrite	5.3	13.1	17.1
CaMg-Oxide(S)	2.6	3.6	2.7
Ca-Oxide	0.3	1.6	7
CaMg-Oxide	0.1	0.2	0.4
Iron Oxide	7.1	6.6	5.4
Quartz	21.2	17.6	11.9
Aluminosilicate	52.5	47	44.2
Muscovite+Illite	1.4	1	0.6
Microcline	4	3.1	1.6
Glass	2.3	2.6	3.1
Char	2.4	2.6	3.3

APPENDIX F: EXAMPLES OF EMISSION CONVERSION AND SULPHUR RETENTION

F.1: The Conversion of Gas Emissions onto Standardise Basis

CO measurements are detected as part per million (ppm).

For test 0.6 (Coal A, Ca/S =2), CO was measured as 210.84 ppm and the O_2 was 5.61%.

- Firstly, the CO value is normalised to 6% O_2 according to this equation

$$X_{i,ppm\ at\ 6\%02} = \frac{X_{i,ppm\ at\ actual\ O2}}{1 + \left(\frac{6 - O_{2,actual}}{20{,}95 - 6}\right)}$$

$$CO_{,ppm\ at\ 6\%02} = \frac{CO_{,ppm\ at\ actual\ O2}}{1 + \left(\frac{6 - O_{2,actual}}{20{,}95 - 6}\right)}$$

$$CO_{,ppm\ at\ 6\%02} = \frac{210.84}{1 + \left(\frac{6 - 5.61}{20{,}95 - 6}\right)}$$

$$CO_{,ppm\ at\ 6\%02} = 205.48\ ppm\ (@6\%O_2)$$

- Then it is converted to mg/Nm^3 by the following equation

$$X_{i,mg/Nm3\ 6\%} = X_{i,ppm\ at\ 6\%02} \times \rho_i$$

$$CO_{mg/Nm3\ 6\%} = CO_{ppm\ at\ 6\%02} \times \rho_{CO}$$

$$\rho_{CO} = 1.2505$$

$$CO_{mg/Nm3\ 6\%} = 205.48 \times 1.2505$$

$$CO_{mg/Nm3\ 6\%} = 256.64 mg/Nm^3 (@6\%O_2, STP)$$

The same principle apply for all gas species

F.2: The Calculation of Sulphur Retention

Sulphur retention is measure by the following steps:

For test 0.6 (Coal A, Ca/S =2): O2 = 5.61%, CO = 210.84 ppm, CO_2 = 12.84%, NO_x = 334.09 ppm, N_2O = 151.98 ppm, SO_2 = 140 ppm, N_2 = 81.47%).

- The individual mass unit for the different species is calculated as follows

$$m_i = v_i \times M_{molar,i} \times 100$$

$$m_{O2} = 5.61 \times 32 \times 100 = 17952$$

$$m_{CO} = 210.84 \times 28 \times 100 \div 10000 = 59.04$$

$$m_{CO2} = 12.84 \times 44 \times 100 = 56496$$

$$m_{NOx} = 334.09 \times 30 \times 100 \div 10000 = 100.23$$

$$m_{N2O} = 151.98 \times 44 \times 100 \div 10000 = 66.87$$

$$m_{SO2} = 140 \times 64 \times 100 \div 10000 = 89.6$$

$$m_{N2} = 81.47 \times 28 \times 100 = 228116$$

- The mass of gas is then calculated as

$$m_{gas\ mass} = m_{CO} + m_{CO2} + m_{NO} + m_{NO2} + m_{N2O} + m_{SO2} + m_{N2} + m_{O2} + m_{H2O}$$

$$= 302879.73$$

- The mass fraction of SO_2 in the gas is determined

$$X_{mass\%SO2} = m_{SO2} \div m_{gas\ mass} \times 100$$

$$= 0.0295827\ \%$$

- Mass of flue gas is determined by

$$\dot{m}_{flue\ gas} = \dot{m}_{total\ air} + \left({}^{X_{moisture}}/_{100} + {}^{X_{volatiles}}/_{100}\ {}^{X_{fixed\ carbon}}/_{100} \right) \times \dot{m}_{coal}$$

$$= 81.31\ \text{kg/hr}$$

- The mass flowrate of SO_2 emitted is calculated as.

$$\dot{m}_{SO2emitted} = \dot{m}_{flue\ gas} \times \left({}^{X_{mass\%SO2}}/_{100} \right)$$

= 0.024055 kg/hr

- Theoretical amount of SO2 that can be emitted is.

$$\dot{m}_{theoSO2} = \dot{m}_{coal} \times n_{S\ in\ coal} \times 2$$

= 0.3043

- Sulphur retention is calculated as.

$$S_{retention} = \left(1 - {}^{\dot{m}_{SO2emitted}}/_{\dot{m}_{theoSO2}} \right) * 100$$

= 92.09 %